



CMS-GEN-14-001

CERN-PH-EP/2015-291
2022/09/01

Event generator tunes obtained from underlying event and multiparton scattering measurements

The CMS Collaboration^{*}

Abstract

New sets of parameters (“tunes”) for the underlying-event (UE) modeling of the PYTHIA8, PYTHIA6 and HERWIG++ Monte Carlo event generators are constructed using different parton distribution functions. Combined fits to CMS UE data at $\sqrt{s} = 7$ TeV and to UE data from the CDF experiment at lower \sqrt{s} , are used to study the UE models and constrain their parameters, providing thereby improved predictions for proton-proton collisions at 13 TeV. In addition, it is investigated whether the values of the parameters obtained from fits to UE observables are consistent with the values determined from fitting observables sensitive to double-parton scattering processes. Finally, comparisons of the UE tunes to “minimum bias” (MB) events, multijet, and Drell-Yan ($q\bar{q} \rightarrow Z/\gamma^* \rightarrow \text{lepton-antilepton+jets}$) observables at 7 and 8 TeV are presented, as well as predictions of MB and UE observables at 13 TeV.

Submitted to the European Physical Journal C

1 Introduction

Monte Carlo (MC) event generators of hadron-hadron collisions based on perturbative quantum chromodynamics (QCD) contain several components. The “hard-scattering” part of the event consists of particles resulting from the hadronization of the two partons (jets) produced in the hardest scattering, and in their associated hard initial- and final-state radiation (ISR and FSR). The underlying event (UE) consists of particles from the hadronization of beam-beam remnants (BBR), of multiple-parton interactions (MPI), and their associated ISR and FSR. The BBR include hadrons from the fragmentation of spectator partons that do not exchange any appreciable transverse momentum (p_T) in the collision. The MPI are additional 2-to-2 parton-parton scatterings that occur within the same hadron-hadron collision, and are softer in transverse momentum ($p_T \lesssim 3 \text{ GeV}$) than the hard scattering.

The perturbative 2-to-2 parton-parton differential cross section diverges like $1/\hat{p}_T^4$, where \hat{p}_T is the transverse momentum of the outgoing partons in the parton-parton center-of-mass (c.m.) frame. Usually, QCD MC models such as PYTHIA [1–5] regulate this divergence by including a smooth phenomenological cutoff p_{T0} as follows:

$$1/\hat{p}_T^4 \rightarrow 1/(\hat{p}_T^2 + p_{T0}^2)^2. \quad (1)$$

This formula approaches the perturbative result for large scales and is finite as $\hat{p}_T \rightarrow 0$. The divergence of the strong coupling α_s at low \hat{p}_T is also regulated through Eq. (1). The primary hard 2-to-2 parton-parton scattering process and the MPI are regulated in the same way through a single p_{T0} parameter. However, this cutoff is expected to have a dependence on the center-of-mass energy of the hadron-hadron collision \sqrt{s} . In the PYTHIA MC event generator this energy dependence is parametrized with a power-law function with exponent ϵ :

$$p_{T0}(\sqrt{s}) = p_{T0}^{\text{ref}} (\sqrt{s}/\sqrt{s_0})^\epsilon, \quad (2)$$

where $\sqrt{s_0}$ is a given reference energy and p_{T0}^{ref} is the value of p_{T0} at $\sqrt{s_0}$. At a given \sqrt{s} , the amount of MPI depends on p_{T0} , the parton distribution functions (PDF), and the overlap of the matter distributions (or centrality) of the two colliding hadrons. Smaller values of p_{T0} provide more MPI due to a larger MPI cross section. Table 1 shows the parameters in PYTHIA6 [1] and PYTHIA8 [5] that, together with the selected PDF, determine the energy dependence of MPI. Recently, in HERWIG++ [6, 7] the same formula has been adopted to provide an energy dependence to their MPI cutoff, which is also shown in Table 1. The QCD MC generators have other parameters that can be adjusted to control the modeling of the full properties of the events, and a specified set of such parameters adjusted to fit certain prescribed aspects of the data is referred to as a “tune” [8–10].

Table 1: Parameters in PYTHIA6 [1], PYTHIA8 [5], and HERWIG++ [6, 7] MC event generators that, together with some chosen PDF, determine the energy dependence of MPI.

Parameter	PYTHIA6	PYTHIA8	HERWIG++
MPI cutoff, p_{T0}^{ref} , at $\sqrt{s} = \sqrt{s_0}$	PARP(82)	MultipartonInteractions:pT0Ref	MPIHandler:pTmin0
Reference energy, $\sqrt{s_0}$	PARP(89)	MultipartonInteractions:ecmRef	MPIHandler:ReferenceScale
Exponent of \sqrt{s} dependence, ϵ	PARP(90)	MultipartonInteractions:ecmPow	MPIHandler:Power

In addition to hard-scattering processes, other processes contribute to the inelastic cross section in hadron-hadron collisions: single-diffraction dissociation (SD), double-diffraction dissociation

tion (DD), and central-diffraction (CD). In SD and DD events, one or both beam particles are excited into high-mass color-singlet states (i.e. into some resonant N^*), which then decay. The SD and DD processes correspond to color-singlet exchanges between the beam hadrons, while CD corresponds to double color-singlet exchange with a diffractive system produced centrally. The outgoing remnants are no longer color singlets, and this separation of color generates a multitude of quark-antiquark pairs that are created via vacuum polarization. The sum of all components except SD corresponds to non single diffraction (NSD) processes.

Minimum bias (MB) is a generic term that refers to events selected by requiring minimal activity within the detector. This selection accepts a large fraction of the overall inelastic cross section. The study of the UE is often based on MB data, but it should be noted that the dominant particle production mechanisms in MB collisions and in the UE are not exactly the same. On the one hand, the UE is studied in collisions in which a hard 2-to-2 parton-parton scattering has occurred, by analyzing the hadronic activity in different regions of the event with respect to the back-to-back azimuthal structure of the hardest particles emitted [11]. On the other hand, MB collisions are often softer and include diffractive interactions which, in the case of PYTHIA, are modeled via a Regge-based approach [12].

Most of the time MPI are much softer than primary hard scatters, however, occasionally two hard 2-to-2 parton scatters can take place within the same hadron-hadron collision. This is referred to as double-parton scattering (DPS) [13–16], and is typically described in terms of an effective cross section parameter, σ_{eff} , defined as:

$$\sigma_{AB} = \frac{\sigma_A \sigma_B}{\sigma_{\text{eff}}}, \quad (3)$$

where σ_A and σ_B are the inclusive cross sections for individual hard scattering processes of generic type A and B, respectively, and σ_{AB} is the cross section for producing both scatters in the same hadron-hadron collision. If A and B are indistinguishable, as in four-jet production, a statistical factor of 1/2 must be inserted on the right-hand side of Eq. (3). Furthermore, σ_{eff} is assumed to be independent of A and B. However, σ_{eff} is not a directly observed quantity but can be calculated from the overlap function of the two transverse profile distributions of the colliding hadrons, implemented in a given MPI model.

The UE tunes have impact in both soft and hard particle production in a given pp collision. First, about half of the particles produced in a MB collision originate from the hadronization of partons scattered in MPI whose p_T -differential cross sections are regulated via Eq.(1), with the same p_{T0} cutoff used to tame the hardest 2-to-2 parton-parton scattering in the event. The tuning of the cross-section regularization thus affects all (soft and hard) parton-parton scatterings and provides a prediction for the behavior of the ND cross section. Secondly, the UE tunes parametrize the transverse overlap distribution of the colliding protons and thereby the probability of two hard parton-parton scatters which can then be used to estimate DPS-sensitive observables.

In this paper, we study the \sqrt{s} dependence of the UE using recent CDF proton-antiproton data at 0.3, 0.9, and 1.96 TeV [11], together with CMS pp data at $\sqrt{s} = 7$ TeV [17]. The 0.3 and 0.9 TeV data are from the “Tevatron energy scan” performed just before the Tevatron was shut down. Using the RIVET (version 1.9.0) and PROFESSOR (version 1.3.3) frameworks [18, 19], we construct: (i) new PYTHIA8 (version 8.185) UE tunes using different PDF sets (CTEQ6L1 [20], HERAPDF1.5LO [21], and NNPDF2.3LO [22, 23]), (ii) new PYTHIA6 (version 6.327) UE tunes (using CTEQ6L1 and HERAPDF1.5LO), and (iii) a new HERWIG++ (version 2.7.0) UE tune for CTEQ6L1. The RIVET software is a tool for producing predictions of physics quantities obtained

from MC event generators. It is used for generating sets of MC predictions with a different choice of parameters related to the UE simulation. The predictions are then included in the PROFESSOR framework, which parametrizes the generator response and returns the set of tuned parameters that best fits the input measurements.

In addition, we construct several new CMS “DPS tunes” and investigate whether the values of the UE parameters determined from fitting the UE observables in a hard-scattering process are consistent with the values determined from fitting DPS-sensitive observables. The PROFESSOR software also offers the possibility of extracting “eigentunes”, which provide an estimate of the uncertainties in the fitted parameters. The eigentunes consist of a collection of additional tunes, obtained through the covariance matrix of the data-theory fitting procedure, to determine independent directions in parameter space that provide a specific modification in the goodness of the fit, χ^2 (Section 2). All of the CMS UE and DPS tunes are provided with eigentunes. In Section 4, predictions using the CMS UE tunes are compared to other UE measurements not used in determining the tunes, and we examine how well Drell-Yan, MB, and multijet observables can be predicted using the UE tunes. In Section 5, predictions of the new tunes are shown for UE observables at 13 TeV, together with a comparison to the first MB distribution measured. Section 6 has a brief summary and conclusions. The appendices contain additional comparisons between the PYTHIA6 and HERWIG++ UE tunes and the data, information about the tune uncertainties, and predictions for some MB and DPS observables at 13 TeV.

2 The CMS UE tunes

Previous UE studies have used the charged-particle jet with largest p_T [24, 25] or a Z boson [11, 26] as the leading (i.e. highest p_T) objects in the event. The CDF and CMS data, used for the tunes, select the charged particle with largest p_T in the event (p_T^{\max}) as the “leading object”, and use just the charged particles with $p_T > 0.5 \text{ GeV}$ and $|\eta| < 0.8$ to characterize the UE.

On an event-by-event basis, the leading object is used to define regions of pseudorapidity-azimuth (η - ϕ) space. The “toward” region relative to this direction, as indicated in Fig. 1, is defined by $|\Delta\phi| < \pi/3$ and $|\eta| < 0.8$, and the “away” region by $|\Delta\phi| > 2\pi/3$ and $|\eta| < 0.8$. The charged-particle and the scalar- p_T sum densities in the transverse region are calculated as the sum of the contribution in the two regions: “Transverse-1” ($\pi/3 < \Delta\phi < 2\pi/3$, $|\eta| < 0.8$) and “Transverse-2” ($\pi/3 < -\Delta\phi < 2\pi/3$, $|\eta| < 0.8$), divided by the area in η - ϕ space, $\Delta\eta\Delta\phi = 1.6 \times 2\pi/3$. The transverse region is further separated into the “TransMAX” and “TransMIN” regions, also shown in Fig. 1. This defines on an event-by-event basis the regions with more (TransMAX) and fewer (TransMIN) charged particles (N_{ch}), or greater (TransMAX) or smaller (TransMIN) scalar- p_T sums (p_T^{sum}). The UE particle and p_T densities are constructed by dividing by the area in η - ϕ space, where the TransMAX and TransMIN regions each have an area of $\Delta\eta\Delta\phi = 1.6 \times 2\pi/6$. The transverse density (also referred to as “TransAVE”) is the average of the TransMAX and the TransMIN densities. For events with hard initial- or final-state radiation, the TransMAX region often contains a third jet, but both the TransMAX and TransMIN regions receive contributions from the MPI and BBR components. The TransMIN region is very sensitive to the MPI and BBR components of the UE, while “TransDIF” (the difference between TransMAX and TransMIN densities) is very sensitive to ISR and FSR [27].

The new UE tunes are determined by fitting UE observables, and using only those parameters that are most sensitive to the UE data. Since it is not possible to tune all parameters of a MC event generator at once, the parameters that affect, for example, the parton shower, the fragmentation, and the intrinsic-parton p_T are fixed to the values given by an initially established reference tune. The initial reference tunes used for PYTHIA8 are Tune 4C [28] and the Monash

Tune [29]. For PYTHIA6, the reference tune is Tune Z2*lep [25], and for HERWIG++ it is Tune UE-EE-5C [30].

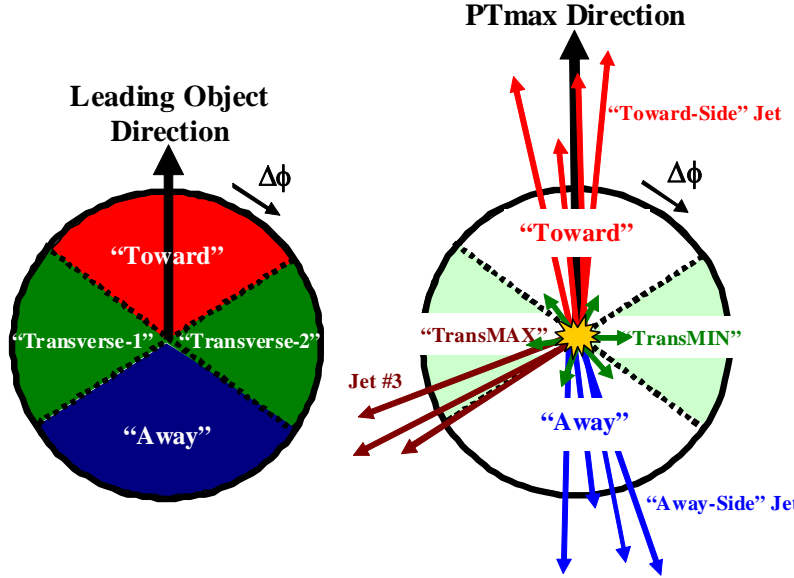


Figure 1: Left: Illustration of the azimuthal regions in an event defined by the $\Delta\phi$ angle relative to the direction of the leading object [11]. Right: Illustration of the topology of a hadron-hadron collision in which a hard parton-parton collision has occurred, and the leading object is taken to be the charged particle of largest p_T in the event, p_T^{\max} .

2.1 The PYTHIA8 UE tunes

Taking as the reference tune the set of parameters of PYTHIA8 Tune 4C [28], we construct two new UE tunes, one using CTEQ6L1 (CUETP8S1-CTEQ6L1) and one using HERAPDF1.5LO (CUETP8S1-HERAPDF1.5LO). CUET (read as “cute”) stands for “CMS UE tune”, and P8S1 stands for PYTHIA8 “Set 1”.

The tunes are extracted by varying the four parameters in Table 2 in fits to the TransMAX and TransMIN charged-particle and p_T^{\sum} densities at three energies, for $p\bar{p}$ collisions at $\sqrt{s} = 0.9$ and 1.96, and pp collisions at 7 TeV. The measurements of TransAVE and TransDIF densities are not included in the fit, since they can be constructed from TransMAX and TransMIN. The new tunes use an exponentially-falling matter-overlap function between the two colliding protons of the form $\exp(-b \exp^{\text{POW}})$, with b being the impact parameter of the collision. The parameters that are varied are \exp^{POW} , the MPI energy-dependence parameters (Table 1) and the range, i.e. the probability, of color reconnection (CR). A small (large) value of the final-state CR parameter tends to increase (reduce) the final particle multiplicities. In PYTHIA8, unlike in PYTHIA6, only one parameter determines the amount of CR, which includes a p_T dependence, as defined in Ref. [5].

The generated inelastic events include ND and diffractive (DD+SD+CD) contributions, although the UE observables used to determine the tunes are sensitive to SD, CD, and DD only at very small p_T^{\max} values (e.g. $p_T^{\max} < 1.5$ GeV). The ND component dominates for p_T^{\max} values greater than ≈ 2.0 GeV, since the cross section of the diffractive components rapidly decreases as a function of \hat{p}_T . The fit is performed by minimizing the χ^2 function:

$$\chi^2(p) = \sum_i \frac{(f^i(p) - R_i)^2}{\Delta_i^2}, \quad (4)$$

where the sum runs over each bin i of every observable. The $f^i(p)$ functions correspond to the interpolated MC response for the simulated observables as a function of the parameter vector p , R_i is the value of the measured observable in bin i , and Δ_i is the total experimental uncertainty of R_i . We do not use the Tevatron data at $\sqrt{s} = 300$ GeV, as we are unable to obtain an acceptable χ^2 in a fit of the four parameters in Table 2. The χ^2 per degree of freedom (dof) listed in Table 2 refers to the quantity $\chi^2(p)$ in Eq. (4), divided by the number of dof in the fit. The eigentunes (see Appendix A) correspond to the tunes in which the changes in the χ^2 ($\Delta\chi^2$) of the fit relative to the best-fit value equals the χ^2 value obtained in the tune, i.e. $\Delta\chi^2 = \chi^2$. For both tunes in Table 2, the fit quality is very good, with χ^2/dof values very close to 1.

The contribution from CR changes in the two new tunes; it is large for the HERAPDF1.5LO and small for the CTEQ6L1 PDF. This is a result of the shape of the parton densities at small fractional momenta x , which is different for the two PDF sets. While the parameter p_{T0}^{ref} in Eq. (2) stays relatively constant between Tune 4C and the new tunes, the energy dependence ϵ tends to increase in the new tunes, as do the matter-overlap profile functions.

Table 2: The PYTHIA8 parameters, tuning range, Tune 4C values [28], and best-fit values for CUETP8S1-CTEQ6L1 and CUETP8S1-HERAPDF1.5LO, obtained from fits to the TransMAX and TransMIN charged-particle and p_T^{sum} densities, as defined by the leading charged-particle p_T^{max} at $\sqrt{s} = 0.9, 1.96$, and 7 TeV. The $\sqrt{s} = 300$ GeV data are excluded from the fit.

PYTHIA8 Parameter	Tuning Range	Tune 4C	CUETP8S1	CUETP8S1
PDF	—	CTEQ6L1	CTEQ6L1	HERAPDF1.5LO
MultipartonInteractions:pT0Ref [GeV]	1.0–3.0	2.085	2.101	2.000
MultipartonInteractions:ecmPow	0.0–0.4	0.19	0.211	0.250
MultipartonInteractions:expPow	0.4–10.0	2.0	1.609	1.691
ColourReconnection:range	0.0–9.0	1.5	3.313	6.096
MultipartonInteractions:ecmRef [GeV]	—	1800	1800*	1800*
χ^2/dof	—	—	0.952	1.13

* Fixed at Tune 4C value.

The PYTHIA8 Monash Tune [29] combines updated fragmentation parameters with the NNPDF2.3LO PDF.

The NNPDF2.3LO PDF has a gluon distribution at small x that is different compared to CTEQ6L1 and HERAPDF1.5LO, and this affects predictions in the forward region of hadron-hadron collisions. Tunes using the NNPDF2.3LO PDF provide a more consistent description of the UE and MB observables in both the central and forward regions, than tunes using other PDF.

A new PYTHIA8 tune CUETP8M1 (labeled with M for Monash) is constructed using the parameters of the Monash Tune and fitting the two MPI energy-dependence parameters of Table 1 to UE data at $\sqrt{s} = 0.9, 1.96$, and 7 TeV. Varying the CR range and the exponential slope of the matter-overlap function freely in the minimization of the χ^2 leads to suboptimal best-fit values. The CR range is therefore fixed to the value of the the Monash Tune, and the exponential slope of the matter-overlap function `expPow` is set to 1.6, which is similar to the value determined

in CUETP8S1-CTEQ6L1. The best-fit values of the two tuned parameters are shown in Table 3. Again, we exclude the 300 GeV data, since we are unable to get a good χ^2 in the fit. The parameters obtained for CUETP8M1 differ slightly from the ones of the Monash Tune. The obtained energy-dependence parameter ϵ is larger, while a very similar value is obtained for p_{T0}^{ref} .

Table 3: The PYTHIA8 parameters, tuning range, Monash values [29], and best-fit values for CUETP8M1, obtained from fits to the TransMAX and TransMIN charged-particle and p_T^{sum} densities, as defined by the leading charged-particle p_T^{max} at $\sqrt{s} = 0.9, 1.96$, and 7 TeV . The $\sqrt{s} = 300 \text{ GeV}$ data are excluded from the fit.

PYTHIA8 Parameter	Tuning Range	Monash	CUETP8M1
PDF	—	NNPDF2.3LO	NNPDF2.3LO
MultipartonInteractions:pT0Ref [GeV]	1.0–3.0	2.280	2.402
MultipartonInteractions:ecmPow	0.0–0.4	0.215	0.252
MultipartonInteractions:expPow	—	1.85	1.6*
ColourReconnection:range	—	1.80	1.80**
MultipartonInteractions:ecmRef [GeV]	—	7000	7000**
χ^2/dof	—	—	1.54

* Fixed at CUETP8S1-CTEQ6L1 value.

** Fixed at Monash Tune value.

Figures 2–5 show the CDF data at 0.3, 0.9, and 1.96 TeV, and the CMS data at 7 TeV for charged-particle and p_T^{sum} densities in the TransMIN and TransMAX regions as a function of p_T^{max} , compared to predictions obtained with the PYTHIA8 Tune 4C and with the new CMS tunes: CUETP8S1-CTEQ6L1, CUETP8S1-HERAPDF1.5LO, and CUETP8M1. Predictions from the new tunes cannot reproduce the $\sqrt{s} = 300 \text{ GeV}$ data, but describe very well the data at the higher $\sqrt{s} = 0.9, 1.96$, and 7 TeV . In particular, the description provided by the new tunes significantly improves relative to the old Tune 4C, which is likely due to the better choice of parameters used in the MPI energy dependence and the extraction of the CR in the retuning.

2.2 The PYTHIA6 UE tunes

The PYTHIA6 Tune Z2*lep [25] uses the improved fragmentation parameters from fits to the LEP e^+e^- data [31], and a double-Gaussian matter profile for the colliding protons but corresponds to an outdated CMS UE tune. It was constructed by fitting the CMS charged-particle jet UE data at 0.9 and 7 TeV [24] using data on the TransAVE charged-particle and p_T^{sum} densities, since data on TransMAX, TransMIN, and TransDIF were not available at that time.

Starting with Tune Z2*lep parameters, two new PYTHIA6 UE tunes are constructed, one using CTEQ6L1 (CUETP6S1-CTEQ6L1) and one using HERAPDF1.5LO (CUETP6S1-HERAPDF1.5LO), with P6S1 standing for PYTHIA6 “Set 1”. The tunes are constructed by fitting the five parameters shown in Table 4 to the TransMAX and TransMIN charged-particle and p_T^{sum} densities at $\sqrt{s} = 0.3, 0.9, 1.96$, and 7 TeV . In addition to varying the MPI energy-dependence parameters (Table 1), we also vary the core-matter fraction PARP(83), which parametrizes the amount of matter contained within the radius of the proton core, the CR strength PARP(78), and the CR suppression PARP(77). The PARP(78) parameter reflects the probability for a given string to retain its color history, and therefore does not change the color and other string pieces, while the PARP(77) parameter introduces a p_T dependence on the CR

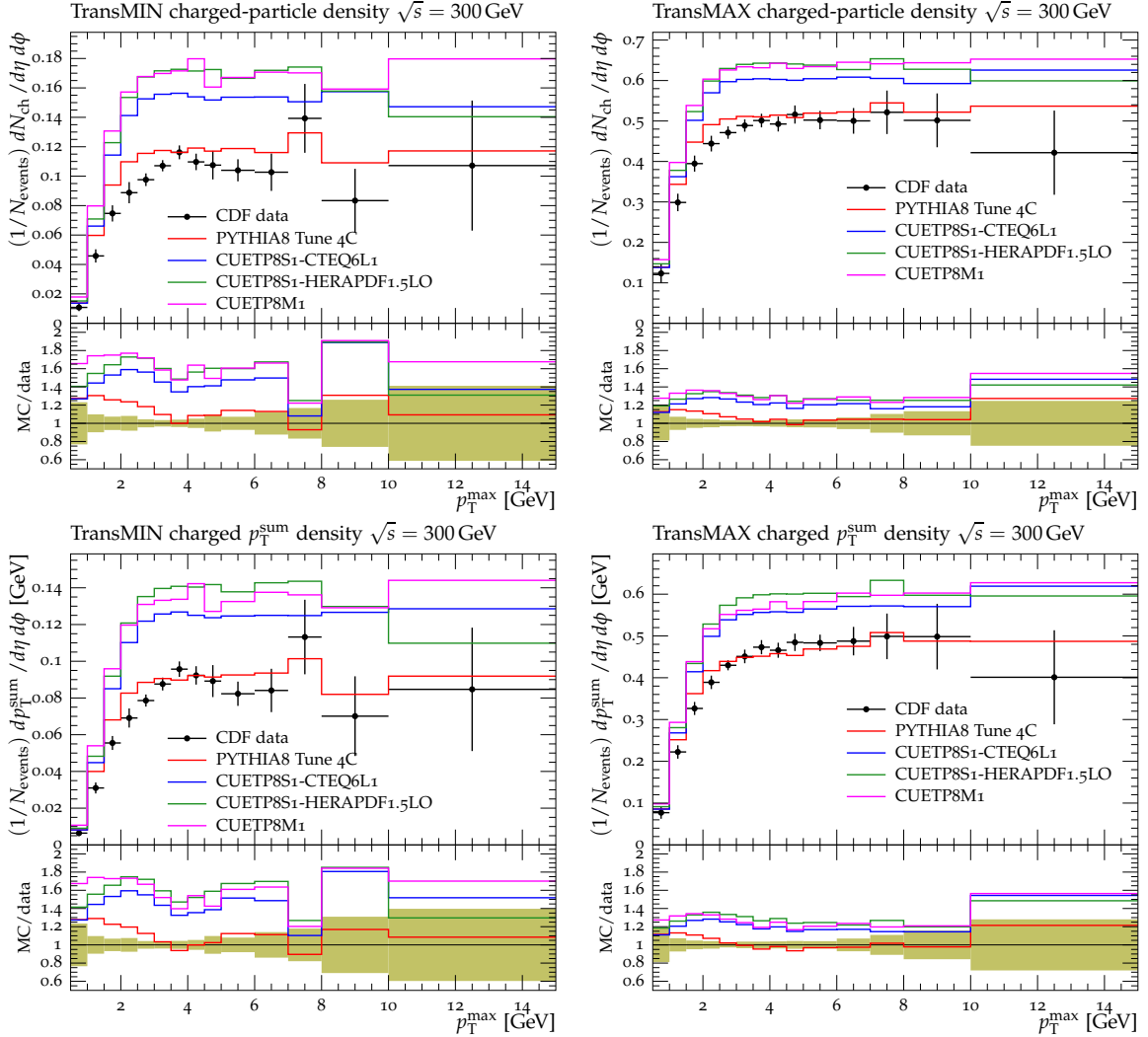


Figure 2: CDF data at $\sqrt{s} = 300 \text{ GeV}$ [11] on particle (top) and p_T^{sum} densities (bottom) for charged particles with $p_T > 0.5 \text{ GeV}$ and $|\eta| < 0.8$ in the TransMIN (left) and TransMAX (right) regions as defined by the leading charged particle, as a function of the transverse momentum of the leading charged-particle p_T^{max} . The data are compared to PYTHIA8 Tune 4C, CUETP8S1-CTEQ6L1, CUETP8S1-HERAPDF1.5LO, and CUETP8M1. The ratios of MC events to data are given below each panel. The data at $\sqrt{s} = 300 \text{ GeV}$ are not used in determining these tunes. The green bands in the ratios represent the total experimental uncertainties.

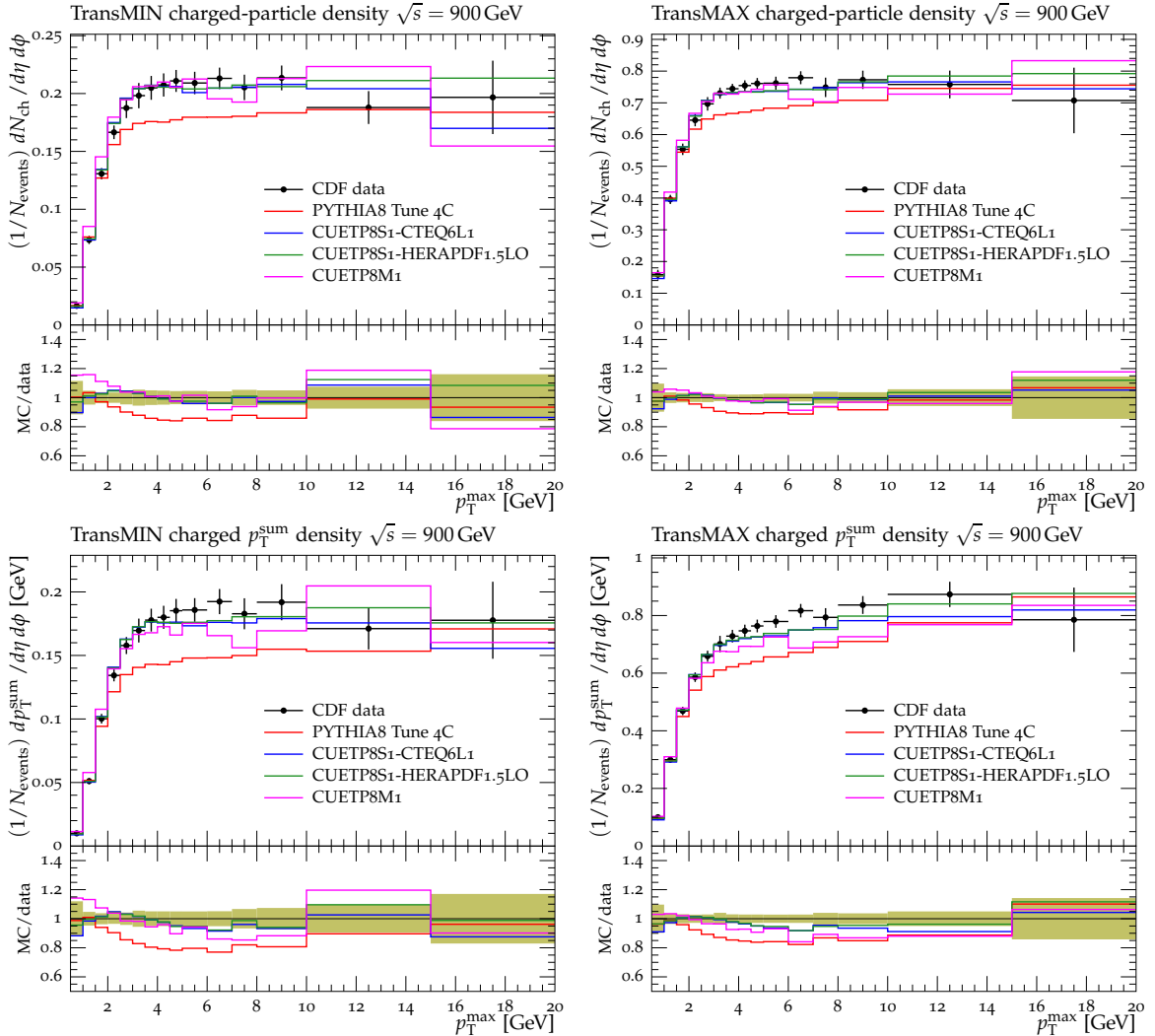


Figure 3: CDF data at $\sqrt{s} = 900 \text{ GeV}$ [11] on particle (top) and p_T^{sum} densities (bottom) for charged particles with $p_T > 0.5 \text{ GeV}$ and $|\eta| < 0.8$ in the TransMIN (left) and TransMAX (right) regions as defined by the leading charged particle, as a function of the transverse momentum of the leading charged-particle p_T^{max} . The data are compared to PYTHIA8 Tune 4C, CUETP8S1-CTEQ6L1, CUETP8S1-HERAPDF1.5LO, and CUETP8M1. The ratios of MC events to data are given below each panel. The green bands in the ratios represent the total experimental uncertainties.

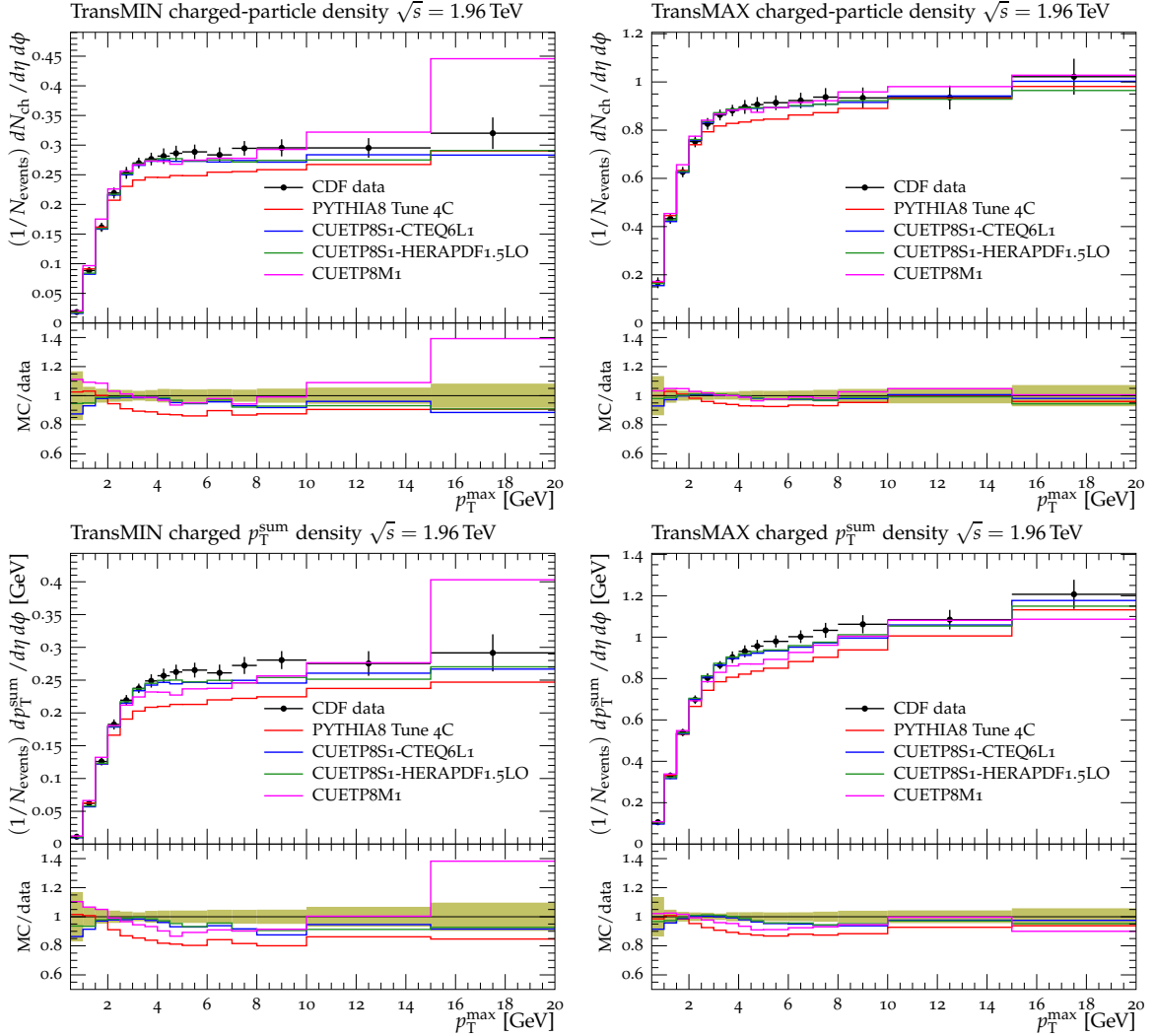


Figure 4: CDF data at $\sqrt{s} = 1.96 \text{ TeV}$ [11] on particle (top) and p_T^{sum} densities (bottom) for charged particles with $p_T > 0.5 \text{ GeV}$ and $|\eta| < 0.8$ in the TransMIN (left) and TransMAX (right) regions as defined by the leading charged particle, as a function of the transverse momentum of the leading charged-particle p_T^{max} . The data are compared to PYTHIA8 Tune 4C, CUETP8S1-CTEQ6L1, CUETP8S1-HERAPDF1.5LO, and CUETP8M1. The ratios of MC events to data are given below each panel. The green bands in the ratios represent the total experimental uncertainties.

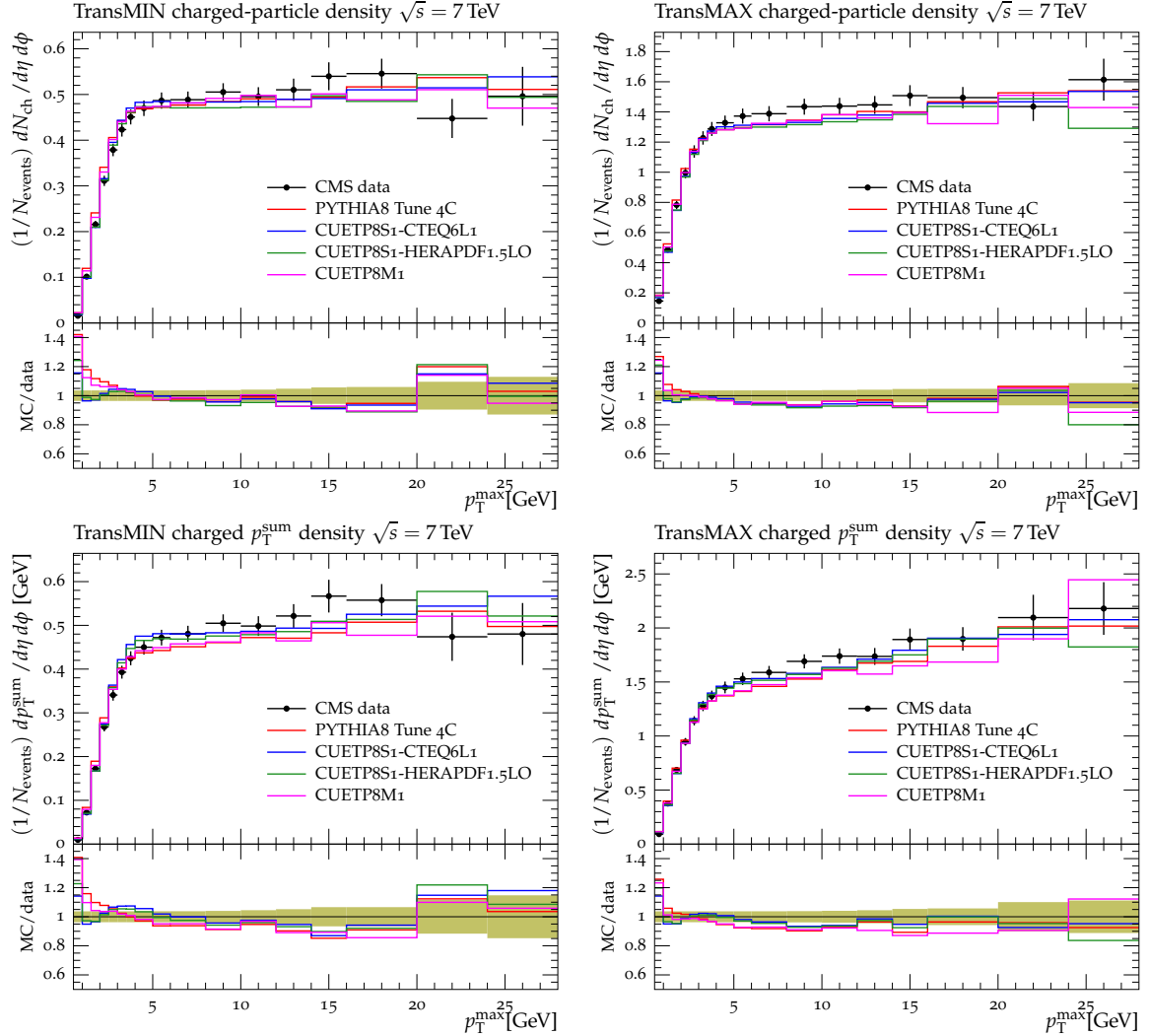


Figure 5: CMS data at $\sqrt{s} = 7 \text{ TeV}$ [17] on particle (top) and p_T^{sum} densities (bottom) for charged particles with $p_T > 0.5 \text{ GeV}$ and $|\eta| < 0.8$ in the TransMIN (left) and TransMAX (right) regions as defined by the leading charged particle, as a function of the transverse momentum of the leading charged-particle p_T^{\max} . The data are compared to PYTHIA8 Tune 4C, and CUETP8S1-CTEQ6L1, CUETP8S1-HERAPDF1.5LO, and CUETP8M1. The ratios of MC events to data are given below each panel. The green bands in the ratios represent the total experimental uncertainties.

probability [1].

Inelastic events (ND+DD+SD+CD) are generated with PYTHIA6. The best-fit values of the five parameters are shown in Table 4. The matter-core fraction is quite different in the two new PYTHIA6 tunes. This is due to the fact that this parameter is very sensitive to the behaviour of the PDF at small x . Predictions obtained with PYTHIA6 Tune Z2*lep, CUETP6S1-CTEQ6L1 and CUETP6S1-HERAPDF1.5LO are compared in Appendix B to the UE data. The new PYTHIA6 tunes significantly improve the description of the UE data relative to PYTHIA6 Tune Z2*lep at all considered energies, due to the better choice of parameters governing the MPI energy dependence.

Table 4: The PYTHIA6 parameters, tuning range, Tune Z2*lep values [31], and best-fit values for CUETP6S1-CTEQ6L1 and CUETP6S1-HERAPDF1.5LO, obtained from fits to the TransMAX and TransMIN charged-particle and p_T^{sum} densities as defined by the p_T^{max} of the leading charged particle at $\sqrt{s} = 0.3, 0.9, 1.96$, and 7 TeV .

PYTHIA6 Parameter	Tuning Range	Tune Z2*lep	CUETP6S1	CUETP6S1
PDF	—	CTEQ6L1	CTEQ6L1	HERAPDF1.5LO
PARP(82) - MPI cutoff [GeV]	1.6–2.2	1.921	1.910	1.946
PARP(90) - Exponent of \sqrt{s} dependence	0.18–0.28	0.227	0.248	0.250
PARP(77) - CR suppression	0.25–1.15	1.016	0.665	0.667
PARP(78) - CR strength	0.2–0.8	0.538	0.545	0.537
PARP(83) - Matter fraction in core	0.1–1.0	0.356	0.822	0.490
PARP(89) - Reference energy [GeV]	—	1800	1800*	1800*
χ^2/dof	—	—	0.915	1.004

* Fixed at Tune Z2*lep value.

2.3 The HERWIG++ UE tunes

Starting with the parameters of HERWIG++ Tune UE-EE-5C [30], we construct a new HERWIG++ UE tune, CUETHppS1, where Hpp stands for HERWIG++. This tune is obtained by varying the four parameters shown in Table 5 in the fit to TransMAX and TransMIN charged-particle and p_T^{sum} densities at the four $\sqrt{s} = 0.3, 0.9, 1.96$, and 7 TeV . We set the MPI cutoff p_{T0} and the reference energy $\sqrt{s_0}$ to the Tune UE-EE-5C values, and vary the MPI c.m. energy extrapolation parameter in Table 1. We also vary the inverse radius that determines the matter overlap and the range of CR. The CR model in HERWIG++ is defined by two parameters, one (`colourDisrupt`) ruling the color structure of soft interactions ($p_T < p_{T0}$), and one (`ReconnectionProbability`) giving the probability of CR without a p_T dependence for color strings. We include all four center-of-mass energies, although at each energy we exclude the first two p_T^{max} bins. These first bins, e.g. for $p_T^{\text{max}} < 1.5 \text{ GeV}$, are sensitive to SD, CD, and DD, but HERWIG++ contains only the ND component.

In Table 5, the parameters of the new CUETHppS1 are listed and compared to those from Tune UE-EE-5C. The parameters of the two tunes are very similar. The χ^2/dof , also indicated in Table 5, is found to be ≈ 0.46 , which is smaller than the value obtained for other CMS UE tunes. This is due to the fact that the first two bins as a function of p_T^{max} , which have much smaller statistical uncertainties than the higher- p_T^{max} bins, are excluded from the fit because they cannot be described by any reasonable fit-values. In Appendix C, predictions obtained with HERWIG++ Tune UE-EE-5C and CUETHppS1 are compared to the UE data. The two

tunes are both able to reproduce the UE data at all energies. With the new CUETHppS1 tune, uncertainties can be estimated using the eigentunes (see Appendix A).

Table 5: The `HERWIG++` parameters, tuning range, Tune UE-EE-5C values [30], and best-fit values for CUETHppS1, obtained from a fit to the TransMAX and TransMIN charged-particle and p_T^{sum} densities as a function of the leading charged-particle p_T^{max} at $\sqrt{s} = 0.3, 0.9, 1.96$, and 7 TeV .

HERWIG++ Parameter	Tuning Range	UE-EE-5C	CUETHppS1
PDF	—	CTEQ6L1	CTEQ6L1
MPIHandler:Power	0.1–0.5	0.33	0.371
RemnantDecayer:colourDisrupt	0.1–0.9	0.8	0.628
MPIHandler:InvRadius [GeV 2]	0.5–2.7	2.30	2.255
ColourReconnector:ReconnectionProbability	0.1–0.9	0.49	0.528
MPIHandler:pTmin0 [GeV]	—	3.91	3.91*
MPIHandler:ReferenceScale [GeV]	—	7000	7000*
χ^2/dof	—	—	0.463

* Fixed at Tune UE-EE-5C value.

In conclusion, both `HERWIG++` tunes, as well as the new CMS PYTHIA6 UE tunes reproduce the UE data at all four \sqrt{s} . The PYTHIA8 UE tunes, however, do not describe well the data at $\sqrt{s} = 300 \text{ GeV}$, which may be related to the modeling of the proton-proton overlap function. The PYTHIA6 Tune Z2*lep, and the new CMS UE tunes use a double-Gaussian matter distribution, while all the PYTHIA8 UE tunes use a single exponential matter overlap. The `HERWIG++` tune, on the other hand, uses a matter-overlap function that is related to the Fourier transform of the electromagnetic form factor with μ^2 [7] playing the role of an effective inverse proton radius (i.e. the `InvRadius` parameter in Table 5). However, predictions from a tune performed with PYTHIA8 using a double-Gaussian matter distribution were not able to improve the quality of the fit as a fit obtained without interleaved FSR in the simulation of the UE (as it is implemented in PYTHIA6) did not show any improvement. Further investigations are needed to resolve this issue.

3 The CMS DPS tunes

Traditionally, σ_{eff} is determined by fitting the DPS-sensitive observables with two templates [32–36] that are often based on distributions obtained from QCD MC models. One template is constructed with no DPS, i.e. just single parton scattering (SPS), while the other represents DPS production. This determines σ_{eff} from the relative amounts of SPS and DPS contributions needed to fit the data. Here we use an alternative method that does not require construction of templates from MC samples. Instead, we fit the DPS-sensitive observables directly and then calculate the resulting σ_{eff} from the model. For example, in PYTHIA8, the value of σ_{eff} is calculated by multiplying the ND cross section by an enhancement or a depletion factor, which expresses the dependence of DPS events on the collision impact parameter. As expected, more central collisions have a higher probability of a second hard scattering than peripheral collisions. The enhancement/depletion factors depend on the UE parameters, namely, on the parameters that characterize the matter-overlap function of the two protons, which for `bProfile = 3` is determined by the exponential parameter `expPow`, on the MPI regulator p_{T0} in Eq. (2), and the range of the CR. PYTHIA8 Tune 4C gives $\sigma_{\text{eff}} \approx 30.3 \text{ mb}$ at $\sqrt{s} = 7 \text{ TeV}$.

In Section 2, we determined the MPI parameters by fitting UE data. Here we determine the MPI parameters by fitting to observables which involve correlations among produced objects in hadron-hadron collisions that are sensitive to DPS. Two such observables used in the fit, ΔS and $\Delta^{\text{rel}} p_T$, are defined as follows:

$$\Delta S = \arccos \left(\frac{\vec{p}_T(\text{object}_1) \cdot \vec{p}_T(\text{object}_2)}{|\vec{p}_T(\text{object}_1)| \times |\vec{p}_T(\text{object}_2)|} \right), \quad (5)$$

$$\Delta^{\text{rel}} p_T = \frac{|\vec{p}_T^{\text{jet}_1} + \vec{p}_T^{\text{jet}_2}|}{|\vec{p}_T^{\text{jet}_1}| + |\vec{p}_T^{\text{jet}_2}|}, \quad (6)$$

where, for W+dijet production, object₁ is the W boson and object₂ is the dijet system. For four-jet production, object₁ is the hard-jet pair and object₂ is the soft-jet pair. For $\Delta^{\text{rel}} p_T$ in W+dijet production, jet₁ and jet₂ are the two jets of the dijet system, while in four-jet production, jet₁ and jet₂ refer to the two softer jets.

The PYTHIA8 UE parameters are fitted to the DPS-sensitive observables measured by CMS in W+dijet [36] and in four-jet production [37]. After extracting the MPI parameters, the value of σ_{eff} in Eq. (3) can be calculated from the underlying MPI model. In PYTHIA8, σ_{eff} depends primarily on the matter-overlap function and, to a lesser extent, on the value of p_{T0} in Eq. (2), and the range of the CR. We obtain two separate tunes for each channel: in the first one, we vary just the matter-overlap parameter `expPow`, to which the σ_{eff} value is most sensitive, and in the second one, the whole set of parameters is varied. These two tunes allow to check whether the value of σ_{eff} is stable relative to the choice of parameters.

The W+dijet and the four-jet channels are fitted separately. The fit to DPS-sensitive observables in the W+dijet channel gives a new determination of σ_{eff} which can be compared to the value measured through the template method in the same final state [36]. Fitting the same way to the observables in the four-jet final state provides an estimate of σ_{eff} for this channel.

3.1 Double-parton scattering in W+dijet production

To study the dependence of the DPS-sensitive observables on MPI parameters, we construct two W+dijet DPS tunes, starting from the parameters of PYTHIA8 Tune 4C. In a partial tune only the parameter of the exponential distribution `expPow` is varied, and in a full tune all four parameters in Table 6 are varied. In a comparison of models with W+dijet events [36], it was shown that higher-order SPS contributions (not present in PYTHIA) fill a similar region of phase-space as the DPS signal. When such higher-order SPS diagrams are neglected, the measured DPS contribution to the W+dijet channel can be overestimated (i.e. σ_{eff} underestimated). We therefore interface the LO matrix elements (ME) generated by MADGRAPH 5 (version 1.5.14) [38] with PYTHIA8, and tune to the normalized distributions of the correlation observables in Eqs. (5) and (6). For this study, we produce MADGRAPH parton-level events with a W boson and up to four partons in the final state. The cross section is calculated using the CTEQ6L1 PDF with a matching scale for ME and parton shower (PS) jets set to 20 GeV. (In Section 4, we show that the CMS UE tunes can be interfaced to higher-order ME generators without additional tuning of MPI parameters). Figure 6 shows the CMS data [36] for the observables ΔS and $\Delta^{\text{rel}} p_T$ measured in W+dijet production, compared to predictions from MADGRAPH interfaced to PYTHIA8 Tune 4C, to Tune 4C with no MPI, to the partial CDPSTP8S1-Wj, as well as to the full CDPSTP8S2-Wj (CDPST stands for ‘‘CMS DPS tune’’). Table 6 gives the best-fit parameters and the resulting σ_{eff} values at $\sqrt{s} = 7$ TeV. The uncertainties quoted for σ_{eff} are computed from the uncertainties of the fitted parameters given by the eigentunes. For

Tune 4C, the uncertainty in σ_{eff} is not provided since no eigentunes are available for that tune. The resulting values of σ_{eff} are compatible with the value measured by CMS using the template method of $\sigma_{\text{eff}} = 20.6 \pm 0.8 \text{ (stat)} \pm 6.6 \text{ (syst)} \text{ mb}$ [36].

Table 6: The PYTHIA8 parameters, tuning ranges, Tune 4C values [28] and best-fit values of CDPSTP8S1-Wj and CDPSTP8S2-Wj, obtained from fits to DPS observables in W+dijet production with the MADGRAPH event generator interfaced to PYTHIA8. Also shown are the predicted values of σ_{eff} at $\sqrt{s} = 7 \text{ TeV}$, and the uncertainties obtained from the eigentunes.

PYTHIA8 Parameter	Tuning Range	Tune 4C	CDPSTP8S1-Wj	CDPSTP8S2-Wj
PDF		CTEQ6L1	CTEQ6L1	CTEQ6L1
MultipartonInteractions:pT0Ref [GeV]	1.0–3.0	2.085	2.085*	2.501
MultipartonInteractions:ecmPow	0.0–0.4	0.19	0.19*	0.179
MultipartonInteractions:expPow	0.4–10.0	2.0	1.523	1.120
ColourReconnection:range	0.0–9.0	1.5	1.5*	2.586
MultipartonInteractions:ecmRef [GeV]	—	1800	1800*	1800*
χ^2/dof	—	—	0.118	0.09
Predicted σ_{eff} (in mb)	—	30.3	$25.9^{+2.4}_{-2.9}$	$25.8^{+8.2}_{-4.2}$

* Fixed at Tune 4C value.

3.2 Double-parton scattering in four-jet production

Starting from the parameters of PYTHIA8 Tune 4C, we construct two different four-jet DPS tunes. As in the W+dijet channel, in the partial tune just the exponential-dependence parameter, `expPow`, while in the full tune all four parameters of Table 7 are varied. We obtain a good fit to the four-jet data without including higher-order ME contributions. However, we also obtain a good fit when higher-order (real) ME terms are generated with MADGRAPH. In Fig. 7 and 8 the correlation observables ΔS and $\Delta^{\text{rel}} p_T$ in four-jet production [37] are compared to predictions obtained with PYTHIA8 Tune 4C, Tune 4C without MPI, CDPSTP8S1-4j, CDPSTP8S2-4j, and MADGRAPH interfaced to CDPSTP8S2-4j. Table 7 gives the best-fit parameters and the resulting σ_{eff} values. The values of σ_{eff} extracted from the CMS PYTHIA8 DPS tunes give the first determination of σ_{eff} in four-jet production at $\sqrt{s} = 7 \text{ TeV}$. The uncertainties quoted for σ_{eff} are obtained from the eigentunes.

4 Validation of CMS tunes

Here we discuss the compatibility of the UE and DPS tunes. In addition, we compare the CMS UE tunes with UE data that have not been used in the fits, and we examine how well Drell–Yan and MB observables can be predicted from MC simulations using the UE tunes. We also show that the CMS UE tunes can be interfaced to higher-order ME generators without additional tuning of the MPI parameters.

4.1 Compatibility of UE and DPS tunes

The values of σ_{eff} obtained from simulations applying the CMS PYTHIA8 UE and DPS tunes at $\sqrt{s} = 7 \text{ TeV}$ and $\sqrt{s} = 13 \text{ TeV}$ are listed in Table 8. The uncertainties, obtained from eigentunes are also quoted in Table 8. At $\sqrt{s} = 7 \text{ TeV}$, the CMS DPS tunes give values of $\sigma_{\text{eff}} \approx 20 \text{ mb}$, while the CMS PYTHIA8 UE tunes give slightly higher values in the range 26–29 mb as shown in Figs. 8 and 9. Figure 8 shows the CMS DPS-sensitive data for four-jet production at

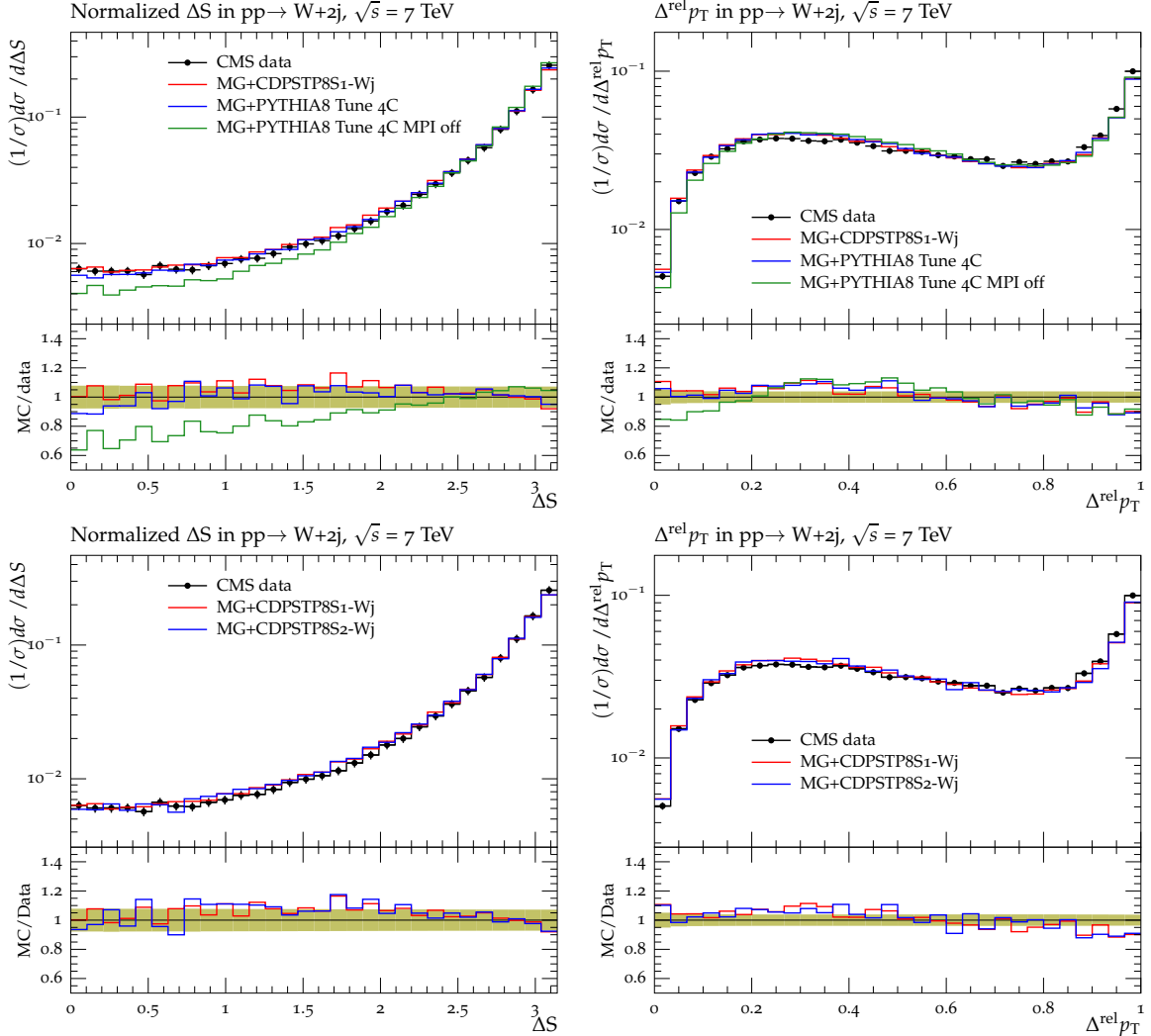


Figure 6: CMS data at $\sqrt{s} = 7 \text{ TeV}$ [36] for the normalized distributions of the correlation observables ΔS (left), and $\Delta^{\text{rel}} p_T$ (right) in the $W + \text{dijet}$ channel, compared to MADGRAPH (MG) interfaced to: PYTHIA8 Tune 4C, Tune 4C with no MPI, and the CMS PYTHIA8 DPS partial CDPSTP8S1-Wj (top); and CDPSTP8S1-Wj, and CDPSTP8S2-Wj (bottom). The bottom panels of each plot show the ratios of these tunes to the data, and the green bands around unity represent the total experimental uncertainty.

Table 7: The PYTHIA8 parameters, tuning ranges, Tune 4C values [28] and best-fit values of CDPSTP8S1-4j and CDPSTP8S2-4j, obtained from fits to DPS observables in four-jet production. Also shown are the predicted values of σ_{eff} at $\sqrt{s} = 7 \text{ TeV}$, and the uncertainties obtained from the eigentunes.

PYTHIA8 Parameter	Tuning Range	Tune 4C	CDPSTP8S1-4j	CDPSTP8S2-4j
PDF		CTEQ6L1	CTEQ6L1	CTEQ6L1
MultipartonInteractions:pT0Ref [GeV]	1.0–3.0	2.085	2.085*	2.125
MultipartonInteractions:ecmPow	0.0–0.4	0.19	0.19*	0.179
MultipartonInteractions:expPow	0.4–10.0	2.0	1.160	0.692
ColourReconnection:range	0.0–9.0	1.5	1.5*	6.526
MultipartonInteractions:ecmRef [GeV]	—	1800	1800*	1800*
χ^2/dof	—	—	0.751	0.428
Predicted σ_{eff} (in mb)	—	30.3	$21.3^{+1.2}_{-1.6}$	$19.0^{+4.7}_{-3.0}$

* Fixed at Tune 4C value.

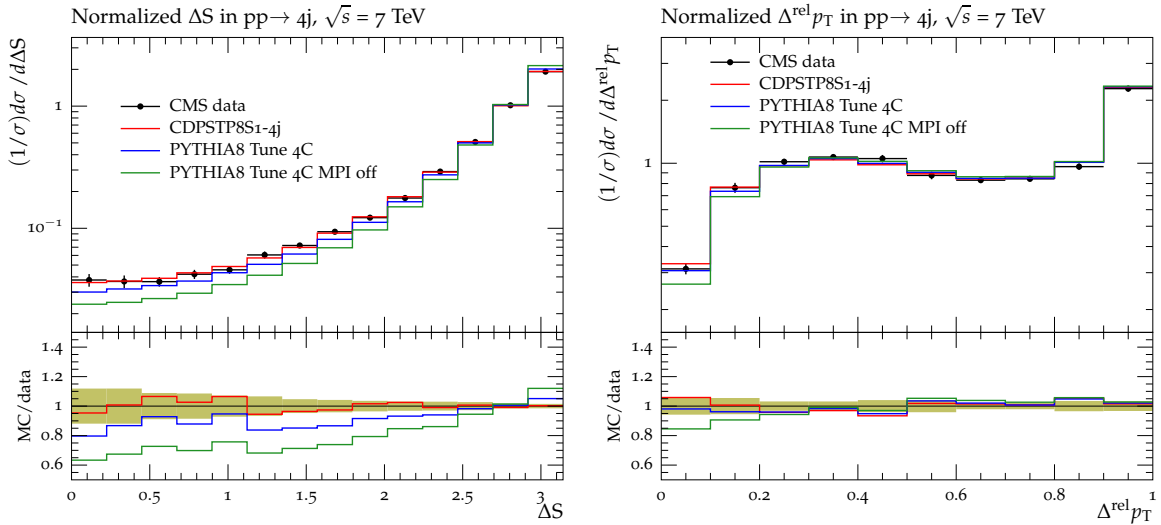


Figure 7: Distributions of the correlation observables ΔS (left) and $\Delta^{\text{rel}} p_T$ (right) measured in four-jet production at $\sqrt{s} = 7 \text{ TeV}$ [37] compared to PYTHIA8 Tune 4C, Tune 4C with no MPI, and CDPSTP8S1-4j. The bottom panels of each plot show the ratios of these predictions to the data, and the green bands around unity represent the total experimental uncertainty.

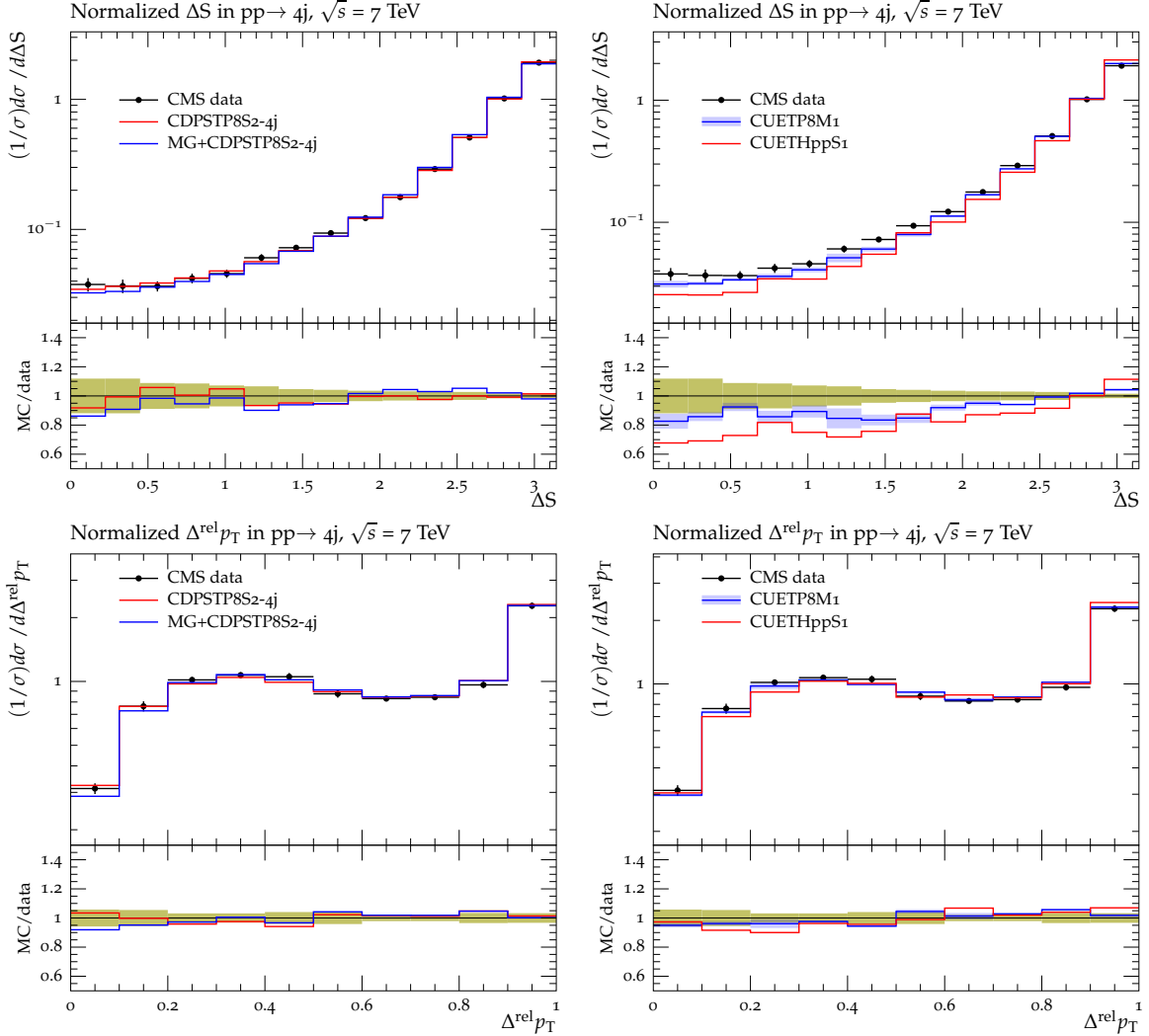


Figure 8: Distributions in the correlation observables ΔS (top) and $\Delta^{\text{rel}} p_T$ (bottom) measured in four-jet production at $\sqrt{s} = 7 \text{ TeV}$ [37], compared to predictions of PYTHIA8 using CDPSTP8S2-4j and of MADGRAPH (MG) interfaced to PYTHIA8 using CDPSTP8S2-4j (left) and PYTHIA8 using CUETP8M1 and HERWIG++ with CUETHppS1 (right). Also shown are the ratios of the predictions to the data. Predictions for CUETP8M1 (right) are shown with an error band corresponding to the total uncertainty obtained from the eigentunes (see Appendix A). The green bands around unity represent the total experimental uncertainty.

$\sqrt{s} = 7 \text{ TeV}$ compared to predictions using CDPSTP8S2-4j, CUETP8M1, and CUETHppS1. Figure 9 shows ATLAS UE data at $\sqrt{s} = 7 \text{ TeV}$ [39] compared to predictions obtained with various tunes: CDPSTP8S2-4j with uncertainty bands, CUETP8S1-CTEQ6L1, CUETP8S1-CTEQ6L1, CUETP8S1-HERAPDF1.5LO, CUETP8M1, and CUETHppS1. Predictions from PYTHIA8 using CUETP8M1 describe reasonably well the DPS observables, but do not fit them as well as predictions using the DPS tunes. On the other hand, predictions using CDPSTP8S2-4j do not fit the UE data as well as the UE tunes do.

Table 8: Values of σ_{eff} at $\sqrt{s} = 7 \text{ TeV}$ and 13 TeV for CUETP8S1-CTEQ6L1, CUETP8S1-HERAPDF1.5LO, and CUETP8M1, CUETHppS1, and for CDPSTP8S1-4j and CDPSTP8S2-4j. At $\sqrt{s} = 7 \text{ TeV}$, also shown are the uncertainties in σ_{eff} obtained from the eigentunes.

CMS Tune	$\sigma_{\text{eff}}(\text{mb})$ at 7 TeV	$\sigma_{\text{eff}}(\text{mb})$ at 13 TeV
CUETP8S1-CTEQ6L1	$27.8^{+1.2}_{-1.3}$	$29.9^{+1.6}_{-2.8}$
CUETP8S1-HERAPDF1.5LO	$29.1^{+2.2}_{-2.0}$	$31.0^{+3.8}_{-2.6}$
CUETP8M1	$26.0^{+0.6}_{-0.2}$	$27.9^{+0.7}_{-0.4}$
CUETHppS1	$15.2^{+0.5}_{-0.6}$	$15.2^{+0.5}_{-0.6}$
CDPSTP8S1-4j	$21.3^{+1.2}_{-1.6}$	$21.8^{+1.0}_{-0.7}$
CDPSTP8S2-4j	$19.0^{+4.7}_{-3.0}$	$22.7^{+10.0}_{-5.2}$

As discussed previously, the PYTHIA8 tunes use a single exponential matter-overlap function, while the HERWIG++ tune uses a matter-overlap function that is related to the Fourier transform of the electromagnetic form factor. The CUETHppS1 gives a value of $\sigma_{\text{eff}} \approx 15 \text{ mb}$, while UE and DPS tunes give higher values of σ_{eff} . It should be noted that σ_{eff} is a parton-level observable and its importance is not in the modeled value of σ_{eff} , but in what is learned about the transverse proton profile (and its energy evolution), and how well the models describe the DPS-sensitive observables. As can be seen in Fig. 8, predictions using CUETP8M1 describe the DPS-sensitive observables better than CUETHppS1, but not quite as well as the DPS tunes. We performed a simultaneous PYTHIA8 tune that included both the UE data and DPS-sensitive observables, however, the quality of the resulting fit was poor. This confirms the difficulty of describing soft and hard MPI within the current PYTHIA and HERWIG++ frameworks. Recent studies [40, 41] suggest the need for introducing parton correlation effects in the MPI framework in order to achieve a consistent description of both the UE and DPS observables.

4.2 Comparisons with other UE measurements

Figure 10 shows charged particle and p_T^{sum} densities [24, 42] at $\sqrt{s} = 0.9, 2.76$, and 7 TeV with $p_T > 0.5 \text{ GeV}$ and $|\eta| < 2.0$ in the TransAVE region, as defined by the leading jet reconstructed by using just the charged particles (also called “leading track-jet”) compared to predictions using the CMS UE tunes. The CMS UE tunes describe quite well the UE measured using the leading charged particle as well as the leading charged-particle jet.

Tunes obtained from fits to UE data and combined with higher-order ME calculations [43] can also be cross-checked against the data. The CMS UE tunes can be interfaced to higher-order ME generators without spoiling their good description of the UE. In Fig. 11, the charged-particle and p_T^{sum} densities in the TransMIN and TransMAX regions as a function of p_T^{max} , are compared to predictions obtained with MADGRAPH and POWHEG [44, 45] interfaced to PYTHIA8 using CUETP8S1-CTEQ6L1 and CUETP8M1. In MADGRAPH, up to four partons are simulated in the final state. The cross section is calculated with the CTEQ6L1 PDF. The ME/PS matching scale is taken to be 10 GeV . The POWHEG predictions are based on next-to-leading-order (NLO)

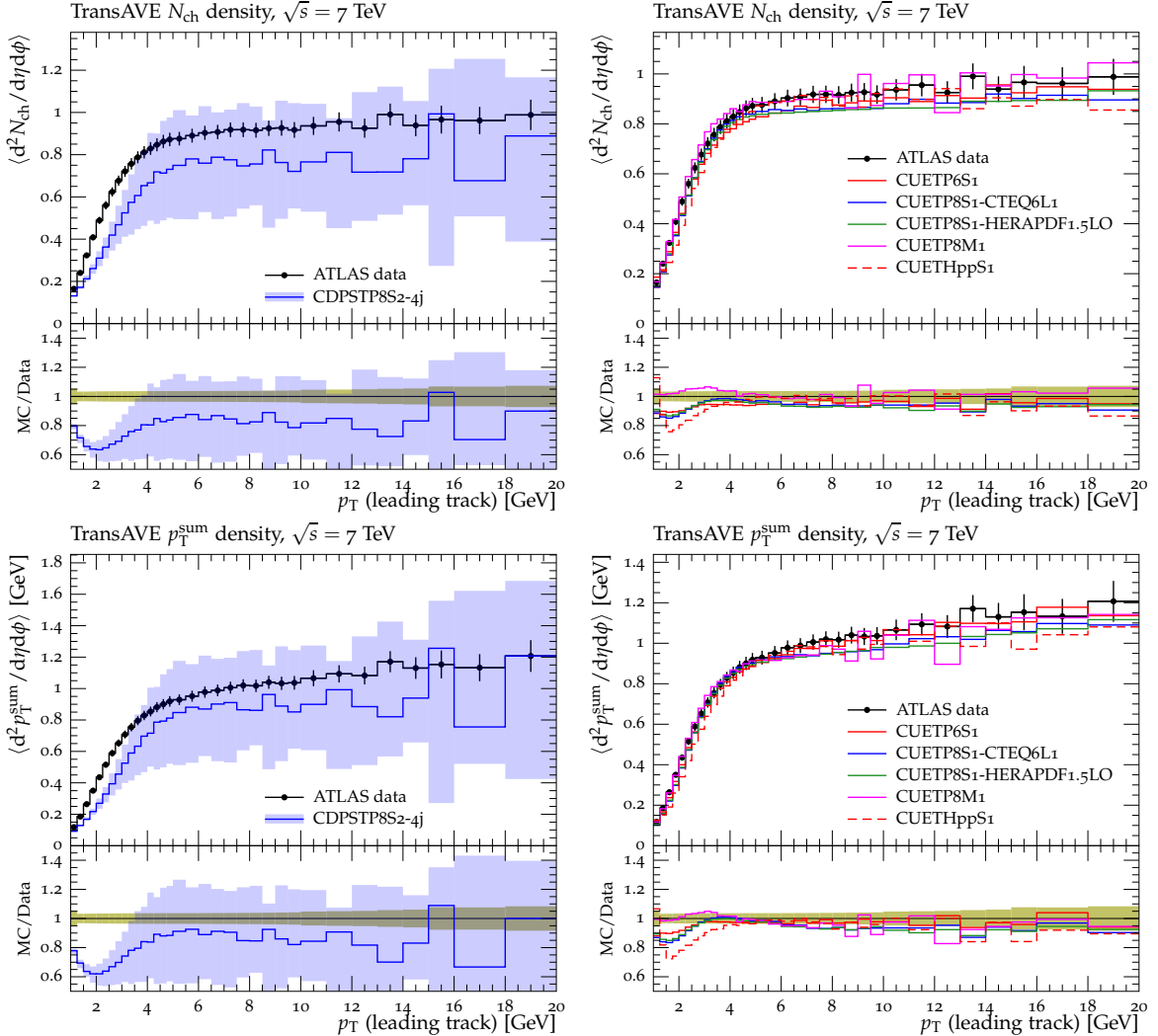


Figure 9: ATLAS data at $\sqrt{s} = 7 \text{ TeV}$ [39] for charged-particle (left) and p_T^{sum} densities (right) with $p_T > 0.5 \text{ GeV}$ and $|\eta| < 2.0$ in the transverse (TransAVE) region compared to predictions of PYTHIA8 using CDPSTP8S2-4j (left) and CUETP8S1-CTEQ6L1, CUETP8S1-HERAPDF1.5LO, and CUETP8M1, plus HERWIG++ using CUETHppS1 (right). The predictions of CDPSTP8S2-4j are shown with an error band corresponding to the total uncertainty obtained from the eigen-tunes (see Appendix A). The bottom panels of each plot show the ratios of these predictions to the data, and the green bands around unity represent the total experimental uncertainty.

dijet using the CT10nlo PDF [46] interfaced to PYTHIA8 based on CUETP8M1, and HERA-PDF1.5NLO [21] interfaced to the PYTHIA8 using CUETP8S1-HERAPDF1.5LO.

The poor agreement below $p_T^{\max} = 5 \text{ GeV}$ in Fig. 11 is not relevant as the minimum \hat{p}_T for MADGRAPH and POWHEG is 5 GeV. The agreement with the UE data in the plateau region of $p_T^{\max} > 5 \text{ GeV}$ is good. All these figures show that CMS UE tunes interfaced to higher-order ME generators do not spoil their good description of the UE data.

4.3 Predicting MB observables

The UE is studied in events containing a hard scatter, whereas most of the MB collisions are softer and can include diffractive scatterings. It is however interesting to see how well predictions based on the CMS UE tunes can describe the properties of MB distributions. Figure 12 shows predictions using CMS UE tunes for the ALICE [47] and TOTEM data [48] at $\sqrt{s} = 7 \text{ TeV}$ for the charged-particle pseudorapidity distribution, $dN_{\text{ch}}/d\eta$, and for $dE/d\eta$ [49] at $\sqrt{s} = 7 \text{ TeV}$. These observables are sensitive to SD, CD, and DD, which are modeled in PYTHIA. Since HERWIG++ does not include a model for SD, CD, and DD, we do not show it here. Figure 13 shows predictions using the CMS UE tunes for the combined CMS+TOTEM data at $\sqrt{s} = 8 \text{ TeV}$ [50] for the charged-particle pseudorapidity distribution, $dN_{\text{ch}}/d\eta$, for inelastic, NSD-enhanced, and SD-enhanced proton-proton collisions.

The PYTHIA8 event generator using the UE tunes describes the MB data better than PYTHIA6 with the UE tune, which is likely due to the improved modeling of SD, CD, and DD in PYTHIA8. Predictions with all the UE tunes describe fairly well MB observables in the central region ($|\eta| < 2$), however, only predictions obtained with CUETP8M1 describe the data in the forward region ($|\eta| > 4$). This is due to the PDF used in CUETP8M1. As can be seen in Fig. 14, the NNPDF2.3LO PDF at scales $Q^2 = 10 \text{ GeV}^2$ (corresponding to hard scatterings with $\hat{p}_T \sim 3 \text{ GeV}$) and small x , features a larger gluon density than in CTEQ6L1 and HERAPDF1.5LO, thereby contributing to more particles (and more energy) produced in the forward region. We have checked that increasing the gluon distribution in HERAPDF1.5LO at values below 10^{-5} improved the description of the charged-particle multiplicity measurements in the forward region.

4.4 Comparisons with inclusive jet production

In Fig. 15 predictions using CUETP8S1-CTEQ6L1, CUETP8S1-HERAPDF1.5LO, and CUETP8M1, and CUETHppS1 are compared to inclusive jet cross section at $\sqrt{s} = 7 \text{ TeV}$ [51] in several rapidity ranges. Predictions using CUETP8M1 describe the data best, however, all the tunes overshoot the jet spectra at small p_T . Predictions from the CUETHppS1 underestimate the high p_T region at central rapidity ($|y| < 2.0$). In Fig. 16, the inclusive jet cross sections are compared to predictions from POWHEG interfaced to PYTHIA8 using CUETP8S1-HERAPDF1.5LO and CUETP8M1. A very good description of the measurement is obtained.

4.5 Comparisons with Z boson production

In Fig. 17 the p_T and rapidity distributions of the Z boson in pp collisions at $\sqrt{s} = 7 \text{ TeV}$ [52] are shown and compared to PYTHIA8 using CUETP8M1, and to POWHEG interfaced to PYTHIA8 using CUETP8S1-CTEQ6L1 and CUETP8M1. The prediction using PYTHIA8 with CUETP8M1 (without POWHEG) agrees reasonably well with the distribution of the Z boson at small p_T values. Also, when interfaced to POWHEG, which implements an inclusive Z boson NLO calculation, the agreement is good over the whole spectrum.

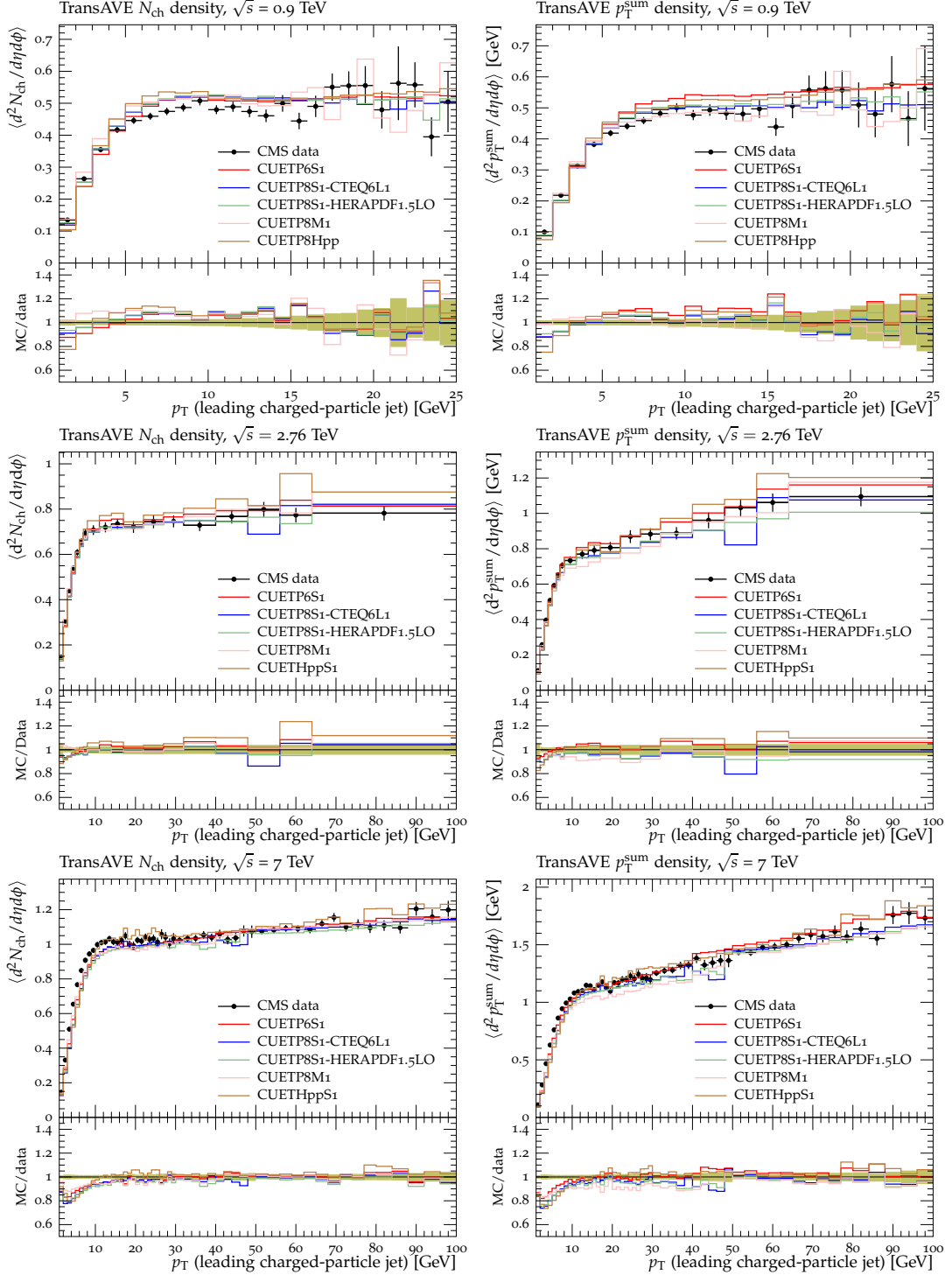


Figure 10: CMS data on charged-particle (left) and $p_{\text{T}}^{\text{sum}}$ (right) densities at $\sqrt{s} = 0.9$ [24] (top), 2.76 [42] (middle), and 7 TeV [24] (bottom) with $p_{\text{T}} > 0.5$ GeV and $|\eta| < 2.0$ in the transverse (TransAVE) region as defined by the leading charged-particle jet. The data are compared to predictions of PYTHIA6 using CUETP6S1-CTEQ6L1, PYTHIA8 using CUETP8S1-CTEQ6L1, CUETP8S1-HERAPDF1.5LO, and CUETP8M1, and HERWIG++ using CUETHppS1. The bottom panels of each plot show the ratios of these predictions to the data, and the green bands around unity represent the total experimental uncertainty.

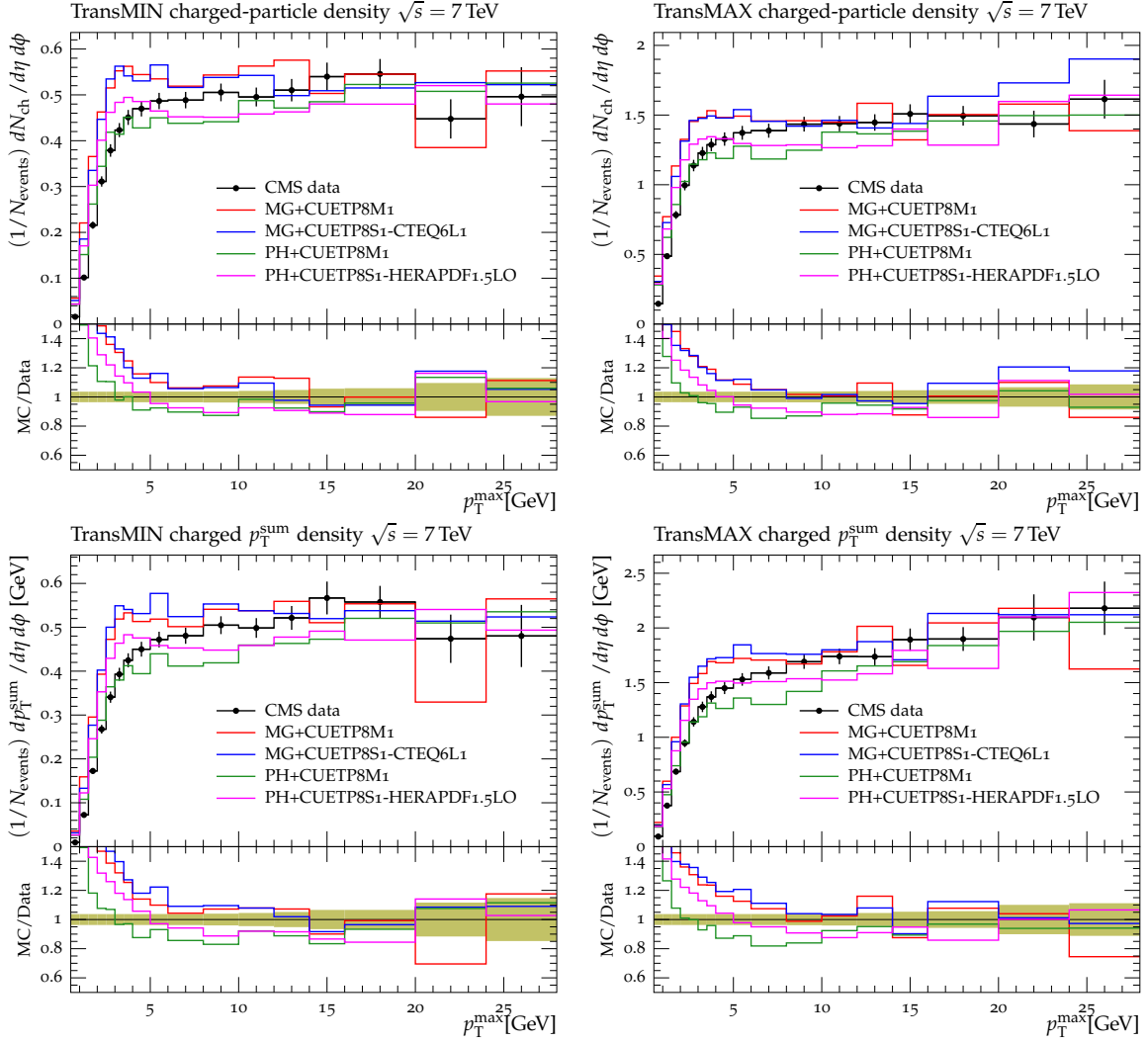


Figure 11: CMS data at $\sqrt{s} = 7 \text{ TeV}$ [17] for particle (top) and p_T^{sum} densities (bottom) for charged particles with $p_T > 0.5 \text{ GeV}$ and $|\eta| < 0.8$ in the TransMIN (left) and TransMAX (right) regions, as defined by the leading charged particle, as a function of the transverse momentum of the leading charged-particle p_T^{max} . The data are compared to MADGRAPH (MG), interfaced to PYTHIA8 using CUETP8S1-CTEQ6L1 and CUETP8M1, and to POWHEG (PH), interfaced to PYTHIA8 using CUETP8S1-HERAPDF1.5LO and CUETP8M1. The bottom panels of each plot show the ratios of these predictions to the data, and the green bands around unity represent the total experimental uncertainty.

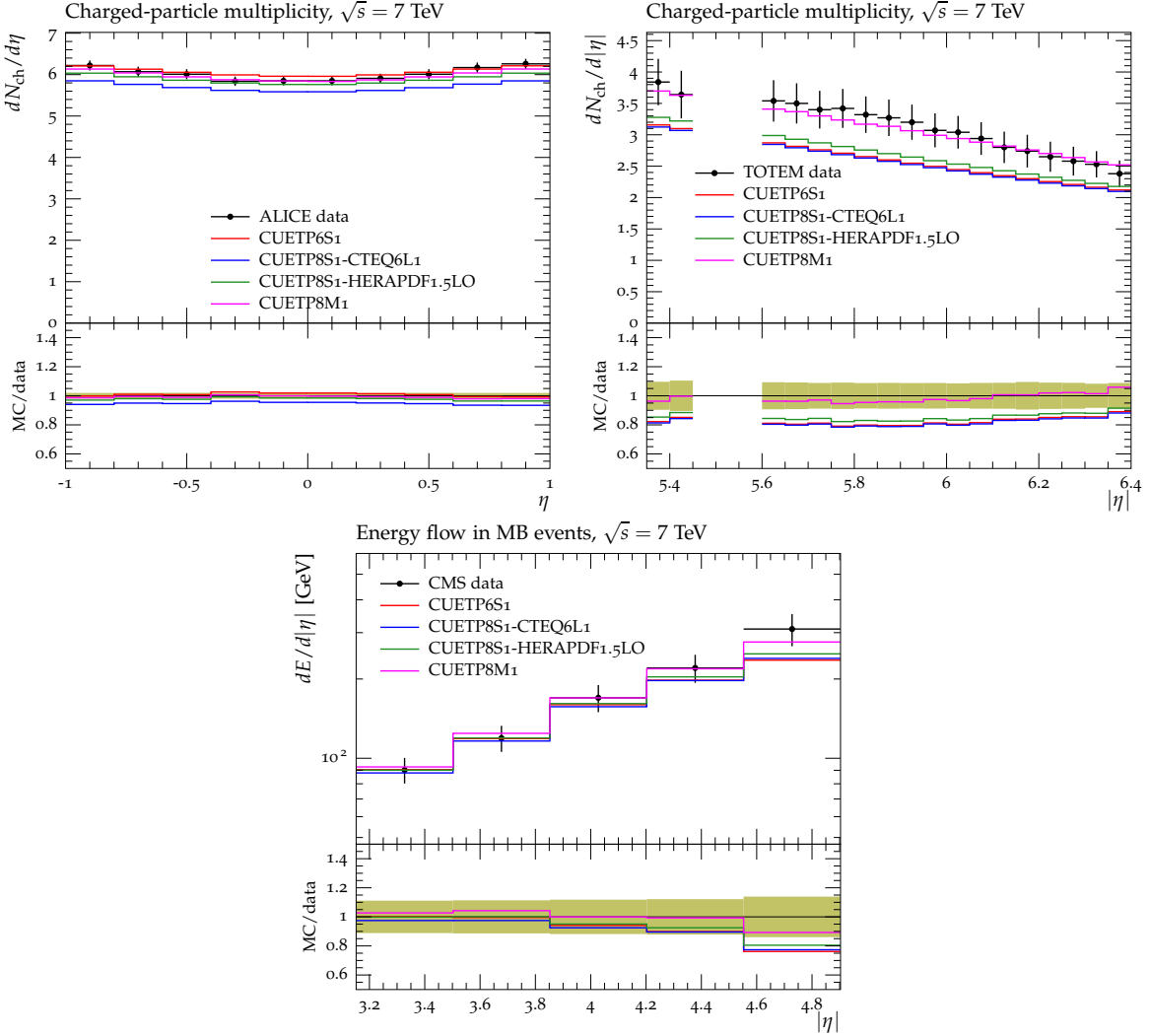


Figure 12: ALICE data at $\sqrt{s} = 7 \text{ TeV}$ [47] for the charged-particle pseudorapidity distribution, $dN_{\text{ch}}/d\eta$, in inclusive inelastic pp collisions (top left). TOTEM data at $\sqrt{s} = 7 \text{ TeV}$ [48] for the charged-particle pseudorapidity distribution, $dN_{\text{ch}}/d\eta$, in inclusive inelastic pp collisions ($p_T > 40 \text{ MeV}$, $N_{\text{chg}} \geq 1$) (top right). CMS data at $\sqrt{s} = 7 \text{ TeV}$ [50] for the energy flow $dE/d\eta$, in MB pp collisions. The data are compared to PYTHIA6 using CUETP6S1-CTEQ6L1, and to PYTHIA8 using CUETP8S1-CTEQ6L1, CUETP8S1-HERAPDF1.5LO, and CUETP8M1. The bottom panels of each plot show the ratios of these predictions to the data, and the green bands around unity represent the total experimental uncertainty.

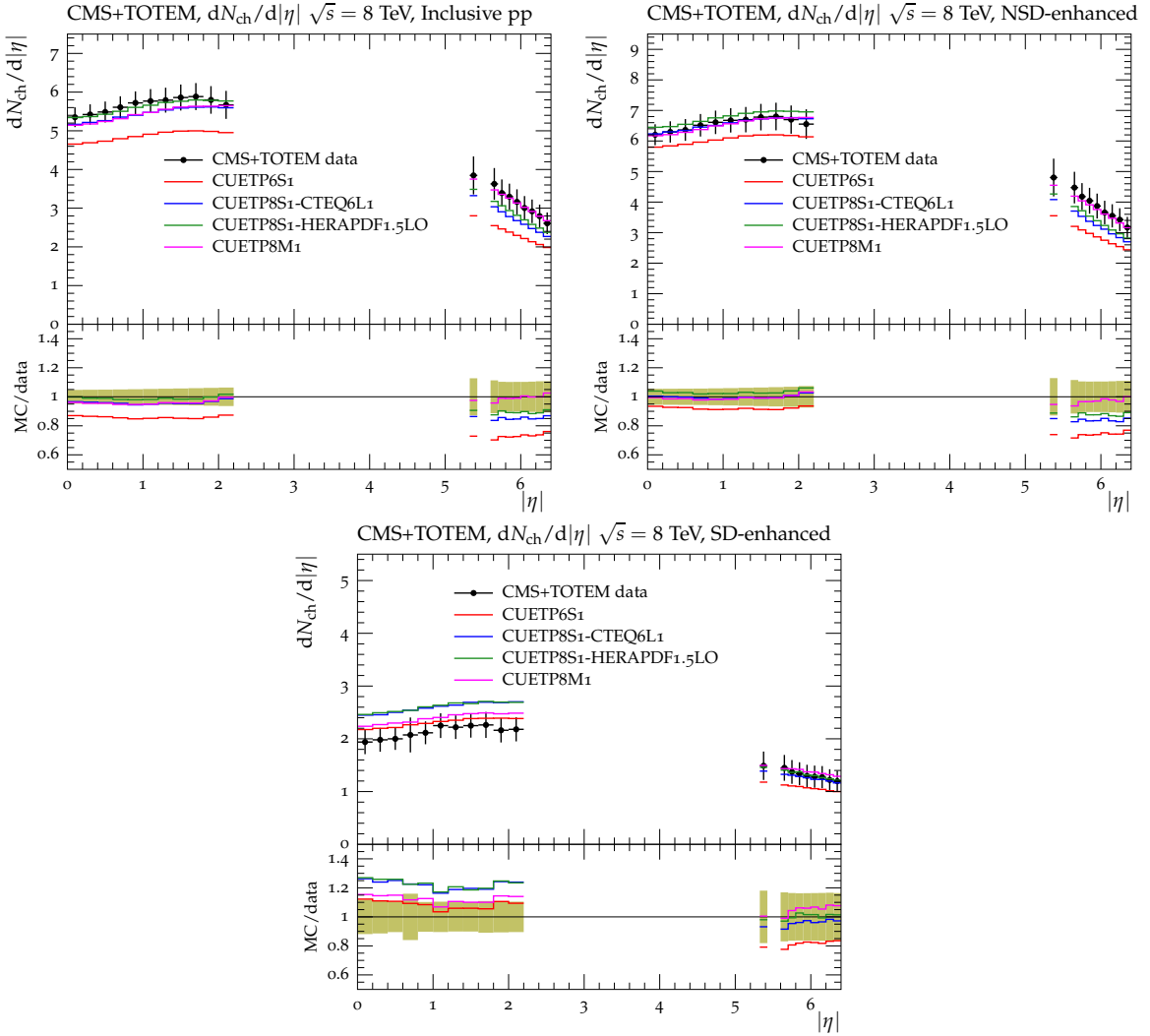


Figure 13: Combined CMS and TOTEM data at $\sqrt{s} = 8 \text{ TeV}$ [50] for the charged-particle distribution $dN_{ch}/d\eta$, in inclusive inelastic (top left), NSD-enhanced (top right), and SD-enhanced (bottom) pp collisions. The data are compared to PYTHIA6 using CUETP6S1-CTEQ6L1, and to PYTHIA8 using CUETP8S1-CTEQ6L1, CUETP8S1-HERAPDF1.5LO, and CUETP8M1. The bottom panels of each plot show the ratios of these predictions to the data, and the green bands around unity represent the total experimental uncertainty.

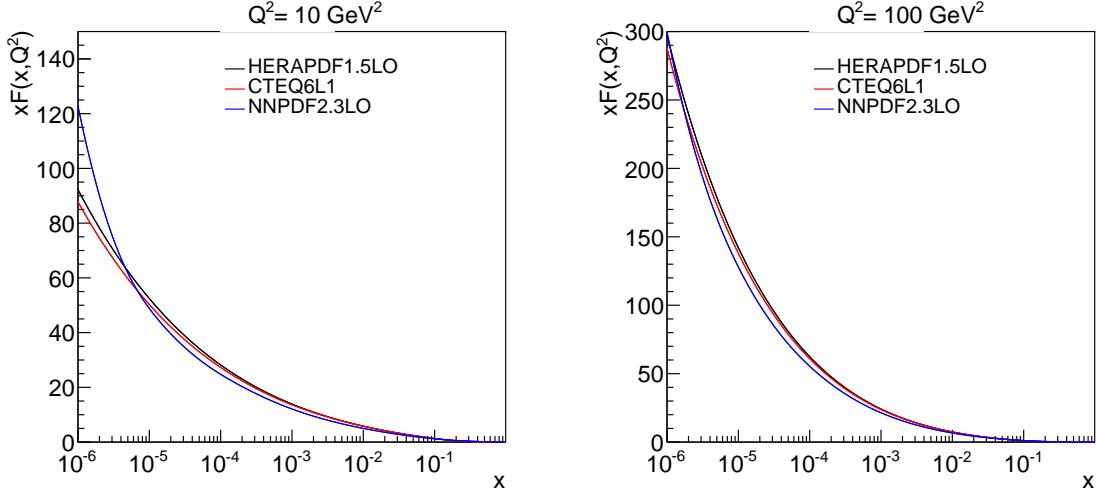


Figure 14: Comparison of gluon distributions in the proton for the CTEQ6L1, HERAPDF1.5LO, and NNPDF2.3LO PDF sets, at the $Q^2 = 10 \text{ GeV}^2$ (left) and 100 GeV^2 (right).

In Fig. 18 the charged-particle and p_T^{sum} densities [26] in the toward, away, and transverse (TransAVE) regions as defined by the Z boson in proton-proton collisions at $\sqrt{s} = 7 \text{ TeV}$ are compared to predictions of PYTHIA8 using CUETP8M1. Also shown are MADGRAPH and POWHEG results interfaced to PYTHIA8 using CUETP8S1-HERAPDF1.5LO and CUETP8M1. The MADGRAPH generator simulates Drell-Yan events with up to four partons, using the CTEQ6L1 PDF. The matching of ME partons and PS is performed at a scale of 20 GeV. The POWHEG events are obtained using NLO inclusive Drell-Yan production, including up to one additional parton. The POWHEG events are interfaced to PYTHIA8 using CUETP8M1 and CUETP8S1-HERAPDF1.5LO. The predictions based on CUETP8M1 do not fit the Z boson data unless they are interfaced to a higher-order ME generator. In PYTHIA8 only the Born term ($q\bar{q} \rightarrow Z$), corrected for single-parton emission, is generated. This ME configuration agrees well with the observables in the away region in data, when the Z boson recoils against one or more jets. In the transverse and toward regions, larger discrepancies between data and PYTHIA8 predictions appear at high p_T , where the occurrence of multijet emission has a large impact. To describe Z boson production at $\sqrt{s} = 7 \text{ TeV}$ in all regions, higher-order contributions (starting with Z+2-jets), as used in interfacing PYTHIA to POWHEG or MADGRAPH, must be included.

5 Extrapolation to 13 TeV

In this section, predictions at $\sqrt{s} = 13 \text{ TeV}$, based on the new tunes, for observables sensitive to the UE are presented. Figure 19 shows the predictions at 13 TeV for the charged-particle and the p_T^{sum} densities in the TransMIN, TransMAX, and TransDIF regions, as defined by the leading charged particle as a function of p_T^{max} based on the five new CMS UE tunes: CUETP6S1-CTEQ6L1, CUETP8S1-CTEQ6L1, CUETP8S1-HERAPDF1.5LO, CUETP8M1, and CUETHppS1. In Fig. 19 the ratio of the predictions using the four CMS tunes to the one using CUETP8M1 is shown. The predictions at 13 TeV of all these tunes are remarkably similar. It does not seem to matter that the new CMS PYTHIA8 UE tunes do not fit very well to the $\sqrt{s} = 300 \text{ GeV}$ UE data. The new PYTHIA8 tunes give results at 13 TeV similar to the new CMS PYTHIA6 tune and the new CMS HERWIG++ tune. The uncertainties on the predictions based on the eigentunes do

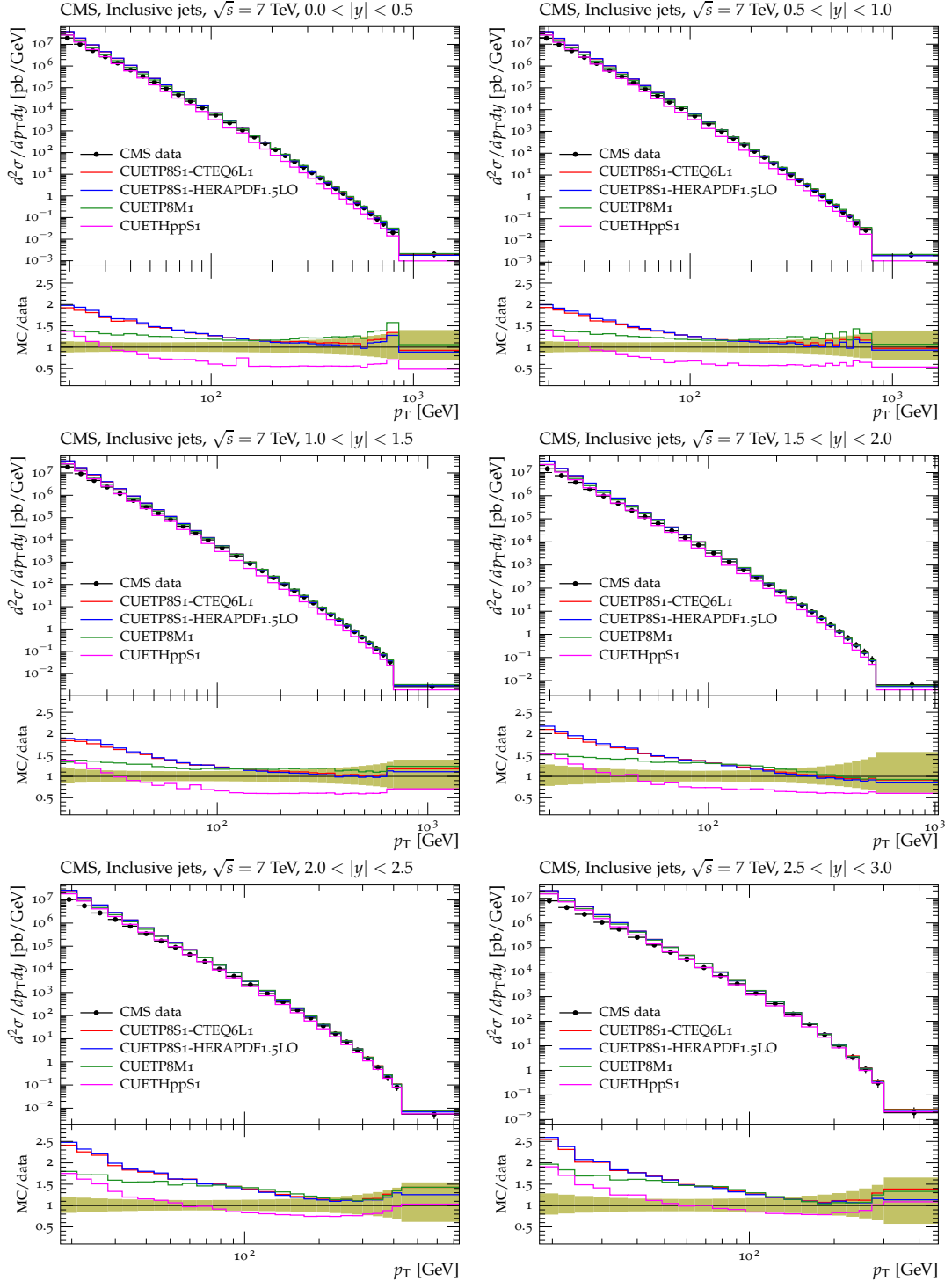


Figure 15: CMS data at $\sqrt{s} = 7$ TeV [51] for the inclusive jet cross section as a function of p_T in different rapidity ranges compared to predictions of PYTHIA8 using CUETP8S1-CTEQ6L1, CUETP8S1-HERAPDF, and CUETP8M1, and of HERWIG++ using CUETHppS1. The bottom panels of each plot show the ratios of these predictions to the data, and the green bands around unity represent the total experimental uncertainty.

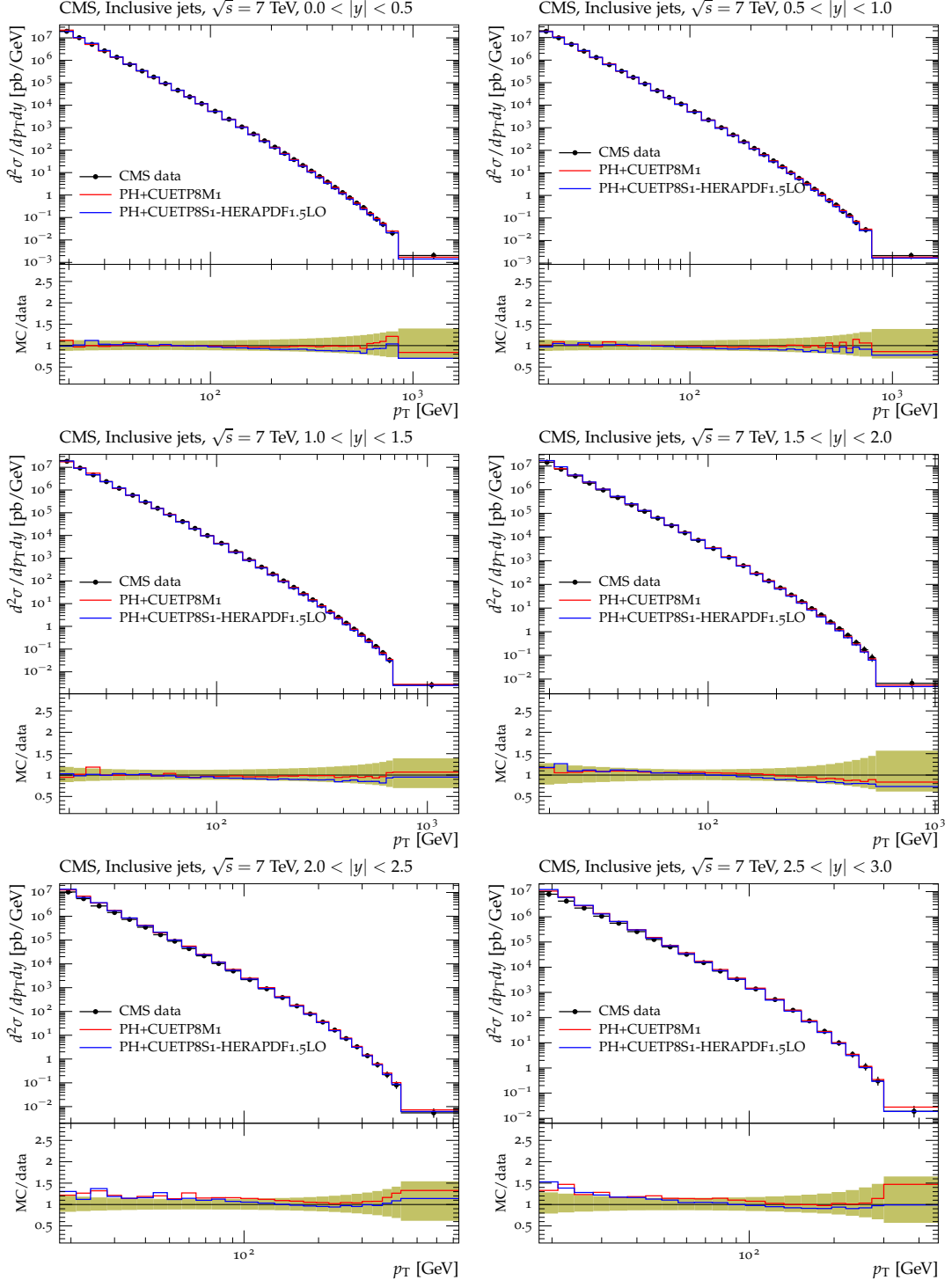


Figure 16: CMS data at $\sqrt{s} = 7$ TeV [51] for the inclusive jet cross section as a function of p_T in different rapidity ranges compared to predictions of POWHEG interfaced to PYTHIA8 using CUETP8S1-HERAPDF1.5LO and CUETP8M1. The bottom panels of each plot show the ratios of these predictions to the data, and the green bands around unity represent the total experimental uncertainty.

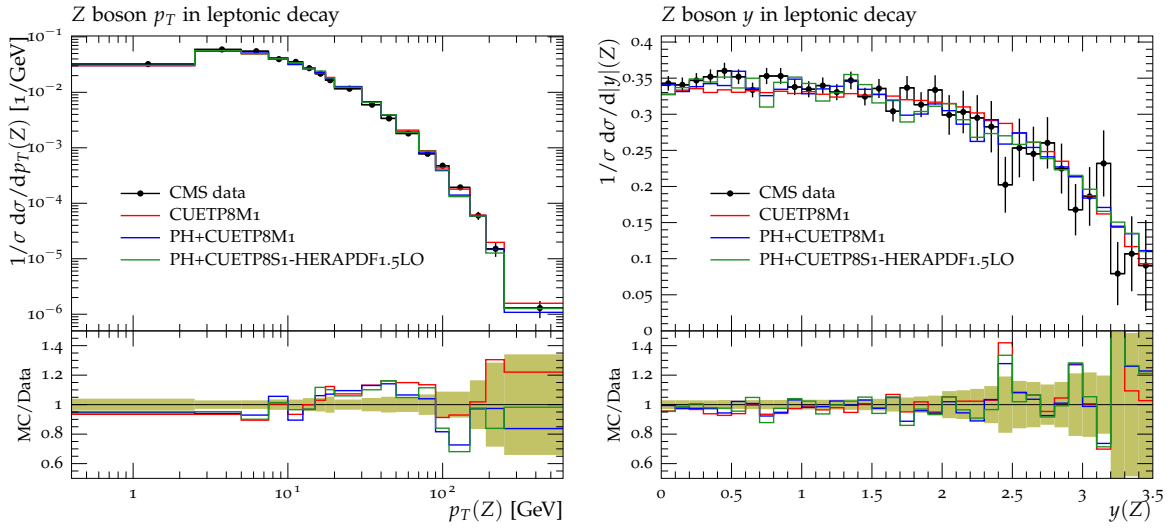


Figure 17: Transverse momentum p_T (left) and rapidity distributions (right) of Z boson production in pp collisions at $\sqrt{s} = 7$ TeV [52]. The data are compared to PYTHIA8 using CUETP8M1, and to POWHEG interfaced to PYTHIA8 using CUETP8S1-CTEQ6L1 and CUETP8M1. The green bands in the ratios represent the total experimental uncertainty.

not exceed 10% relative to the central value.

In Fig. 20 and 21 the predictions at $\sqrt{s} = 13$ TeV obtained using the new tunes from 7 TeV are shown for the charged-particle and the p_T^{sum} densities in the TransMIN, TransMAX, and TransDIF regions, defined as a function of p_T^{max} . Also shown is the ratio of 13 TeV to 7 TeV results for the five tunes. The TransMIN region increases much more rapidly with energy than the TransDIF region. For example, when using CUETP8M1, the charged-particle and the p_T^{sum} densities in the TransMIN region for $5.0 < p_T^{\text{max}} < 6.0$ GeV is predicted to increase by 28% and 37%, respectively, while the TransDIF region is predicted to increase by a factor of two less, i.e. by 13% and 18% respectively.

In Fig. 22, predictions obtained with PYTHIA8 using CUETP8S1-CTEQ6L1 and CUETP8M1, and Tune 4C are compared to the recent CMS data measured at $\sqrt{s} = 13$ TeV [53] on charged-particle multiplicity as a function of pseudorapidity. Predictions from CUETP8S1-CTEQ6L1 and CUETP8M1 are shown with the error bands corresponding to the uncertainties obtained from the eigentunes. These two new CMS tunes, although obtained from fits to UE data at 7 TeV, agree well with the MB measurements over the whole pseudorapidity range, while predictions from PYTHIA8 Tune 4C overestimate the data by about 10%. This confirms that the collision-energy dependence of the CMS UE tunes parameters can be trusted for predictions of MB observables.

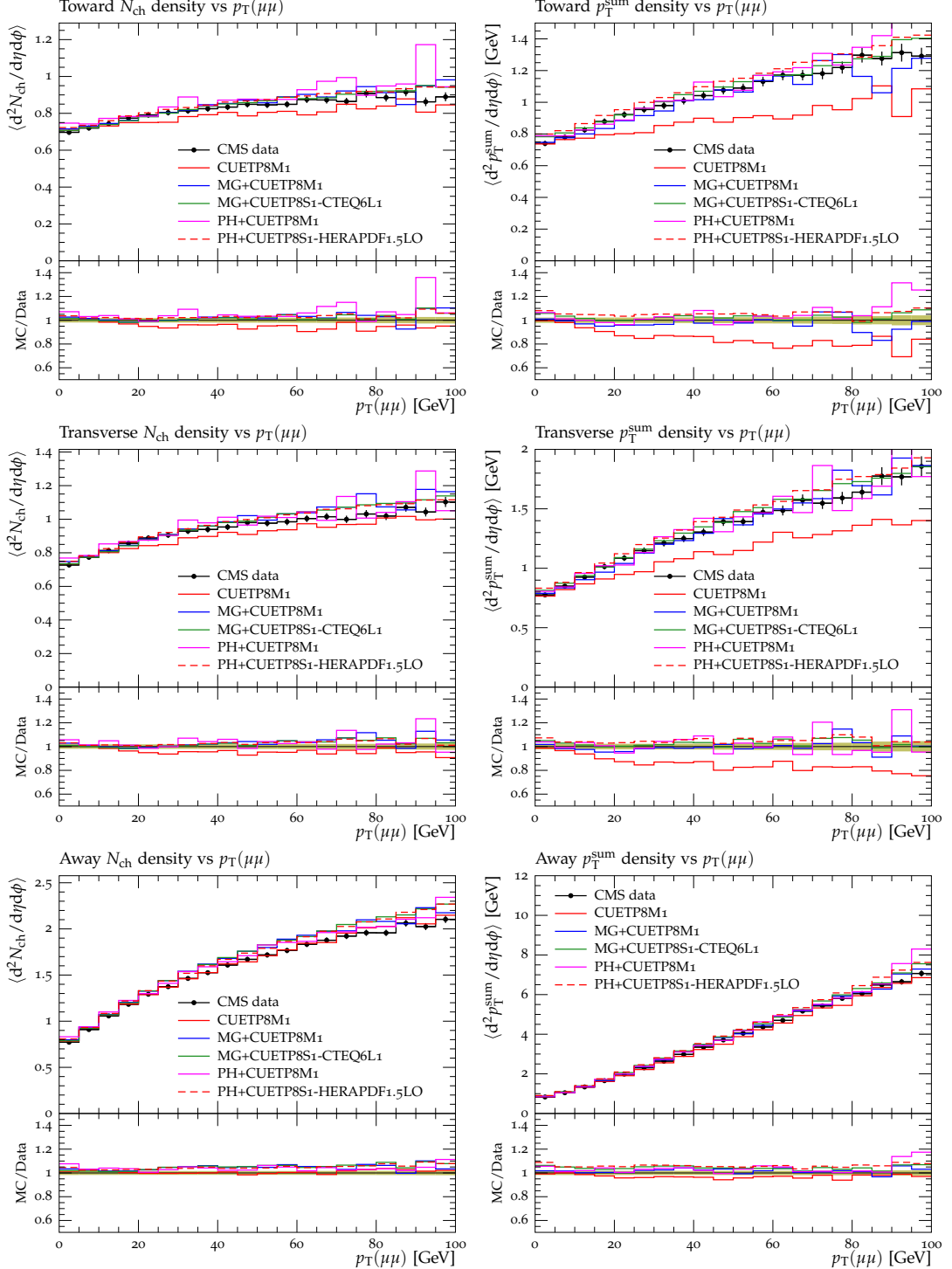


Figure 18: Charged-particle (left) and p_T^{sum} densities (right) in the toward (top), away (middle), and transverse (TransAVE) (bottom) regions, as defined by the Z-boson direction in Drell-Yan production at $\sqrt{s} = 7 \text{ TeV}$ [26]. The data are compared to PYTHIA8 using CUETP8M1, to MADGRAPH (MG) interfaced to PYTHIA8 using CUETP8S1-CTEQ6L1 and CUETP8M1, and to POWHEG (PH) interfaced to PYTHIA8 using CUETP8S1-HERAPDF1.5LO and CUETP8M1. The green bands in the ratios represent the total experimental uncertainty.

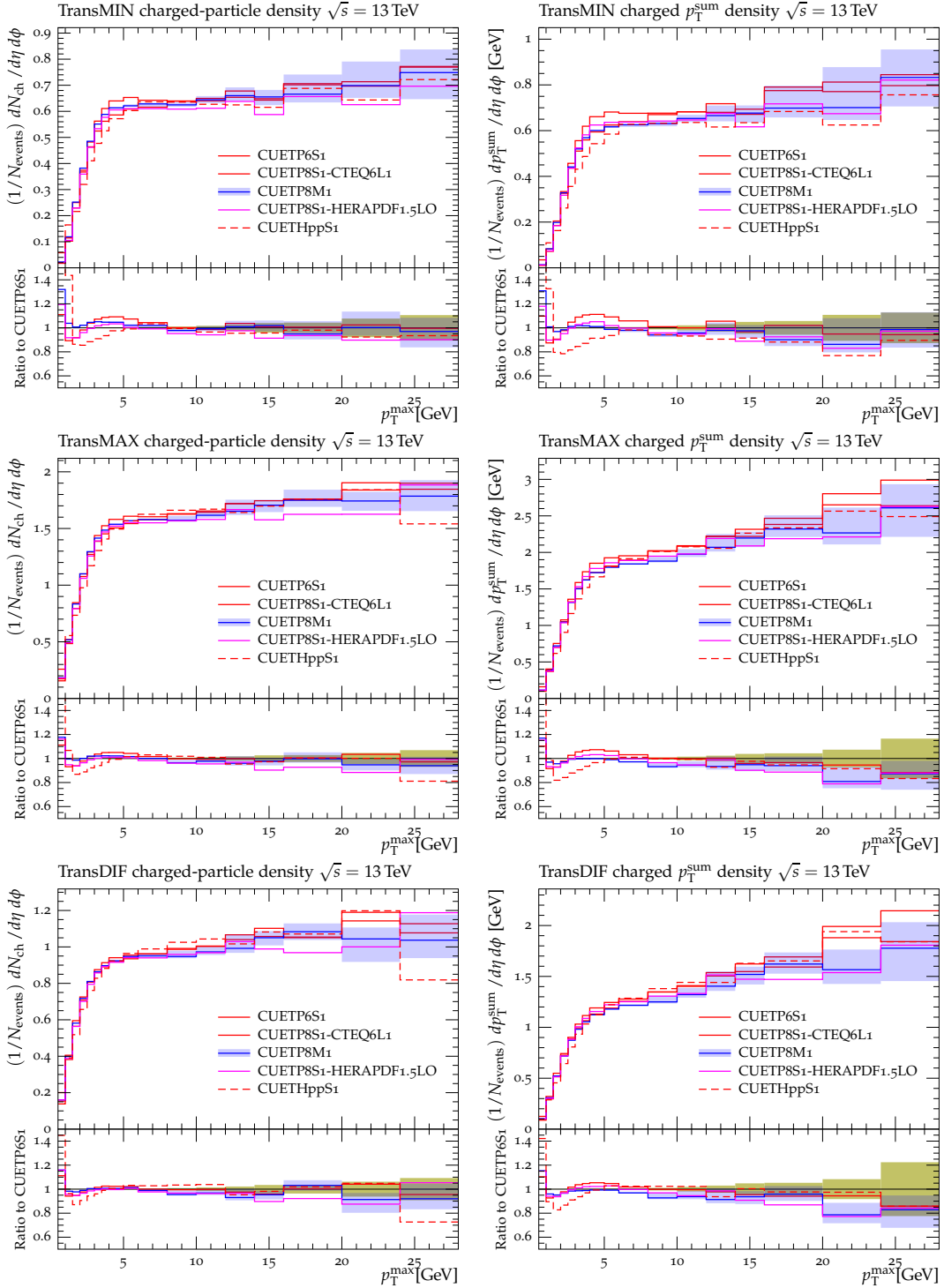


Figure 19: Predictions at $\sqrt{s} = 13$ TeV for the particle (left) and the p_T^{sum} densities (right) for charged particles with $p_T > 0.5$ GeV and $|\eta| < 0.8$ in the TransMIN (top), TransMAX (middle), and TransDIF (bottom) regions, as defined by the leading charged particle, as a function of the leading charged-particle p_T^{max} for the five CMS UE tunes: PYTHIA6 CUETP6S1-CTEQ6L1, and PYTHIA8 CUETP8S1-CTEQ6L1, CUETP8S1-HERAPDF1.5LO, and CUETP8M1, and HERWIG++ CUETHppS1. Also shown are the ratio of the tunes to predictions of CUETP8S1-CTEQ6L1. Predictions for CUETP8M1 are shown along with the envelope (green bands) of the corresponding eigenfunctions.

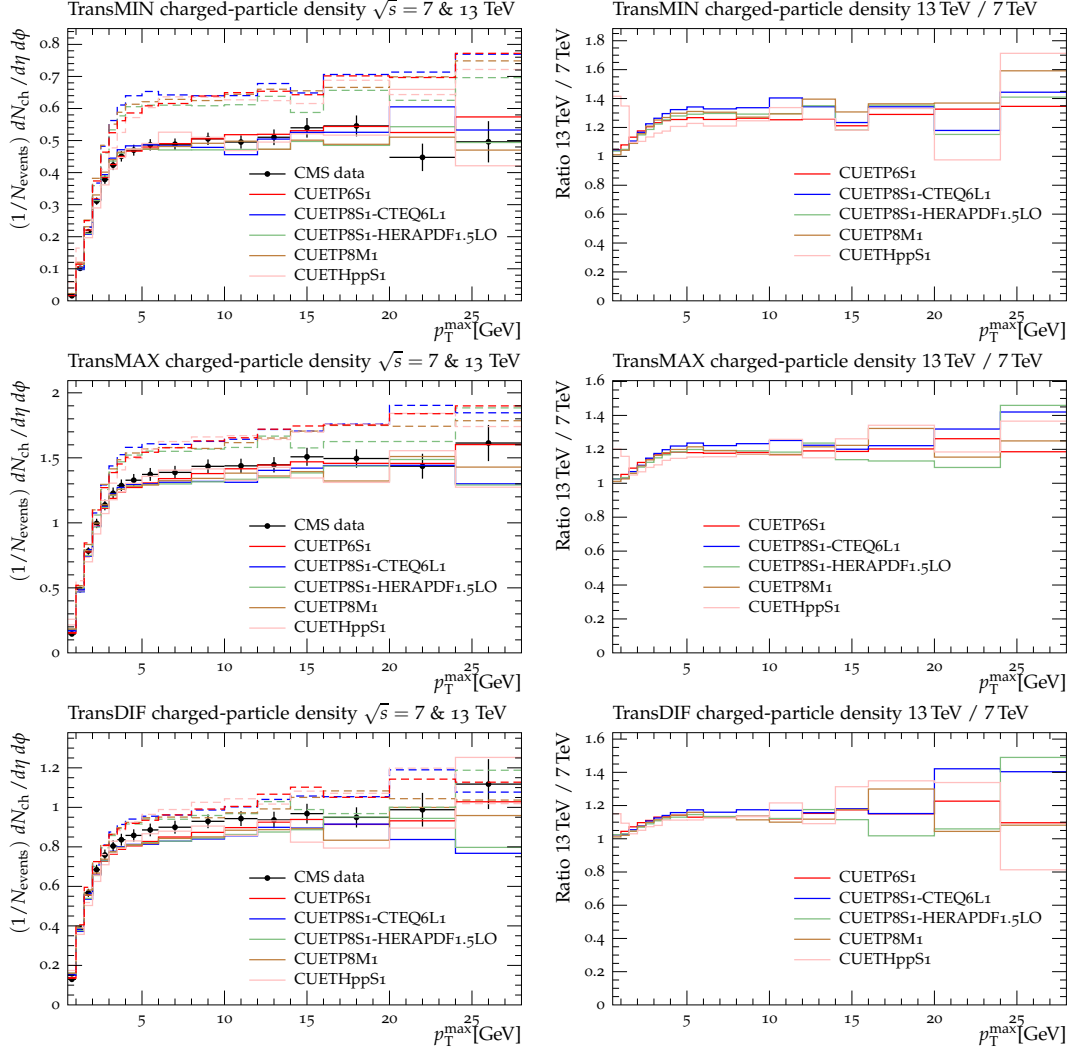


Figure 20: Charged-particle density at $\sqrt{s} = 7$ TeV for particles with $p_T > 0.5$ GeV and $|\eta| < 0.8$ in the TransMIN (top), TransMAX (middle), and TransDIF (bottom) regions, as defined by the leading charged particle, as a function of the leading charged-particle p_T^{\max} . The data are compared to PYTHIA6 using CUETP6S1-CTEQ6L1, to PYTHIA8 using CUETP8S1-CTEQ6L1, CUETP8S1-HERAPDF1.5LO, and CUETP8M1, and to HERWIG++ using CUETHppS1. Also shown are the predictions (left) based on the CMS UE tunes at 13 TeV (dashed lines), and the ratio of the 13 TeV to 7 TeV results for the five tunes (right).

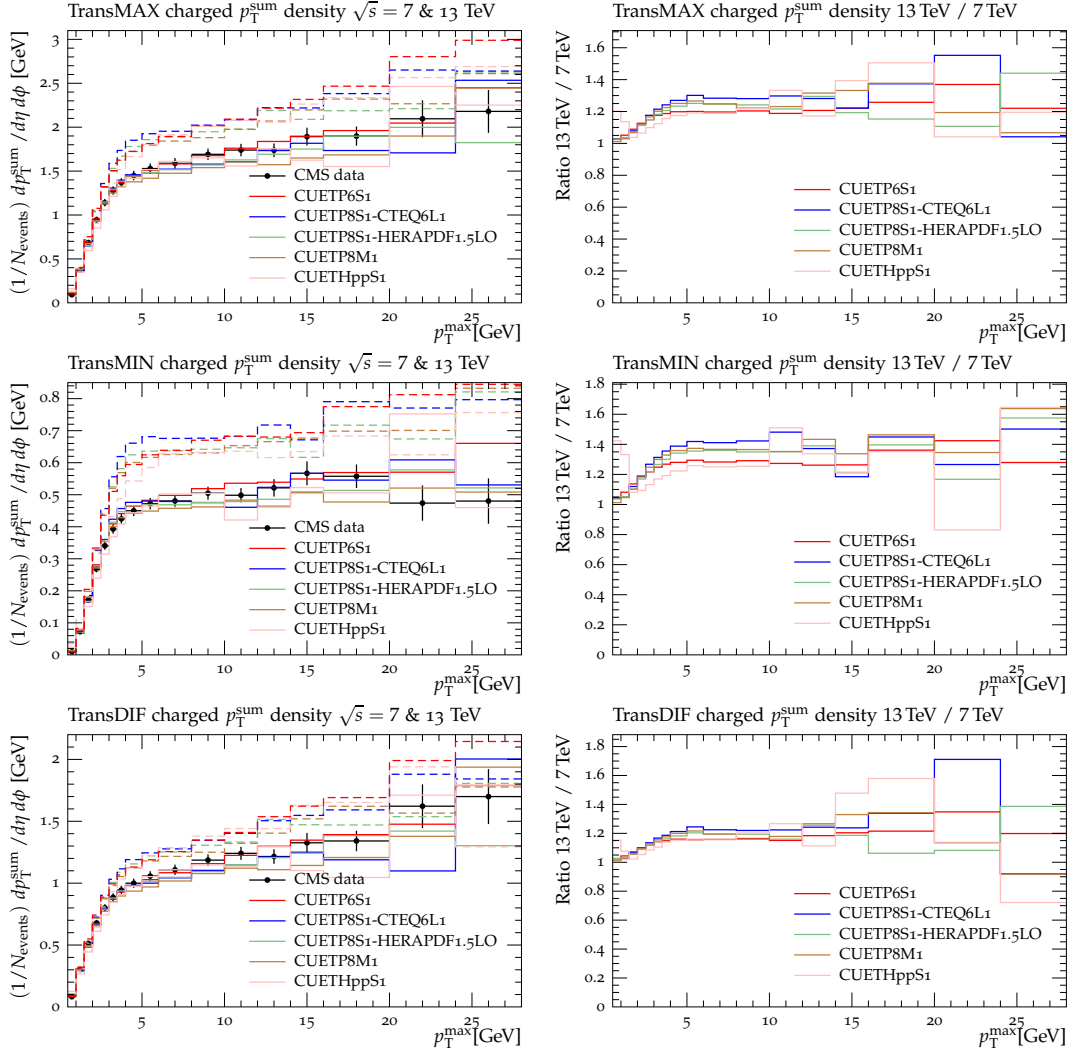


Figure 21: Charged p_T^{sum} density at $\sqrt{s} = 7 \text{ TeV}$ for particles with $p_T > 0.5 \text{ GeV}$ and $|\eta| < 0.8$ in the TransMIN (top), TransMAX (middle), and TransDIF (bottom) regions, as defined by the leading charged particle, as a function of the leading charged-particle p_T^{max} . The data are compared to PYTHIA6 using CUETP6S1-CTEQ6L1, to PYTHIA8 using CUETP8S1-CTEQ6L1, CUETP8S1-HERAPDF1.5LO, and CUETP8M1, and to HERWIG++ using CUETHppS1. Also shown are the predictions (left) based on the CMS UE tunes at 13 TeV (dashed lines), and the ratio of the 13 TeV to 7 TeV results for the five tunes (right).

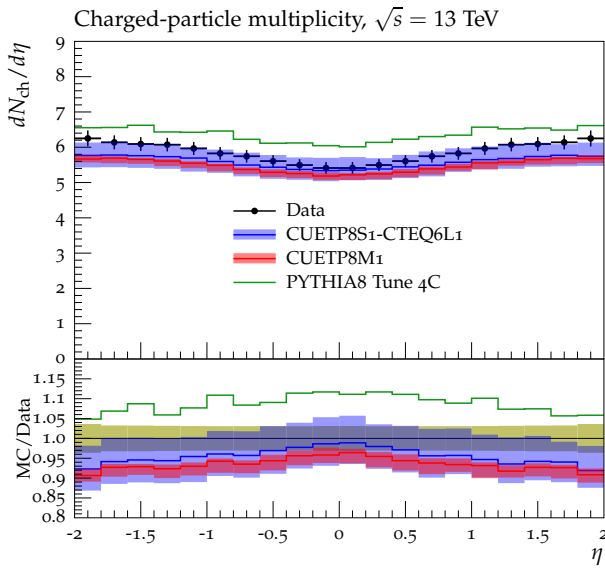


Figure 22: CMS data at $\sqrt{s} = 13 \text{ TeV}$ [53] for the charged-particle pseudorapidity distribution, $dN_{\text{ch}}/d\eta$, in inelastic proton-proton collisions. The data are compared to predictions of PYTHIA8 using CUETP8S1-CTEQ6L1, CUETP8M1, and Tune 4C. The predictions based on CUETP8S1-CTEQ6L1 and CUETP8M1 are shown with an error band corresponding to the total uncertainty obtained from the eigentunes. Also shown are the ratios of these predictions to the data. The green band represents the total experimental uncertainty on the data.

6 Summary and conclusions

We have constructed new tunes of the PYTHIA event generator using various sets of underlying-event (UE) data, for different parton distribution functions. By simultaneously fitting UE data at several center-of-mass energies, models for UE have been tested and their parameters constrained. The improvement in the description of UE data provided by the new CMS tunes at different collision energies gives confidence that they can provide reliable predictions at $\sqrt{s} = 13$ TeV, where all the new UE tunes predict similar results for the UE observables.

The observables sensitive to double-parton scattering (DPS) were fitted directly by tuning the MPI parameters. To study the dependence of the DPS-sensitive observables on the MPI parameters, two W+dijet DPS tunes and two four-jet DPS tunes were constructed. The CMS UE tunes perform fairly well in the description of DPS observables, but they do not fit the DPS data as well as the DPS tunes do. On the other hand, the CMS DPS tunes do not fit the UE data as well as the UE tunes. At present, we are not able to accurately describe both soft and hard MPI within the current PYTHIA and HERWIG++ frameworks. By fitting DPS-sensitive observables, we have also calculated the DPS effective cross section σ_{eff} associated to each model. This method can be applied to any final-state with two hard particles produced, in order to determine the σ_{eff} values associated to the different MPI models implemented in the current MC event generators.

Predictions of PYTHIA8 using the CMS UE tunes agree fairly well with the MB observables in the central region ($|\eta| < 2$) and can be interfaced to higher-order and multileg matrix-element generators, such as POWHEG and MADGRAPH, while maintaining their good description of the UE. It is not necessary to produce separate tunes for these generators. In addition, we have verified that the measured particle pseudorapidity density at 13 TeV is well reproduced by the new CMS UE Tunes. Furthermore, all of the new CMS tunes come with their eigentunes, which can be used to determine the uncertainties associated with the theoretical predictions. These new CMS tunes will play an important role in predicting and analyzing LHC data at 13 and 14 TeV.

A Tables of tune uncertainties

This section provides the values of the parameters corresponding to the eigentunes of the new CMS PYTHIA8 and the HERWIG++ tunes. A change in the χ^2 of the fit that equals the absolute χ^2 value obtained in the tune defines the eigentunes listed in Tables 9–12 for the new PYTHIA8 and the new HERWIG++ tunes. The different parameter values indicated refer to the deviation tunes along each of the maximally independent directions in the parameter space, obtained by using the covariance matrix in the region of the best tune. The number of directions defined in the parameter space equals the number of free parameters n used in the fit and results into $2n$ parameter variations, i.e. eigentunes. These variations represent a good set of systematic errors on the given tune.

Table 9: Eigentunes sets for CUETP8S1-CTEQ6L1.

PYTHIA8 Parameter	1-	1+	2-	2+	3-	3+	4-	4+
MultipartonInteractions:pT0Ref [GeV]	2.101	2.101	2.068	2.135	2.100	2.102	2.079	2.123
MultipartonInteractions:ecmPow	0.191	0.231	0.210	0.211	0.231	0.191	0.191	0.231
MultipartonInteractions:expPow	1.609	1.609	1.602	1.616	1.613	1.605	1.714	1.503
ColourReconnection:range	3.030	3.609	3.313	3.313	3.311	3.314	3.314	3.311

Table 10: Eigentunes sets for CUETP8S1-HERAPDF.

PYTHIA8 Parameter	1-	1+	2-	2+	3-	3+	4-	4+
MultipartonInteractions:pT0Ref [GeV]	2.000	2.000	1.960	2.043	1.999	2.001	1.968	2.030
MultipartonInteractions:ecmPow	0.275	0.226	0.250	0.250	0.226	0.275	0.274	0.227
MultipartonInteractions:expPow	1.691	1.690	1.681	1.700	1.695	1.686	1.831	1.559
ColourReconnection:range	6.224	5.972	6.096	6.096	6.101	6.091	6.091	6.101

Table 11: Eigentunes sets for CUETP8M1.

PYTHIA8 Parameter	1-	1+	2-	2+
MultipartonInteractions:pT0Ref [GeV]	2.403	2.402	2.400	2.405
MultipartonInteractions:ecmPow	0.253	0.251	0.253	0.252

B Comparisons of PYTHIA6 UE tunes to data

Figures 23–26 show the CDF data at $\sqrt{s} = 0.3, 0.9$, and 1.96 TeV , and the CMS data at $\sqrt{s} = 7\text{ TeV}$ on charged-particle and p_T^{sum} densities in the TransMIN and TransMAX regions, as a function of the transverse momentum of the leading charged-particle p_T^{max} . The distributions are compared to predictions obtained with PYTHIA6 Tune Z2*lep and the two new CUETP6S1-CTEQ6L1 and CUETP6S1-HERAPDF1.5LO. The new CMS PYTHIA6 tunes are able to describe the measurements better than Tune Z2*lep, in both the rising and the plateau regions of the spectra.

C Comparisons to HERWIG++ UE tunes to data

Figures 27–30 show the CDF data at $\sqrt{s} = 0.3, 0.9$, and 1.96 TeV , and the CMS data at $\sqrt{s} = 7\text{ TeV}$ on the charged-particle and p_T^{sum} densities in the TransMIN and TransMAX regions as a function of p_T^{max} , and compared with predictions obtained with the HERWIG++ Tune UE-EE-5C and the new CUETHppS1. These two HERWIG++ tunes are very similar and adequately describe the UE data at all four energies.

D Additional comparisons at 13 TeV

In this section, a supplementary collection of comparisons among predictions of the new tunes are shown for DPS and MB observables at 13 TeV.

D.1 DPS predictions at 13 TeV

In Fig. 31, the predictions for the DPS-sensitive observables at 13 TeV are shown for the three CMS PYTHIA8 UE tunes: CUETP8S1-CTEQ6L1, CUETP8S1-HERAPDF1.5LO, and CUETP8M1,

Table 12: Eigentunes sets for CUETHppS1.

HERWIG++ Parameter	1-	1+	2-	2+	3-	3+	4-	4+
MPIHandler:InvRadius	2.290	2.227	2.318	2.196	2.272	2.237	2.254	2.256
RemnantDecayer:colourDisrupt	0.396	0.811	0.634	0.623	0.632	0.625	0.596	0.666
MPIHandler:Power	0.396	0.351	0.331	0.408	0.399	0.342	0.361	0.381
ColourReconnector:ReconnectionProbability	0.615	0.460	0.529	0.527	0.523	0.533	0.444	0.626

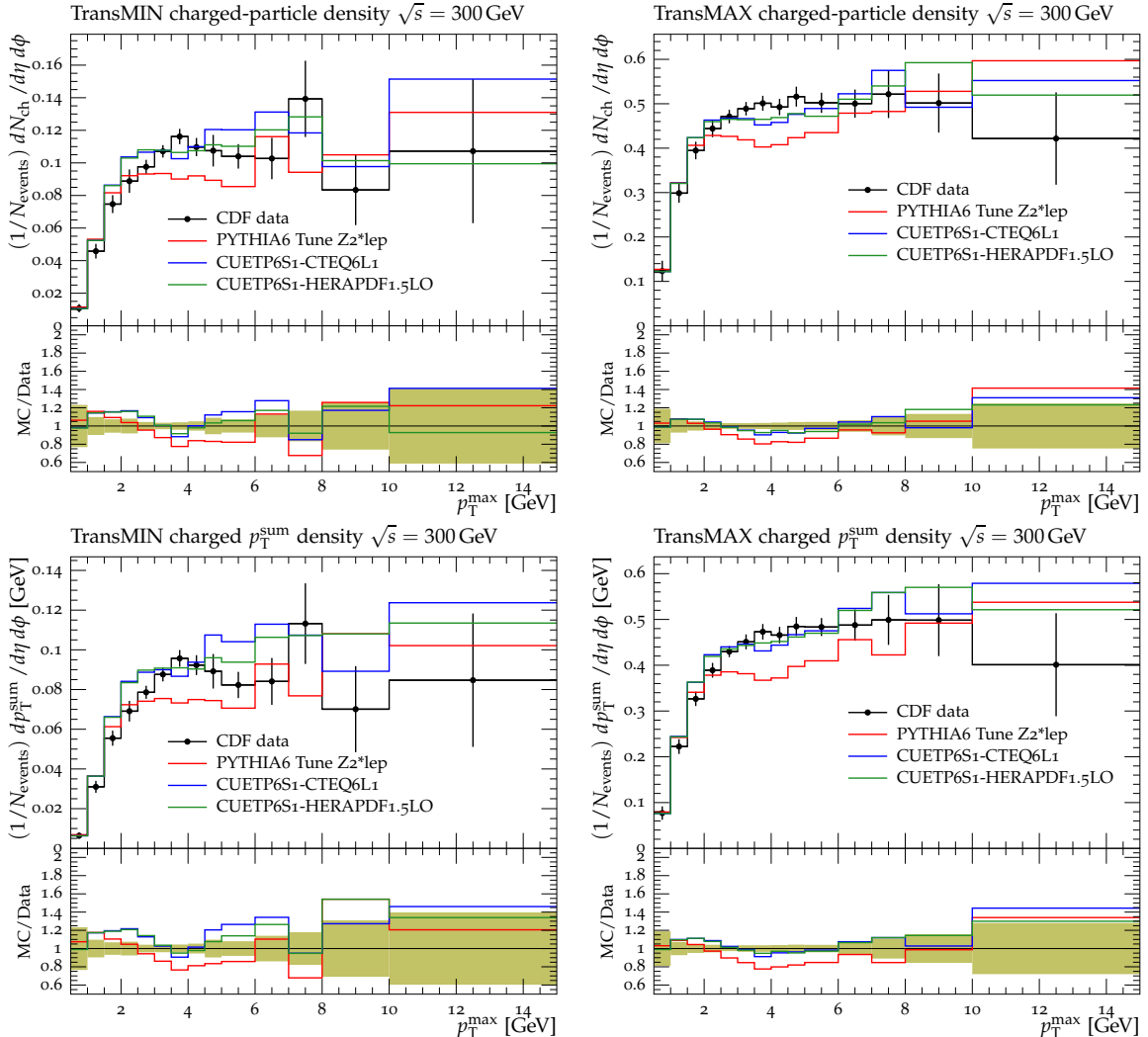


Figure 23: CDF data at $\sqrt{s} = 300 \text{ GeV}$ [11] on the particle (top) and p_T^{sum} densities (bottom) for charged particles with $p_T > 0.5 \text{ GeV}$ and $|\eta| < 0.8$ in the TransMIN (left) and TransMAX (right) regions as defined by the leading charged particle, as a function of the transverse momentum of the leading charged-particle p_T^{max} . The data are compared to the PYTHIA6 Tune Z2*lep, CUETP6S1-CTEQ6L1 and CUETP6S1-HERAPDF1.5LO. The green bands in the ratios represent the total experimental uncertainties.

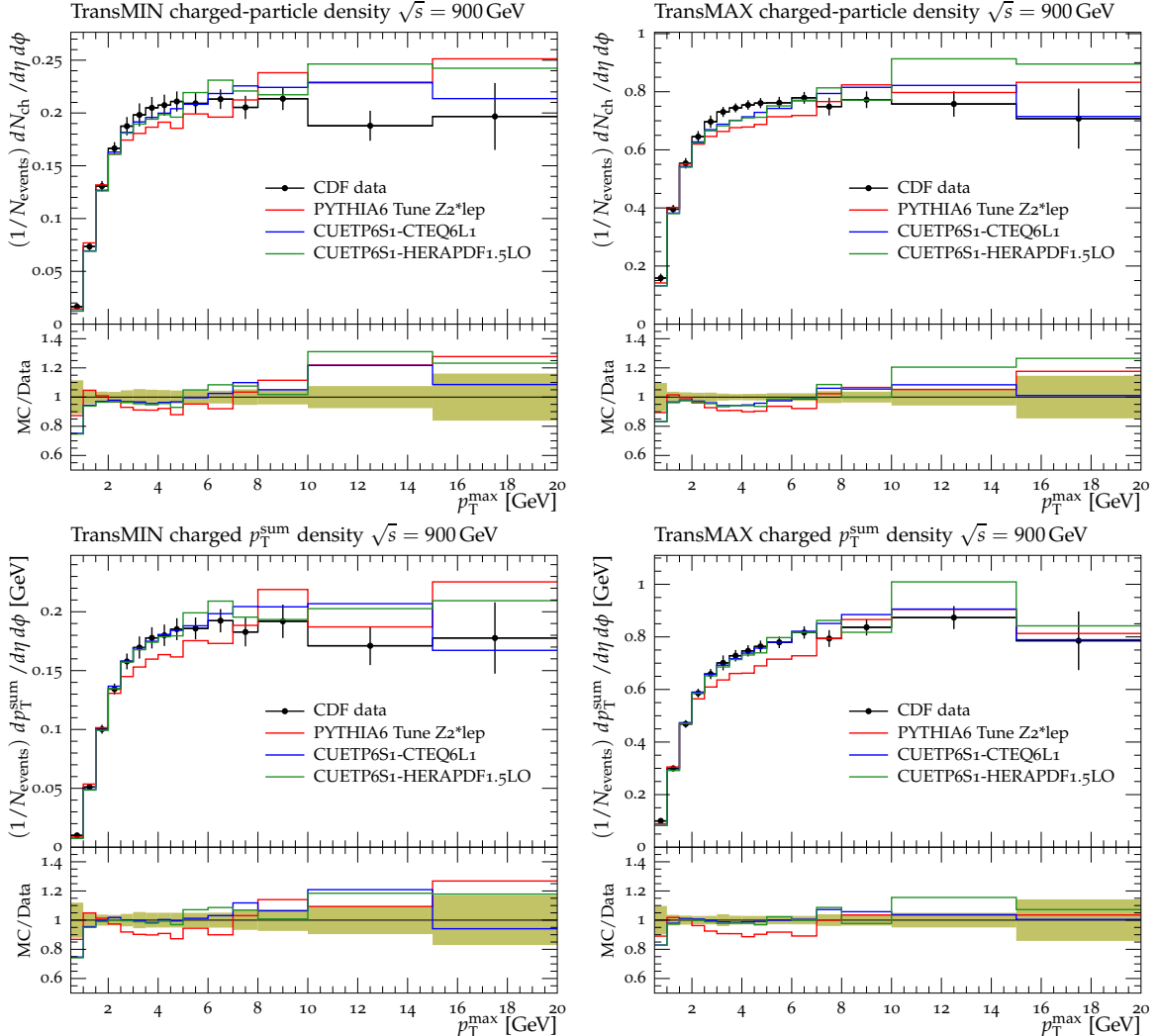


Figure 24: CDF data at $\sqrt{s} = 900 \text{ GeV}$ [11] on the particle (top) and p_T^{sum} densities (bottom) for charged particles with $p_T > 0.5 \text{ GeV}$ and $|\eta| < 0.8$ in the TransMIN (left) and TransMAX (right) regions as defined by the leading charged particle, as a function of the transverse momentum of the leading-charged particle p_T^{\max} . The data are compared to the PYTHIA6 Tune Z2*lep, CUETP6S1-CTEQ6L1 and CUETP6S1-HERAPDF1.5LO. The green bands in the ratios represent the total experimental uncertainties.

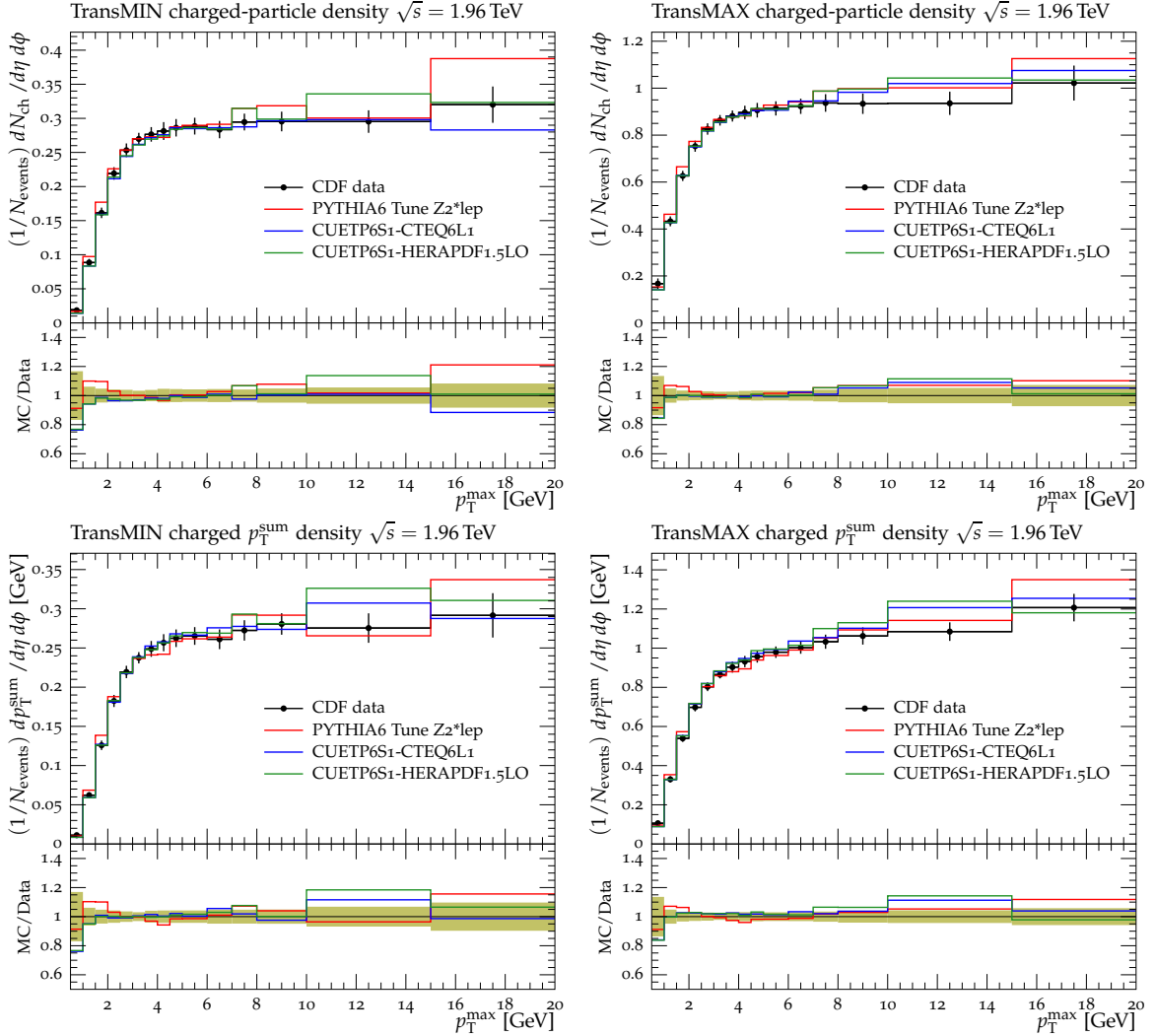


Figure 25: CDF data at $\sqrt{s} = 1.96$ TeV [11] on the particle (top) and p_T^{sum} densities (bottom) for charged particles with $p_T > 0.5$ GeV and $|\eta| < 0.8$ in the TransMIN (left) and TransMAX (right) regions as defined by the leading charged particle, as a function of the transverse momentum of the leading charged-particle p_T^{max} . The data are compared to the PYTHIA6 Tune Z2*lep, CUETP6S1-CTEQ6L1 and CUETP6S1-HERAPDF1.5LO. The green bands in the ratios represent the total experimental uncertainties.

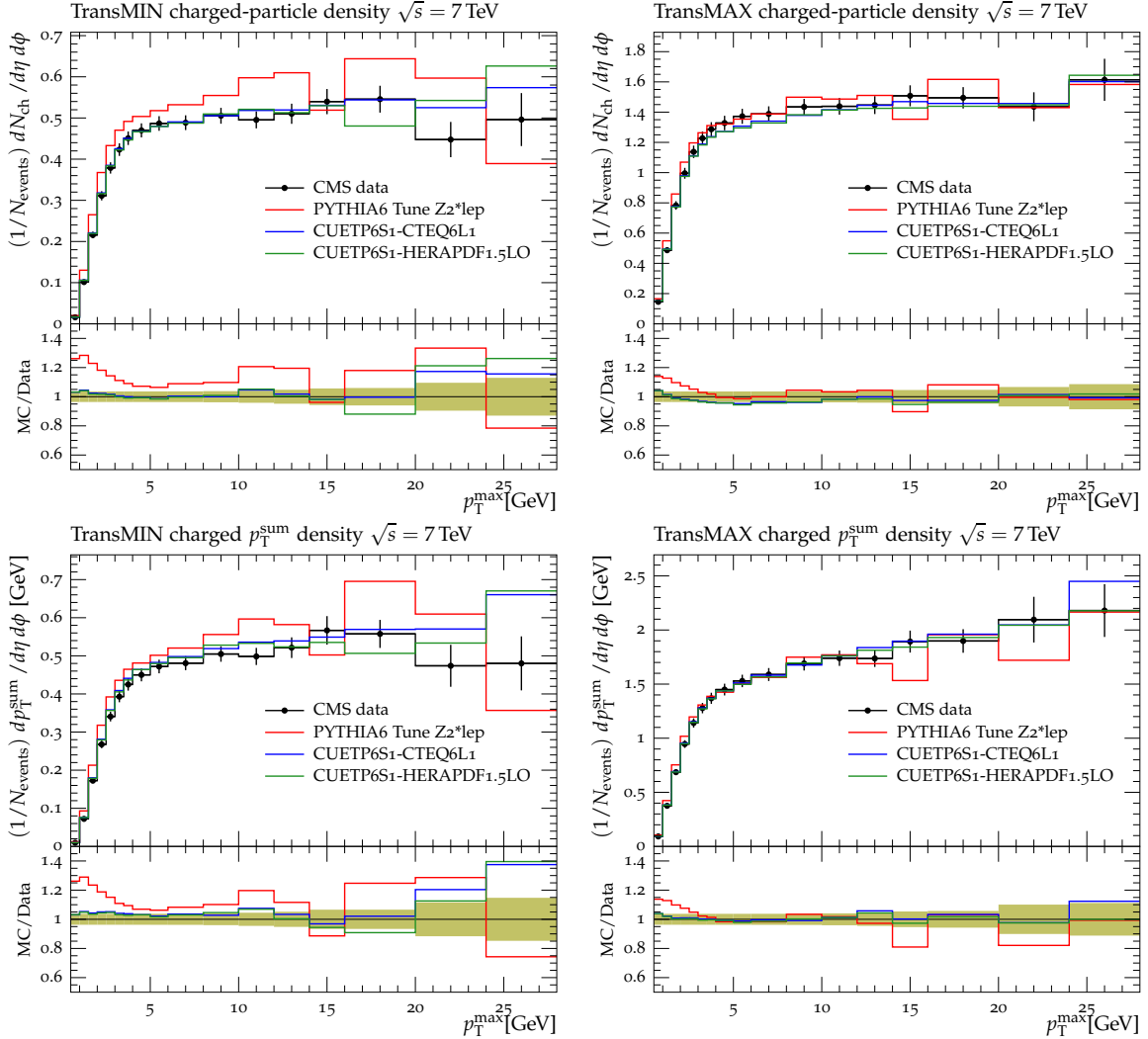


Figure 26: CMS data at $\sqrt{s} = 7 \text{ TeV}$ [17] on the particle (top) and p_T^{sum} densities (bottom) for charged particles with $p_T > 0.5 \text{ GeV}$ and $|\eta| < 0.8$ in the TransMIN (left) and TransMAX (right) regions as defined by the leading charged particle, as a function of the transverse momentum of the leading charged-particle p_T^{max} . The data are compared to the PYTHIA6 Tune Z2*lep, CUETP6S1-CTEQ6L1 and CUETP6S1-HERAPDF1.5LO. The green bands in the ratios represent the total experimental uncertainties.

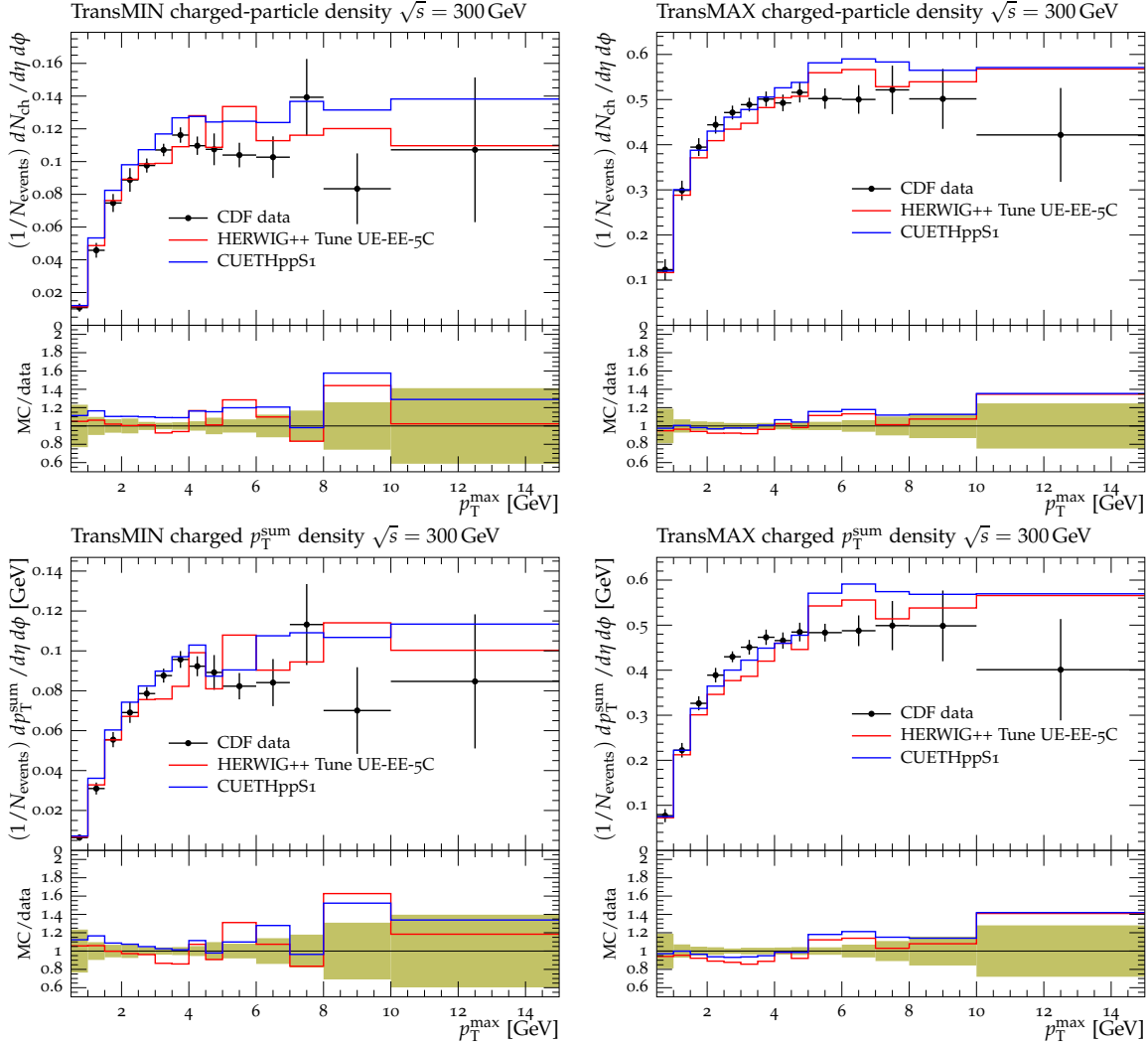


Figure 27: CDF data at $\sqrt{s} = 300 \text{ GeV}$ [11] on particle (top) and p_T^{sum} densities (bottom) for charged particles with $p_T > 0.5 \text{ GeV}$ and $|\eta| < 0.8$ in the TransMIN (left) and TransMAX (right) regions as defined by the leading charged particle, as a function of the transverse momentum of the leading charged-particle p_T^{\max} . The data are compared to the HERWIG++ Tune UE-EE-5C and CUETHppS1. The green bands in the ratios represent the total experimental uncertainties.

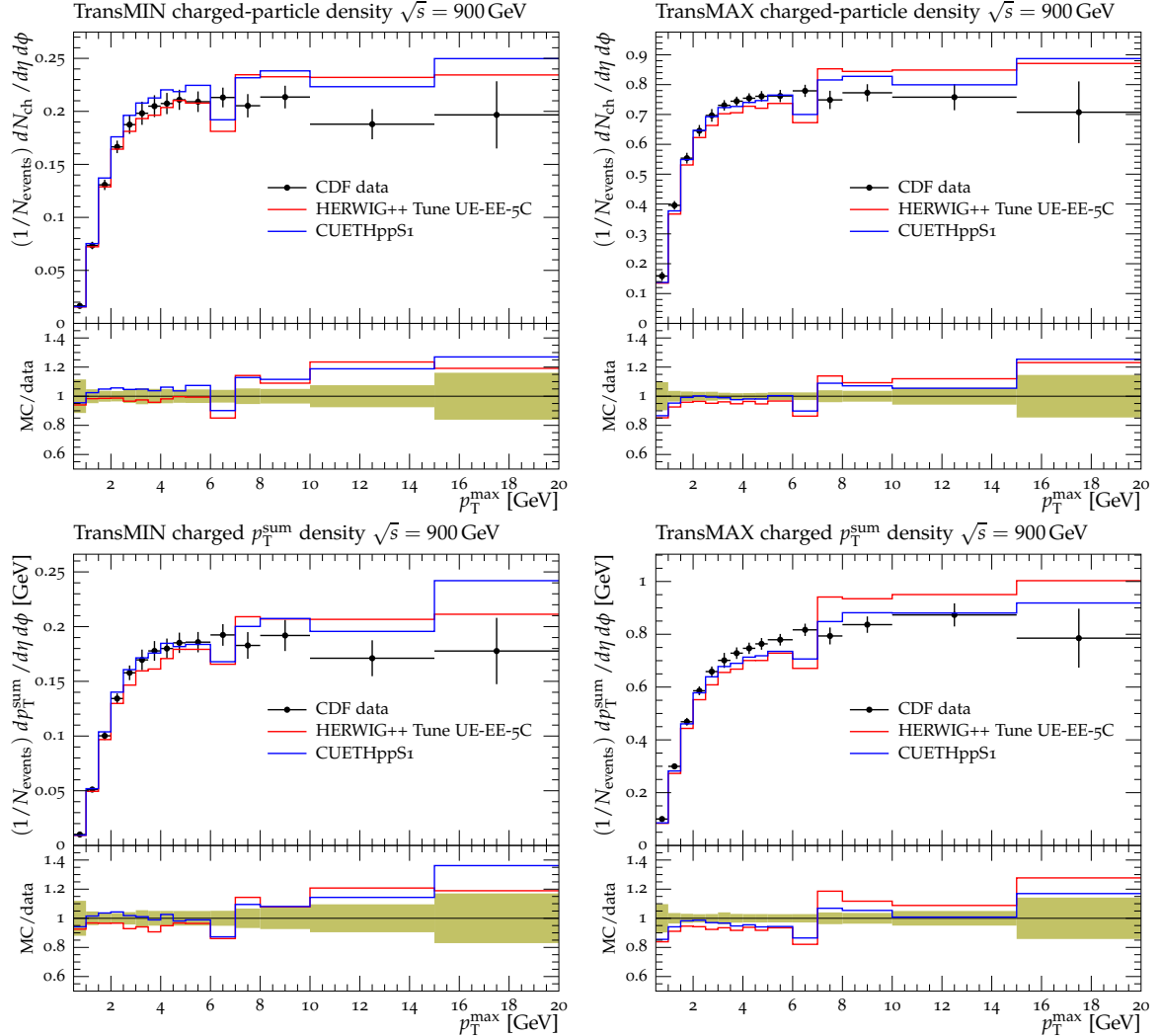


Figure 28: CDF data at $\sqrt{s} = 900 \text{ GeV}$ [11] on particle (top) and p_T^{sum} densities (bottom) for charged particles with $p_T > 0.5 \text{ GeV}$ and $|\eta| < 0.8$ in the TransMIN (left) and TransMAX (right) regions as defined by the leading charged particle, as a function of the transverse momentum of the leading charged-particle p_T^{\max} . The data are compared to the HERWIG++ Tune UE-EE-5C and CUETHppS1. The green bands in the ratios represent the total experimental uncertainties.

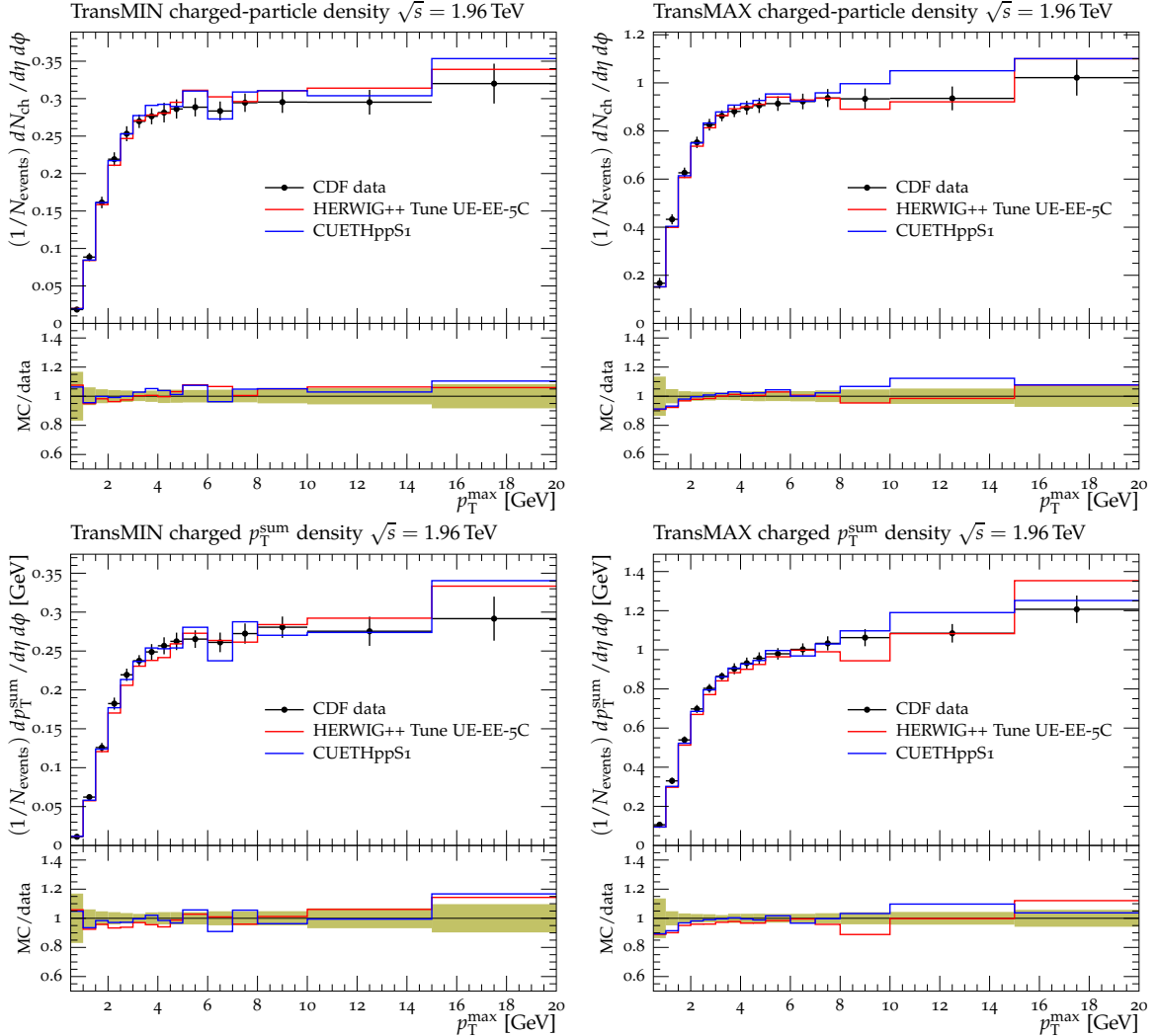


Figure 29: CDF data at $\sqrt{s} = 1.96 \text{ TeV}$ [11] on particle (top) and p_T^{sum} densities (bottom) for charged particles with $p_T > 0.5 \text{ GeV}$ and $|\eta| < 0.8$ in the TransMIN (left) and TransMAX (right) regions as defined by the leading charged particle, as a function of the transverse momentum of the leading charged-particle p_T^{max} . The data are compared to the HERWIG++ Tune UE-EE-5C and CUETHppS1. The green bands in the ratios represent the total experimental uncertainties.

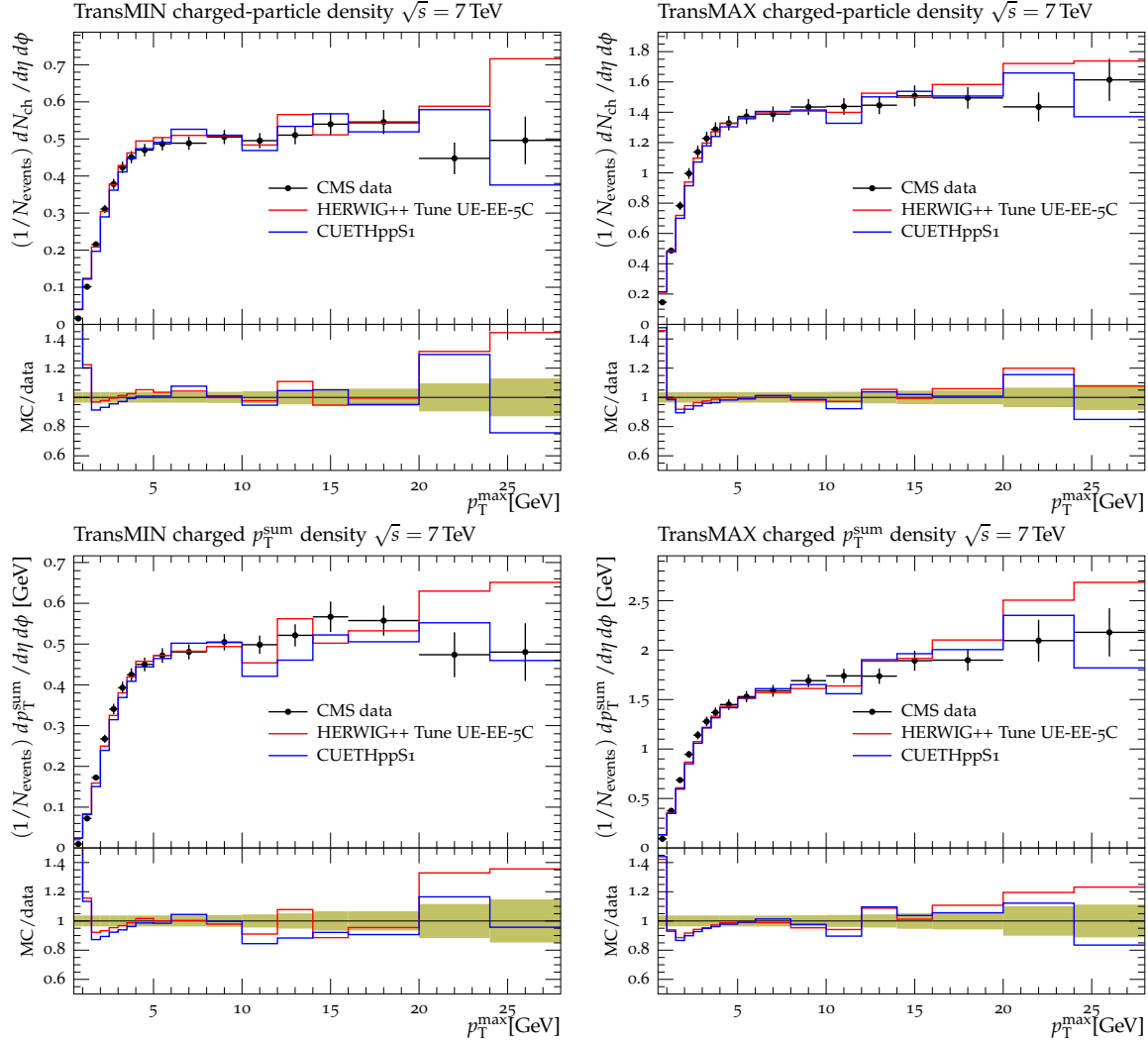


Figure 30: CMS data at $\sqrt{s} = 7 \text{ TeV}$ [17] on particle (top) and p_T^{sum} densities (bottom) for charged particles with $p_T > 0.5 \text{ GeV}$ and $|\eta| < 0.8$ in the TransMIN (left) and TransMAX (right) regions as defined by the leading charged particle, as a function of the transverse momentum of the leading charged-particle p_T^{max} . The data are compared to the HERWIG++ Tune UE-EE-5C and CUETHppS1. The green bands in the ratios represent the total experimental uncertainties.

for CUETHppS1, and for the two CMS PYTHIA8 DPS tunes CDPSTP8S1-4j and CDPSTP8S2-4j. In HERWIG++, σ_{eff} is independent of the center-of-mass energy, while PYTHIA8 gives a σ_{eff} that increases with energy. The PYTHIA8 UE tunes predict that σ_{eff} will increase by about 7% between 7 TeV and 13 TeV, while the CDPSTP8S2-4j predicts an increase of about 20%. This results in slightly different predictions for the DPS-sensitive observables at 13 TeV for the CMS UE tunes and the CMS DPS tunes.

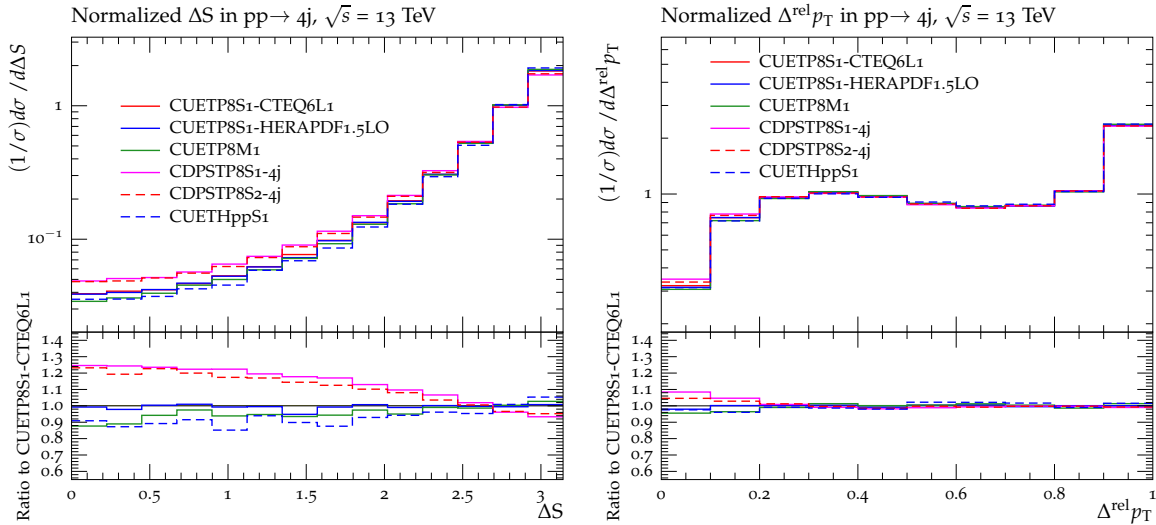


Figure 31: Predictions at $\sqrt{s} = 13$ TeV for the normalized distributions of the correlation observables ΔS (left), and $\Delta^{\text{rel}} p_T$ (right) for four-jet production in pp collisions for the three CMS PYTHIA8 UE tunes CUETP8S1-CTEQ6L1, CUETP8S1-HERAPDF1.5LO, and CUETP8M1, for CUETHppS1, and for CDPSTP8S1-4j and CDPSTP8S2-4j. Also shown are the ratios of the tunes to predictions of CUETP8S1-CTEQ6L1.

D.2 MB predictions at 13 TeV

Predictions of the CMS UE tunes at $\sqrt{s} = 13$ TeV are shown in Fig. 32 for the charged-particle pseudorapidity distribution, $dN_{\text{ch}}/d\eta$, for inelastic, NSD-enhanced, and SD-enhanced proton-proton collisions. In Fig. 32, the ratio of 13 TeV to 8 TeV results is shown for each of the tunes. The densities in the forward region are predicted to increase more rapidly than the central region between 8 TeV and 13 TeV. However, the UE observables in Figs. 20 and 21 increase much faster with center-of-mass energy than do these MB observables.

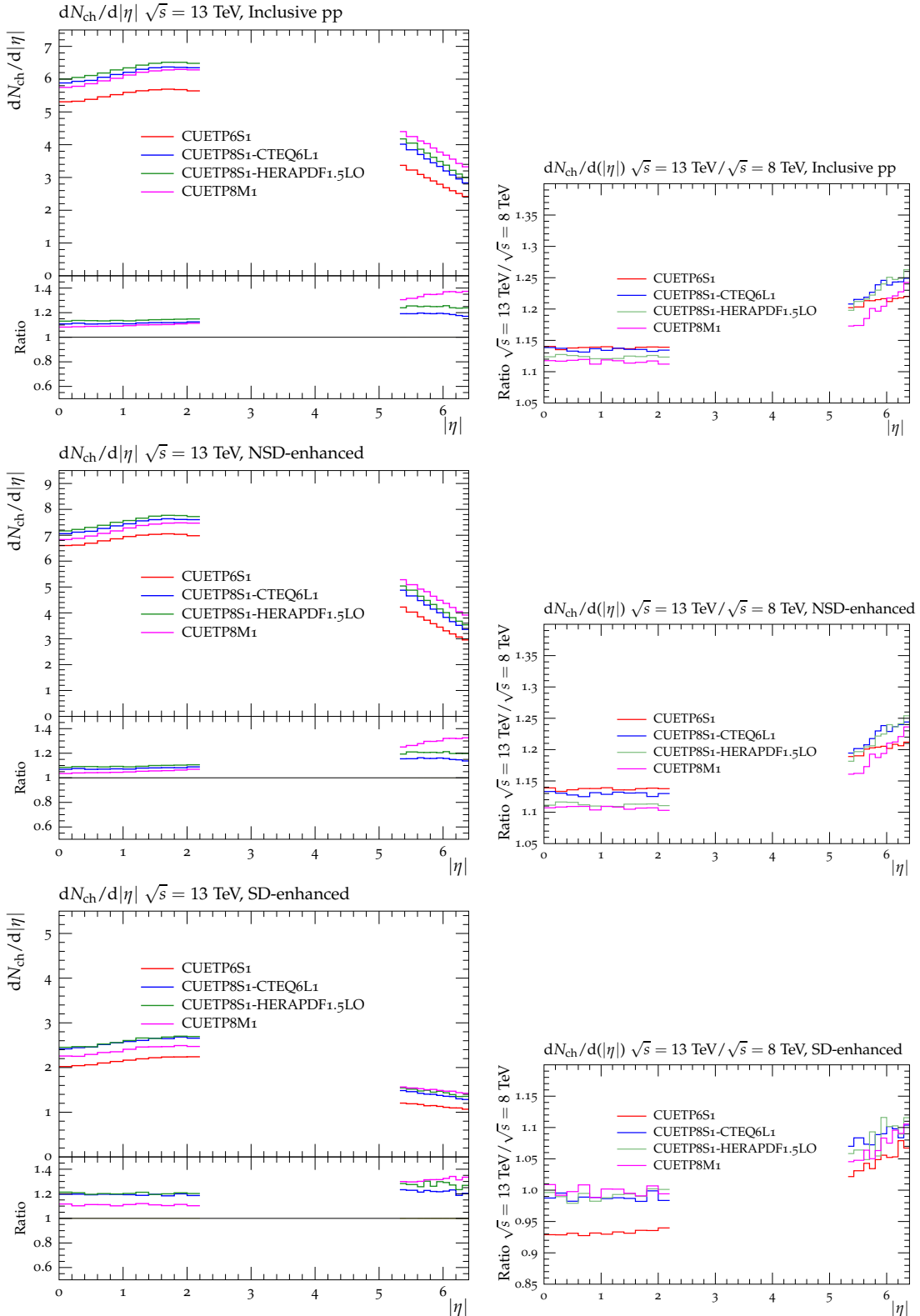


Figure 32: Predictions at $\sqrt{s} = 13$ TeV for the charged-particle pseudorapidity distribution $dN_{ch}/d\eta$, for (top) inelastic, (middle) NSD-enhanced, and (bottom) SD-enhanced pp collisions from CUETP6S1-CTEQ6L1, CUETP8S1-CTEQ6L1, CUETP8S1-HERAPDF1.5LO, and CUETP8M1. Also shown are the ratios of the tunes to predictions of CUETP8M1, and the ratio of 13 TeV to 8 TeV results for each of the tunes (right).

Acknowledgments

We congratulate our colleagues in the CERN accelerator departments for the excellent performance of the LHC and thank the technical and administrative staffs at CERN and at other CMS institutes for their contributions to the success of the CMS effort. In addition, we gratefully acknowledge the computing centres and personnel of the Worldwide LHC Computing Grid for delivering so effectively the computing infrastructure essential to our analyses. Finally, we acknowledge the enduring support for the construction and operation of the LHC and the CMS detector provided by the following funding agencies: the Austrian Federal Ministry of Science, Research and Economy and the Austrian Science Fund; the Belgian Fonds de la Recherche Scientifique, and Fonds voor Wetenschappelijk Onderzoek; the Brazilian Funding Agencies (CNPq, CAPES, FAPERJ, and FAPESP); the Bulgarian Ministry of Education and Science; CERN; the Chinese Academy of Sciences, Ministry of Science and Technology, and National Natural Science Foundation of China; the Colombian Funding Agency (COLCIENCIAS); the Croatian Ministry of Science, Education and Sport, and the Croatian Science Foundation; the Research Promotion Foundation, Cyprus; the Ministry of Education and Research, Estonian Research Council via IUT23-4 and IUT23-6 and European Regional Development Fund, Estonia; the Academy of Finland, Finnish Ministry of Education and Culture, and Helsinki Institute of Physics; the Institut National de Physique Nucléaire et de Physique des Particules / CNRS, and Commissariat à l'Énergie Atomique et aux Énergies Alternatives / CEA, France; the Bundesministerium für Bildung und Forschung, Deutsche Forschungsgemeinschaft, and Helmholtz-Gemeinschaft Deutscher Forschungszentren, Germany; the General Secretariat for Research and Technology, Greece; the National Scientific Research Foundation, and National Innovation Office, Hungary; the Department of Atomic Energy and the Department of Science and Technology, India; the Institute for Studies in Theoretical Physics and Mathematics, Iran; the Science Foundation, Ireland; the Istituto Nazionale di Fisica Nucleare, Italy; the Ministry of Science, ICT and Future Planning, and National Research Foundation (NRF), Republic of Korea; the Lithuanian Academy of Sciences; the Ministry of Education, and University of Malaya (Malaysia); the Mexican Funding Agencies (CINVESTAV, CONACYT, SEP, and UASLP-FAI); the Ministry of Business, Innovation and Employment, New Zealand; the Pakistan Atomic Energy Commission; the Ministry of Science and Higher Education and the National Science Centre, Poland; the Fundação para a Ciência e a Tecnologia, Portugal; JINR, Dubna; the Ministry of Education and Science of the Russian Federation, the Federal Agency of Atomic Energy of the Russian Federation, Russian Academy of Sciences, and the Russian Foundation for Basic Research; the Ministry of Education, Science and Technological Development of Serbia; the Secretaría de Estado de Investigación, Desarrollo e Innovación and Programa Consolider-Ingenio 2010, Spain; the Swiss Funding Agencies (ETH Board, ETH Zurich, PSI, SNF, UniZH, Canton Zurich, and SER); the Ministry of Science and Technology, Taipei; the Thailand Center of Excellence in Physics, the Institute for the Promotion of Teaching Science and Technology of Thailand, Special Task Force for Activating Research and the National Science and Technology Development Agency of Thailand; the Scientific and Technical Research Council of Turkey, and Turkish Atomic Energy Authority; the National Academy of Sciences of Ukraine, and State Fund for Fundamental Researches, Ukraine; the Science and Technology Facilities Council, UK; the US Department of Energy, and the US National Science Foundation.

Individuals have received support from the Marie-Curie programme and the European Research Council and EPLANET (European Union); the Leventis Foundation; the A. P. Sloan Foundation; the Alexander von Humboldt Foundation; the Belgian Federal Science Policy Office; the Fonds pour la Formation à la Recherche dans l'Industrie et dans l'Agriculture (FRIA-Belgium); the Agentschap voor Innovatie door Wetenschap en Technologie (IWT-Belgium); the

Ministry of Education, Youth and Sports (MEYS) of the Czech Republic; the Council of Science and Industrial Research, India; the HOMING PLUS programme of the Foundation for Polish Science, cofinanced from European Union, Regional Development Fund; the OPUS programme of the National Science Center (Poland); the Compagnia di San Paolo (Torino); MIUR project 20108T4XTM (Italy); the Thalis and Aristeia programmes cofinanced by EU-ESF and the Greek NSRF; the National Priorities Research Program by Qatar National Research Fund; the Rachadapisek Sompot Fund for Postdoctoral Fellowship, Chulalongkorn University (Thailand); and the Welch Foundation, contract C-1845.

References

- [1] T. Sjöstrand, S. Mrenna, and P. Skands, “PYTHIA 6.4 physics and manual”, *JHEP* **05** (2006) 026, doi:10.1088/1126-6708/2006/05/026, arXiv:hep-ph/0603175.
- [2] T. Sjöstrand, L. Lonnblad, and S. Mrenna, “PYTHIA 6.2: physics and manual”, (2001). arXiv:hep-ph/0108264.
- [3] T. Sjöstrand and M. van Zijl, “A multiple interaction model for the event structure in hadron collisions”, *Phys. Rev. D* **36** (1987) 2019, doi:10.1103/PhysRevD.36.2019.
- [4] M. Bengtsson, T. Sjöstrand, and M. van Zijl, “Initial state radiation effects on W and jet production”, *Z. Phys. C* **32** (1986) 67, doi:10.1007/BF01441353.
- [5] T. Sjöstrand, S. Mrenna, and P. Z. Skands, “A brief introduction to PYTHIA 8.1”, *Comput. Phys. Commun.* **178** (2008) 852, doi:10.1016/j.cpc.2008.01.036, arXiv:0710.3820.
- [6] M. Bahr et al., “Herwig++ physics and manual”, *Eur. Phys. J. C* **58** (2008) 639, doi:10.1140/epjc/s10052-008-0798-9, arXiv:0803.0883.
- [7] J. Bellm et al., “Herwig++ 2.7 Release Note”, (2013). arXiv:1310.6877.
- [8] M. G. Albrow et al., “Tevatron-for-LHC report of the QCD working group”, (2006). arXiv:hep-ph/0610012.
- [9] CDF Collaboration, “Studying the ‘underlying event’ at CDF and the LHC”, (2009). FERMILAB-CONF-09-792-E.
- [10] P. Z. Skands, “The Perugia tunes”, in *Proceedings, 1st International Workshop on Multiple Partonic Interactions at the LHC (MPI08)*. 2009. arXiv:0905.3418.
- [11] CDF Collaboration, “A study of the energy dependence of the underlying event in proton-antiproton collisions”, *Phys. Rev. D* **92** (2015), no. 9, 092009, doi:10.1103/PhysRevD.92.092009, arXiv:1508.05340.
- [12] G. A. Schuler and T. Sjöstrand, “Hadronic diffractive cross-sections and the rise of the total cross-section”, *Phys. Rev. D* **49** (1994) 2257, doi:10.1103/PhysRevD.49.2257.
- [13] A. V. Manohar and W. J. Waalewijn, “What is double parton scattering?”, *Phys. Lett. B* **713** (2012) 196, doi:10.1016/j.physletb.2012.05.044, arXiv:1202.5034.
- [14] A. Del Fabbro and D. Treleani, “Double parton scatterings at the CERN LHC”, in *Multiparticle production: New frontiers in soft physics and correlations on the threshold of the third millennium. Proceedings, 9th International Workshop, Torino, Italy, June 12-17, 2000*, volume 92, p. 130. 2001. doi:10.1016/S0920-5632(00)01027-6.

- [15] B. Blok, Y. Dokshitzer, L. Frankfurt, and M. Strikman, “Perturbative QCD correlations in multi-parton collisions”, *Eur. Phys. J. C* **74** (2014) 2926,
`doi:10.1140/epjc/s10052-014-2926-z`, `arXiv:1306.3763`.
- [16] P. Bartalini et al., “Multi-parton interactions at the LHC”, (2011). `arXiv:1111.0469`.
- [17] CMS Collaboration, “Measurement of the underlying event activity at the LHC at 7 TeV and comparison with 0.9 TeV”, CMS Physics Analysis Summary CMS-PAS-FSQ-12-020, 2012.
- [18] A. Buckley et al., “Rivet user manual”, *Comput. Phys. Commun.* **184** (2013) 2803,
`doi:10.1016/j.cpc.2013.05.021`, `arXiv:1003.0694`.
- [19] A. Buckley et al., “Systematic event generator tuning for the LHC”, *Eur. Phys. J. C* **65** (2010) 331, `doi:10.1140/epjc/s10052-009-1196-7`, `arXiv:0907.2973`.
- [20] J. Pumplin et al., “New generation of parton distributions with uncertainties from global QCD analysis”, *JHEP* **07** (2002) 012, `doi:10.1088/1126-6708/2002/07/012`,
`arXiv:hep-ph/0201195`.
- [21] A. M. Cooper-Sarkar, “HERAPDF1.5LO PDF set with experimental uncertainties”, in *Proceedings, 22nd International Workshop on Deep-Inelastic Scattering and Related Subjects (DIS 2014)*, volume DIS2014, p. 032. 2014.
- [22] NNPDF Collaboration, “Parton distributions with QED corrections”, *Nucl. Phys. B* **877** (2013) 290, `doi:10.1016/j.nuclphysb.2013.10.010`, `arXiv:1308.0598`.
- [23] NNPDF Collaboration, “Unbiased global determination of parton distributions and their uncertainties at NNLO and at LO”, *Nucl. Phys. B* **855** (2012) 153,
`doi:10.1016/j.nuclphysb.2011.09.024`, `arXiv:1107.2652`.
- [24] CMS Collaboration, “Measurement of the underlying event activity at the LHC with $\sqrt{s} = 7 \text{ TeV}$ and comparison with $\sqrt{s} = 0.9 \text{ TeV}$ ”, *JHEP* **09** (2011) 109,
`doi:10.1007/JHEP09(2011)109`, `arXiv:1107.0330`.
- [25] CMS Collaboration, “Study of the underlying event at forward rapidity in pp collisions at $\sqrt{s} = 0.9, 2.76$, and 7 TeV ”, *JHEP* **04** (2013) 072, `doi:10.1007/JHEP04(2013)072`,
`arXiv:1302.2394`.
- [26] CMS Collaboration, “Measurement of the underlying event in the Drell-Yan process in proton-proton collisions at $\sqrt{s} = 7 \text{ TeV}$ ”, *Eur. Phys. J. C* **72** (2012) 2080,
`doi:10.1140/epjc/s10052-012-2080-4`, `arXiv:1204.1411`.
- [27] J. Pumplin, “Hard underlying event correction to inclusive jet cross-sections”, *Phys. Rev. D* **57** (1998) 5787, `doi:10.1103/PhysRevD.57.5787`, `arXiv:hep-ph/9708464`.
- [28] R. Corke and T. Sjöstrand, “Interleaved parton showers and tuning prospects”, *JHEP* **03** (2011) 032, `doi:10.1007/JHEP03(2011)032`, `arXiv:1011.1759`.
- [29] P. Skands, S. Carrazza, and J. Rojo, “Tuning PYTHIA 8.1: the Monash 2013 tune”, *Eur. Phys. J. C* **74** (2014) 3024, `doi:10.1140/epjc/s10052-014-3024-y`,
`arXiv:1404.5630`.
- [30] M. H. Seymour and A. Siódmiok, “Constraining MPI models using σ_{eff} and recent Tevatron and LHC underlying event data”, *JHEP* **10** (2013) 113,
`doi:10.1007/JHEP10(2013)113`, `arXiv:1307.5015`.

- [31] P. Z. Skands, "Tuning Monte Carlo generators: the Perugia tunes", *Phys. Rev. D* **82** (2010) 074018, doi:10.1103/PhysRevD.82.074018, arXiv:1005.3457.
- [32] AFS Collaboration, "Double parton scattering in pp collisions at $\sqrt{s} = 63 \text{ GeV}$ ", *Z. Phys. C* **34** (1987) doi:10.1007/BF01566757.
- [33] CDF Collaboration, "Double parton scattering in $\bar{p}p$ collisions at $\sqrt{s} = 1.8 \text{ TeV}$ ", *Z. Phys. D* **56** (1997) doi:10.1103/PhysRevD.56.3811.
- [34] UA2 Collaboration, "A study of multi-jet events at the CERN $\bar{p}p$ collider and a search for double parton scattering", *Phys. Lett. B* **268** (1991) 145, doi:10.1016/0370-2693(91)90937-L.
- [35] ATLAS Collaboration, "Measurement of hard double-parton interactions in $W(\rightarrow \ell\nu) + 2\text{-jet}$ events at $\sqrt{s} = 7 \text{ TeV}$ with the ATLAS detector", *New J. Phys.* **15** (2013) 033038, doi:10.1088/1367-2630/15/3/033038, arXiv:1301.6872.
- [36] CMS Collaboration, "Study of double parton scattering using W + 2-jet events in proton-proton collisions at $\sqrt{s} = 7 \text{ TeV}$ ", *JHEP* **03** (2014) 032, doi:10.1007/JHEP03(2014)032, arXiv:1312.5729.
- [37] CMS Collaboration, "Measurement of four-jet production in proton-proton collisions at $\sqrt{s} = 7 \text{ TeV}$ ", *Phys. Rev. D* **89** (2014) 092010, doi:10.1103/PhysRevD.89.092010, arXiv:1312.6440.
- [38] J. Alwall et al., "MadGraph 5 : going beyond", *JHEP* **06** (2011) 128, doi:10.1007/JHEP06(2011)128, arXiv:1106.0522.
- [39] ATLAS Collaboration, "Measurement of underlying event characteristics using charged particles in pp collisions at $\sqrt{s} = 900 \text{ GeV}$ and 7 TeV with the ATLAS detector", *Phys. Rev. D* **83** (2011) 112001, doi:10.1103/PhysRevD.83.112001, arXiv:1012.0791.
- [40] B. Blok and P. Gunnellini, "Dynamical approach to MPI four-jet production in Pythia", *Eur. Phys. J. C* **75** (2015) 282, doi:10.1140/epjc/s10052-015-3520-8, arXiv:1503.08246.
- [41] M. Diehl, T. Kasemets, and S. Keane, "Correlations in double parton distributions: effects of evolution", *JHEP* **05** (2014) 118, doi:10.1007/JHEP05(2014)118, arXiv:1401.1233.
- [42] CMS Collaboration, "Measurement of the underlying event activity using charged-particle jets in proton-proton collisions at $\sqrt(s) = 2.76 \text{ TeV}$ ", *JHEP* **09** (2015) 137, doi:10.1007/JHEP09(2015)137, arXiv:1507.07229.
- [43] B. Cooper et al., "Importance of a consistent choice of α_s in the matching of AlpGen and Pythia", *Eur. Phys. J.C* **72** (2012) 2078, doi:10.1140/epjc/s10052-012-2078-y, arXiv:1109.5295.
- [44] P. A. Nason, "Recent developments in POWHEG", in *Proceedings, 9th International Symposium on Radiative Corrections: Applications of quantum field theory to phenomenology*. (RADCOR 2009), volume RADCOR2009, p. 018. 2010. arXiv:1001.2747.
- [45] S. Alioli, P. Nason, C. Oleari, and E. Re, "A general framework for implementing NLO calculations in shower Monte Carlo programs: the POWHEG BOX", *JHEP* **06** (2010) 043, doi:10.1007/JHEP06(2010)043, arXiv:1002.2581.

- [46] H.-L. Lai et al., “New parton distributions for collider physics”, *Phys. Rev. D* **82** (2010) 074024, doi:[10.1103/PhysRevD.82.074024](https://doi.org/10.1103/PhysRevD.82.074024), arXiv:[1007.2241](https://arxiv.org/abs/1007.2241).
- [47] ALICE Collaboration, “Charged-particle multiplicity measurement in proton-proton collisions at $\sqrt{s} = 7$ TeV with ALICE at LHC”, *Eur. Phys. J. C* **68** (2010) 345, doi:[10.1140/epjc/s10052-010-1350-2](https://doi.org/10.1140/epjc/s10052-010-1350-2), arXiv:[1004.3514](https://arxiv.org/abs/1004.3514).
- [48] TOTEM Collaboration, “First measurement of the total proton-proton cross section at the LHC energy of $\sqrt{s} = 7$ TeV”, *Europhys. Lett.* **96** (2011) 21002, doi:[10.1209/0295-5075/96/21002](https://doi.org/10.1209/0295-5075/96/21002), arXiv:[1110.1395](https://arxiv.org/abs/1110.1395).
- [49] CMS Collaboration, “Measurement of energy flow at large pseudorapidities in pp collisions at $\sqrt{s} = 0.9$ and 7 TeV”, *JHEP* **11** (2011) 148, doi:[10.1007/JHEP02\(2012\)055](https://doi.org/10.1007/JHEP02(2012)055), arXiv:[1110.0211](https://arxiv.org/abs/1110.0211).
- [50] CMS and TOTEM Collaborations, “Measurement of pseudorapidity distributions of charged particles in proton-proton collisions at $\sqrt{s} = 8$ TeV by the CMS and TOTEM experiments”, *Eur. Phys. J. C* **74** (2014) 3053, doi:[10.1140/epjc/s10052-014-3053-6](https://doi.org/10.1140/epjc/s10052-014-3053-6), arXiv:[1405.0722](https://arxiv.org/abs/1405.0722).
- [51] CMS Collaboration, “Measurement of the inclusive jet cross section in pp collisions at $\sqrt{s} = 7$ TeV”, *Phys. Rev. Lett.* **107** (2011) 132001, doi:[10.1103/PhysRevLett.107.132001](https://doi.org/10.1103/PhysRevLett.107.132001), arXiv:[1106.0208](https://arxiv.org/abs/1106.0208).
- [52] CMS Collaboration, “Measurement of the rapidity and transverse momentum distributions of Z bosons in pp collisions at $\sqrt{s} = 7$ TeV”, *Phys. Rev. D* **85** (2012) 032002, doi:[10.1103/PhysRevD.85.032002](https://doi.org/10.1103/PhysRevD.85.032002), arXiv:[1110.4973](https://arxiv.org/abs/1110.4973).
- [53] CMS Collaboration, “Pseudorapidity distribution of charged hadrons in proton-proton collisions at $\sqrt{s} = 13$ TeV”, *Phys. Lett. B* **751** (2015) 143, doi:[10.1016/j.physletb.2015.10.004](https://doi.org/10.1016/j.physletb.2015.10.004), arXiv:[1507.05915](https://arxiv.org/abs/1507.05915).

E The CMS Collaboration

Yerevan Physics Institute, Yerevan, Armenia
V. Khachatryan, A.M. Sirunyan, A. Tumasyan

Institut für Hochenergiephysik der OeAW, Wien, Austria

W. Adam, E. Asilar, T. Bergauer, J. Brandstetter, E. Brondolin, M. Dragicevic, J. Erö, M. Flechl, M. Friedl, R. Frühwirth¹, V.M. Ghete, C. Hartl, N. Hörmann, J. Hrubec, M. Jeitler¹, V. Knünz, A. König, M. Krammer¹, I. Krätschmer, D. Liko, T. Matsushita, I. Mikulec, D. Rabady², B. Rahbaran, H. Rohringer, J. Schieck¹, R. Schöfbeck, J. Strauss, W. Treberer-Treberspurg, W. Waltenberger, C.-E. Wulz¹

National Centre for Particle and High Energy Physics, Minsk, Belarus

V. Mossolov, N. Shumeiko, J. Suarez Gonzalez

Universiteit Antwerpen, Antwerpen, Belgium

S. Alderweireldt, T. Cornelis, E.A. De Wolf, X. Janssen, A. Knutsson, J. Lauwers, S. Luyckx, M. Van De Klundert, H. Van Haevermaet, P. Van Mechelen, N. Van Remortel, A. Van Spilbeeck

Vrije Universiteit Brussel, Brussel, Belgium

S. Abu Zeid, F. Blekman, J. D'Hondt, N. Daci, I. De Bruyn, K. Deroover, N. Heracleous, J. Keaveney, S. Lowette, L. Moreels, A. Olbrechts, Q. Python, D. Strom, S. Tavernier, W. Van Doninck, P. Van Mulders, G.P. Van Onsem, I. Van Parijs

Université Libre de Bruxelles, Bruxelles, Belgium

P. Barria, H. Brun, C. Caillol, B. Clerbaux, G. De Lentdecker, G. Fasanella, L. Favart, A. Grebenyuk, G. Karapostoli, T. Lenzi, A. Léonard, T. Maerschalk, A. Marinov, L. Perniè, A. Randle-conde, T. Seva, C. Vander Velde, P. Vanlaer, R. Yonamine, F. Zenoni, F. Zhang³

Ghent University, Ghent, Belgium

K. Beernaert, L. Benucci, A. Cimmino, S. Crucy, D. Dobur, A. Fagot, G. Garcia, M. Gul, J. Mccartin, A.A. Ocampo Rios, D. Poyraz, D. Ryckbosch, S. Salva, M. Sigamani, M. Tytgat, W. Van Driessche, E. Yazgan, N. Zaganidis

Université Catholique de Louvain, Louvain-la-Neuve, Belgium

S. Basegmez, C. Beluffi⁴, O. Bondu, S. Brochet, G. Bruno, A. Caudron, L. Ceard, G.G. Da Silveira, C. Delaere, D. Favart, L. Forthomme, A. Giannanco⁵, J. Hollar, A. Jafari, P. Jez, M. Komm, V. Lemaitre, A. Mertens, M. Musich, C. Nuttens, L. Perrini, A. Pin, K. Piotrkowski, A. Popov⁶, L. Quertenmont, M. Selvaggi, M. Vidal Marono

Université de Mons, Mons, Belgium

N. Belyi, G.H. Hammad

Centro Brasileiro de Pesquisas Fisicas, Rio de Janeiro, Brazil

W.L. Aldá Júnior, F.L. Alves, G.A. Alves, L. Brito, M. Correa Martins Junior, M. Hamer, C. Hensel, A. Moraes, M.E. Pol, P. Rebello Teles

Universidade do Estado do Rio de Janeiro, Rio de Janeiro, Brazil

E. Belchior Batista Das Chagas, W. Carvalho, J. Chinellato⁷, A. Custódio, E.M. Da Costa, D. De Jesus Damiao, C. De Oliveira Martins, S. Fonseca De Souza, L.M. Huertas Guativa, H. Malbouisson, D. Matos Figueiredo, C. Mora Herrera, L. Mundim, H. Nogima, W.L. Prado Da Silva, A. Santoro, A. Sznajder, E.J. Tonelli Manganote⁷, A. Vilela Pereira

Universidade Estadual Paulista ^a, Universidade Federal do ABC ^b, São Paulo, Brazil

S. Ahuja^a, C.A. Bernardes^b, A. De Souza Santos^b, S. Dogra^a, T.R. Fernandez Perez Tomei^a,

E.M. Gregores^b, P.G. Mercadante^b, C.S. Moon^{a,8}, S.F. Novaes^a, Sandra S. Padula^a, D. Romero Abad, J.C. Ruiz Vargas

Institute for Nuclear Research and Nuclear Energy, Sofia, Bulgaria

A. Aleksandrov, R. Hadjiiska, P. Iaydjiev, M. Rodozov, S. Stoykova, G. Sultanov, M. Vutova

University of Sofia, Sofia, Bulgaria

A. Dimitrov, I. Glushkov, L. Litov, B. Pavlov, P. Petkov

Institute of High Energy Physics, Beijing, China

M. Ahmad, J.G. Bian, G.M. Chen, H.S. Chen, M. Chen, T. Cheng, R. Du, C.H. Jiang, R. Plestina⁹, F. Romeo, S.M. Shaheen, A. Spiezja, J. Tao, C. Wang, Z. Wang, H. Zhang

State Key Laboratory of Nuclear Physics and Technology, Peking University, Beijing, China

C. Asawatangtrakuldee, Y. Ban, Q. Li, S. Liu, Y. Mao, S.J. Qian, D. Wang, Z. Xu

Universidad de Los Andes, Bogota, Colombia

C. Avila, A. Cabrera, L.F. Chaparro Sierra, C. Florez, J.P. Gomez, B. Gomez Moreno, J.C. Sanabria

University of Split, Faculty of Electrical Engineering, Mechanical Engineering and Naval Architecture, Split, Croatia

N. Godinovic, D. Lelas, I. Puljak, P.M. Ribeiro Cipriano

University of Split, Faculty of Science, Split, Croatia

Z. Antunovic, M. Kovac

Institute Rudjer Boskovic, Zagreb, Croatia

V. Brigljevic, K. Kadija, J. Luetic, S. Micanovic, L. Sudic

University of Cyprus, Nicosia, Cyprus

A. Attikis, G. Mavromanolakis, J. Mousa, C. Nicolaou, F. Ptochos, P.A. Razis, H. Rykaczewski

Charles University, Prague, Czech Republic

M. Bodlak, M. Finger¹⁰, M. Finger Jr.¹⁰

Academy of Scientific Research and Technology of the Arab Republic of Egypt, Egyptian Network of High Energy Physics, Cairo, Egypt

A.A. Abdelalim^{11,12}, A. Awad, A. Mahrous¹¹, Y. Mohammed¹³, A. Radi^{14,15}

National Institute of Chemical Physics and Biophysics, Tallinn, Estonia

B. Calpas, M. Kadastik, M. Murumaa, M. Raidal, A. Tiko, C. Veelken

Department of Physics, University of Helsinki, Helsinki, Finland

P. Eerola, J. Pekkanen, M. Voutilainen

Helsinki Institute of Physics, Helsinki, Finland

J. Häkkinen, V. Karimäki, R. Kinnunen, T. Lampén, K. Lassila-Perini, S. Lehti, T. Lindén, P. Luukka, T. Mäenpää, T. Peltola, E. Tuominen, J. Tuominiemi, E. Tuovinen, L. Wendland

Lappeenranta University of Technology, Lappeenranta, Finland

J. Talvitie, T. Tuuva

DSM/IRFU, CEA/Saclay, Gif-sur-Yvette, France

M. Besancon, F. Couderc, M. Dejardin, D. Denegri, B. Fabbro, J.L. Faure, C. Favaro, F. Ferri, S. Ganjour, A. Givernaud, P. Gras, G. Hamel de Monchenault, P. Jarry, E. Locci, M. Machet, J. Malcles, J. Rander, A. Rosowsky, M. Titov, A. Zghiche

Laboratoire Leprince-Ringuet, Ecole Polytechnique, IN2P3-CNRS, Palaiseau, France

I. Antropov, S. Baffioni, F. Beaudette, P. Busson, L. Cadamuro, E. Chapon, C. Charlot, T. Dahms, O. Davignon, N. Filipovic, R. Granier de Cassagnac, M. Jo, S. Lisniak, L. Mastrolorenzo, P. Miné, I.N. Naranjo, M. Nguyen, C. Ochando, G. Ortona, P. Paganini, P. Pigard, S. Regnard, R. Salerno, J.B. Sauvan, Y. Sirois, T. Strebler, Y. Yilmaz, A. Zabi

Institut Pluridisciplinaire Hubert Curien, Université de Strasbourg, Université de Haute Alsace Mulhouse, CNRS/IN2P3, Strasbourg, France

J.-L. Agram¹⁶, J. Andrea, A. Aubin, D. Bloch, J.-M. Brom, M. Buttignol, E.C. Chabert, N. Chanon, C. Collard, E. Conte¹⁶, X. Coubez, J.-C. Fontaine¹⁶, D. Gelé, U. Goerlach, C. Goetzmann, A.-C. Le Bihan, J.A. Merlin², K. Skovpen, P. Van Hove

Centre de Calcul de l’Institut National de Physique Nucléaire et de Physique des Particules, CNRS/IN2P3, Villeurbanne, France

S. Gadrat

Université de Lyon, Université Claude Bernard Lyon 1, CNRS-IN2P3, Institut de Physique Nucléaire de Lyon, Villeurbanne, France

S. Beauceron, C. Bernet, G. Boudoul, E. Bouvier, C.A. Carrillo Montoya, R. Chierici, D. Contardo, B. Courbon, P. Depasse, H. El Mamouni, J. Fan, J. Fay, S. Gascon, M. Gouzevitch, B. Ille, F. Lagarde, I.B. Laktineh, M. Lethuillier, L. Mirabito, A.L. Pequegnot, S. Perries, J.D. Ruiz Alvarez, D. Sabes, L. Sgandurra, V. Sordini, M. Vander Donckt, P. Verdier, S. Viret

Georgian Technical University, Tbilisi, Georgia

T. Toriashvili¹⁷

Tbilisi State University, Tbilisi, Georgia

D. Lomidze

RWTH Aachen University, I. Physikalisches Institut, Aachen, Germany

C. Autermann, S. Beranek, M. Edelhoff, L. Feld, A. Heister, M.K. Kiesel, K. Klein, M. Lipinski, A. Ostapchuk, M. Preuten, F. Raupach, S. Schael, J.F. Schulte, T. Verlage, H. Weber, B. Wittmer, V. Zhukov⁶

RWTH Aachen University, III. Physikalisches Institut A, Aachen, Germany

M. Ata, M. Brodski, E. Dietz-Laursonn, D. Duchardt, M. Endres, M. Erdmann, S. Erdweg, T. Esch, R. Fischer, A. Güth, T. Hebbeker, C. Heidemann, K. Hoepfner, S. Knutzen, P. Kreuzer, M. Merschmeyer, A. Meyer, P. Millet, M. Olszewski, K. Padeken, P. Papacz, T. Pook, M. Radziej, H. Reithler, M. Rieger, F. Scheuch, L. Sonnenschein, D. Teyssier, S. Thüer

RWTH Aachen University, III. Physikalisches Institut B, Aachen, Germany

V. Cherepanov, Y. Erdogan, G. Flügge, H. Geenen, M. Geisler, F. Hoehle, B. Kargoll, T. Kress, Y. Kuessel, A. Künsken, J. Lingemann, A. Nehrkorn, A. Nowack, I.M. Nugent, C. Pistone, O. Pooth, A. Stahl

Deutsches Elektronen-Synchrotron, Hamburg, Germany

M. Aldaya Martin, I. Asin, N. Bartosik, O. Behnke, U. Behrens, A.J. Bell, K. Borras¹⁸, A. Burgmeier, A. Campbell, S. Choudhury¹⁹, F. Costanza, C. Diez Pardos, G. Dolinska, S. Dooling, T. Dorland, G. Eckerlin, D. Eckstein, T. Eichhorn, G. Flucke, E. Gallo²⁰, J. Garay Garcia, A. Geiser, A. Gzhko, P. Gunnellini, J. Hauk, M. Hempel²¹, H. Jung, A. Kalogeropoulos, O. Karacheban²¹, M. Kasemann, P. Katsas, J. Kieseler, C. Kleinwort, I. Korol, W. Lange, J. Leonard, K. Lipka, A. Lobanov, W. Lohmann²¹, R. Mankel, I. Marfin²¹, I.-A. Melzer-Pellmann, A.B. Meyer, G. Mittag, J. Mnich, A. Mussgiller, S. Naumann-Emme, A. Nayak, E. Ntomari,

H. Perrey, D. Pitzl, R. Placakyte, A. Raspereza, B. Roland, M.Ö. Sahin, P. Saxena, T. Schoerner-Sadenius, M. Schröder, C. Seitz, S. Spannagel, K.D. Trippkewitz, R. Walsh, C. Wissing

University of Hamburg, Hamburg, Germany

V. Blobel, M. Centis Vignali, A.R. Draeger, J. Erfle, E. Garutti, K. Goebel, D. Gonzalez, M. Görner, J. Haller, M. Hoffmann, R.S. Höing, A. Junkes, R. Klanner, R. Kogler, N. Kovalchuk, T. Lapsien, T. Lenz, I. Marchesini, D. Marconi, M. Meyer, D. Nowatschin, J. Ott, F. Pantaleo², T. Peiffer, A. Perieanu, N. Pietsch, J. Poehlsen, D. Rathjens, C. Sander, C. Scharf, H. Schettler, P. Schleper, E. Schlieckau, A. Schmidt, J. Schwandt, V. Sola, H. Stadie, G. Steinbrück, H. Tholen, D. Troendle, E. Usai, L. Vanelder, A. Vanhoefer, B. Vormwald

Institut für Experimentelle Kernphysik, Karlsruhe, Germany

C. Barth, C. Baus, J. Berger, C. Böser, E. Butz, T. Chwalek, F. Colombo, W. De Boer, A. Descroix, A. Dierlamm, S. Fink, F. Frensch, R. Friese, M. Giffels, A. Gilbert, D. Haitz, F. Hartmann², S.M. Heindl, U. Husemann, I. Katkov⁶, A. Kornmayer², P. Lobelle Pardo, B. Maier, H. Mildner, M.U. Mozer, T. Müller, Th. Müller, M. Plagge, G. Quast, K. Rabbertz, S. Röcker, F. Roscher, G. Sieber, H.J. Simonis, F.M. Stober, R. Ulrich, J. Wagner-Kuhr, S. Wayand, M. Weber, T. Weiler, S. Williamson, C. Wöhrmann, R. Wolf

Institute of Nuclear and Particle Physics (INPP), NCSR Demokritos, Aghia Paraskevi, Greece

G. Anagnostou, G. Daskalakis, T. Geralis, V.A. Giakoumopoulou, A. Kyriakis, D. Loukas, A. Psallidas, I. Topsis-Giotis

University of Athens, Athens, Greece

A. Agapitos, S. Kesisoglou, A. Panagiotou, N. Saoulidou, E. Tziaferi

University of Ioánnina, Ioánnina, Greece

I. Evangelou, G. Flouris, C. Foudas, P. Kokkas, N. Loukas, N. Manthos, I. Papadopoulos, E. Paradas, J. Strologas

Wigner Research Centre for Physics, Budapest, Hungary

G. Bencze, C. Hajdu, A. Hazi, P. Hidas, D. Horvath²², F. Sikler, V. Veszpremi, G. Vesztergombi²³, A.J. Zsigmond

Institute of Nuclear Research ATOMKI, Debrecen, Hungary

N. Beni, S. Czellar, J. Karancsi²⁴, J. Molnar, Z. Szillasi²

University of Debrecen, Debrecen, Hungary

M. Bartók²⁵, A. Makovec, P. Raics, Z.L. Trocsanyi, B. Ujvari

National Institute of Science Education and Research, Bhubaneswar, India

P. Mal, K. Mandal, D.K. Sahoo, N. Sahoo, S.K. Swain

Panjab University, Chandigarh, India

S. Bansal, S.B. Beri, V. Bhatnagar, R. Chawla, R. Gupta, U.Bhawandeep, A.K. Kalsi, A. Kaur, M. Kaur, R. Kumar, A. Mehta, M. Mittal, J.B. Singh, G. Walia

University of Delhi, Delhi, India

Ashok Kumar, A. Bhardwaj, B.C. Choudhary, R.B. Garg, A. Kumar, S. Malhotra, M. Naimuddin, N. Nishu, K. Ranjan, R. Sharma, V. Sharma

Saha Institute of Nuclear Physics, Kolkata, India

S. Bhattacharya, K. Chatterjee, S. Dey, S. Dutta, Sa. Jain, N. Majumdar, A. Modak, K. Mondal, S. Mukherjee, S. Mukhopadhyay, A. Roy, D. Roy, S. Roy Chowdhury, S. Sarkar, M. Sharan

Bhabha Atomic Research Centre, Mumbai, India

A. Abdulsalam, R. Chudasama, D. Dutta, V. Jha, V. Kumar, A.K. Mohanty², L.M. Pant, P. Shukla, A. Topkar

Tata Institute of Fundamental Research, Mumbai, India

T. Aziz, S. Banerjee, S. Bhowmik²⁶, R.M. Chatterjee, R.K. Dewanjee, S. Dugad, S. Ganguly, S. Ghosh, M. Guchait, A. Gurtu²⁷, G. Kole, S. Kumar, B. Mahakud, M. Maity²⁶, G. Majumder, K. Mazumdar, S. Mitra, G.B. Mohanty, B. Parida, T. Sarkar²⁶, N. Sur, B. Sutar, N. Wickramage²⁸

Indian Institute of Science Education and Research (IISER), Pune, India

S. Chauhan, S. Dube, A. Kapoor, K. Kotekar, S. Sharma

Institute for Research in Fundamental Sciences (IPM), Tehran, Iran

H. Bakhshiansohi, H. Behnamian, S.M. Etesami²⁹, A. Fahim³⁰, R. Goldouzian, M. Khakzad, M. Mohammadi Najafabadi, M. Naseri, S. Pakhtinat Mehdiabadi, F. Rezaei Hosseinabadi, B. Safarzadeh³¹, M. Zeinali

University College Dublin, Dublin, Ireland

M. Felcini, M. Grunewald

INFN Sezione di Bari ^a, Università di Bari ^b, Politecnico di Bari ^c, Bari, Italy

M. Abbrescia^{a,b}, C. Calabria^{a,b}, C. Caputo^{a,b}, A. Colaleo^a, D. Creanza^{a,c}, L. Cristella^{a,b}, N. De Filippis^{a,c}, M. De Palma^{a,b}, L. Fiore^a, G. Iaselli^{a,c}, G. Maggi^{a,c}, M. Maggi^a, G. Miniello^{a,b}, S. My^{a,c}, S. Nuzzo^{a,b}, A. Pompili^{a,b}, G. Pugliese^{a,c}, R. Radogna^{a,b}, A. Ranieri^a, G. Selvaggi^{a,b}, L. Silvestris^{a,2}, R. Venditti^{a,b}, P. Verwilligen^a

INFN Sezione di Bologna ^a, Università di Bologna ^b, Bologna, Italy

G. Abbiendi^a, C. Battilana², A.C. Benvenuti^a, D. Bonacorsi^{a,b}, S. Braibant-Giacomelli^{a,b}, L. Brigliadori^{a,b}, R. Campanini^{a,b}, P. Capiluppi^{a,b}, A. Castro^{a,b}, F.R. Cavallo^a, S.S. Chhibra^{a,b}, G. Codispoti^{a,b}, M. Cuffiani^{a,b}, G.M. Dallavalle^a, F. Fabbri^a, A. Fanfani^{a,b}, D. Fasanella^{a,b}, P. Giacomelli^a, C. Grandi^a, L. Guiducci^{a,b}, S. Marcellini^a, G. Masetti^a, A. Montanari^a, F.L. Navarria^{a,b}, A. Perrotta^a, A.M. Rossi^{a,b}, T. Rovelli^{a,b}, G.P. Siroli^{a,b}, N. Tosi^{a,b,2}, R. Travaglini^{a,b}

INFN Sezione di Catania ^a, Università di Catania ^b, Catania, Italy

G. Cappello^a, M. Chiorboli^{a,b}, S. Costa^{a,b}, A. Di Mattia^a, F. Giordano^{a,b}, R. Potenza^{a,b}, A. Tricomi^{a,b}, C. Tuve^{a,b}

INFN Sezione di Firenze ^a, Università di Firenze ^b, Firenze, Italy

G. Barbagli^a, V. Ciulli^{a,b}, C. Civinini^a, R. D'Alessandro^{a,b}, E. Focardi^{a,b}, S. Gonzi^{a,b}, V. Gori^{a,b}, P. Lenzi^{a,b}, M. Meschini^a, S. Paoletti^a, G. Sguazzoni^a, A. Tropiano^{a,b}, L. Viliani^{a,b,2}

INFN Laboratori Nazionali di Frascati, Frascati, Italy

L. Benussi, S. Bianco, F. Fabbri, D. Piccolo, F. Primavera²

INFN Sezione di Genova ^a, Università di Genova ^b, Genova, Italy

V. Calvelli^{a,b}, F. Ferro^a, M. Lo Vetere^{a,b}, M.R. Monge^{a,b}, E. Robutti^a, S. Tosi^{a,b}

INFN Sezione di Milano-Bicocca ^a, Università di Milano-Bicocca ^b, Milano, Italy

L. Brianza, M.E. Dinardo^{a,b}, S. Fiorendi^{a,b}, S. Gennai^a, R. Gerosa^{a,b}, A. Ghezzi^{a,b}, P. Govoni^{a,b}, S. Malvezzi^a, R.A. Manzoni^{a,b,2}, B. Marzocchi^{a,b,2}, D. Menasce^a, L. Moroni^a, M. Paganoni^{a,b}, D. Pedrini^a, S. Ragazzi^{a,b}, N. Redaelli^a, T. Tabarelli de Fatis^{a,b}

INFN Sezione di Napoli ^a, Università di Napoli 'Federico II' ^b, Napoli, Italy, Università della Basilicata ^c, Potenza, Italy, Università G. Marconi ^d, Roma, Italy

S. Buontempo^a, N. Cavallo^{a,c}, S. Di Guida^{a,d,2}, M. Esposito^{a,b}, F. Fabozzi^{a,c}, A.O.M. Iorio^{a,b}, G. Lanza^a, L. Lista^a, S. Meola^{a,d,2}, M. Merola^a, P. Paolucci^{a,2}, C. Sciacca^{a,b}, F. Thyssen

INFN Sezione di Padova ^a, Università di Padova ^b, Padova, Italy, Università di Trento ^c, Trento, Italy

P. Azzi^{a,2}, N. Bacchetta^a, L. Benato^{a,b}, D. Bisello^{a,b}, A. Boletti^{a,b}, A. Branca^{a,b}, R. Carlin^{a,b}, P. Checchia^a, M. Dall'Osso^{a,b,2}, T. Dorigo^a, U. Dosselli^a, S. Fantinel^a, F. Fanzago^a, F. Gasparini^{a,b}, U. Gasparini^{a,b}, A. Gozzelino^a, K. Kanishchev^{a,c}, S. Lacaprara^a, M. Margoni^{a,b}, A.T. Meneguzzo^{a,b}, J. Pazzini^{a,b,2}, N. Pozzobon^{a,b}, P. Ronchese^{a,b}, F. Simonetto^{a,b}, E. Torassa^a, M. Tosi^{a,b}, M. Zanetti, P. Zotto^{a,b}, A. Zucchetta^{a,b,2}

INFN Sezione di Pavia ^a, Università di Pavia ^b, Pavia, Italy

A. Braghieri^a, A. Magnani^a, P. Montagna^{a,b}, S.P. Ratti^{a,b}, V. Re^a, C. Riccardi^{a,b}, P. Salvini^a, I. Vai^a, P. Vitulo^{a,b}

INFN Sezione di Perugia ^a, Università di Perugia ^b, Perugia, Italy

L. Alunni Solestizi^{a,b}, G.M. Bilei^a, D. Ciangottini^{a,b,2}, L. Fanò^{a,b}, P. Lariccia^{a,b}, G. Mantovani^{a,b}, M. Menichelli^a, A. Saha^a, A. Santocchia^{a,b}

INFN Sezione di Pisa ^a, Università di Pisa ^b, Scuola Normale Superiore di Pisa ^c, Pisa, Italy

K. Androsov^{a,32}, P. Azzurri^{a,2}, G. Bagliesi^a, J. Bernardini^a, T. Boccali^a, R. Castaldi^a, M.A. Ciocci^{a,32}, R. Dell'Orso^a, S. Donato^{a,c,2}, G. Fedi, L. Foà^{a,c†}, A. Giassi^a, M.T. Grippo^{a,32}, F. Ligabue^{a,c}, T. Lomtadze^a, L. Martini^{a,b}, A. Messineo^{a,b}, F. Palla^a, A. Rizzi^{a,b}, A. Savoy-Navarro^{a,33}, A.T. Serban^a, P. Spagnolo^a, R. Tenchini^a, G. Tonelli^{a,b}, A. Venturi^a, P.G. Verdini^a

INFN Sezione di Roma ^a, Università di Roma ^b, Roma, Italy

L. Barone^{a,b}, F. Cavallari^a, G. D'imperio^{a,b,2}, D. Del Re^{a,b,2}, M. Diemoz^a, S. Gelli^{a,b}, C. Jorda^a, E. Longo^{a,b}, F. Margaroli^{a,b}, P. Meridiani^a, G. Organtini^{a,b}, R. Paramatti^a, F. Preiato^{a,b}, S. Rahatlou^{a,b}, C. Rovelli^a, F. Santanastasio^{a,b}, P. Traczyk^{a,b,2}

INFN Sezione di Torino ^a, Università di Torino ^b, Torino, Italy, Università del Piemonte Orientale ^c, Novara, Italy

N. Amapane^{a,b}, R. Arcidiacono^{a,c,2}, S. Argiro^{a,b}, M. Arneodo^{a,c}, R. Bellan^{a,b}, C. Biino^a, N. Cartiglia^a, M. Costa^{a,b}, R. Covarelli^{a,b}, A. Degano^{a,b}, N. Demaria^a, L. Finco^{a,b,2}, B. Kiani^{a,b}, C. Mariotti^a, S. Maselli^a, E. Migliore^{a,b}, V. Monaco^{a,b}, E. Monteil^{a,b}, M.M. Obertino^{a,b}, L. Pacher^{a,b}, N. Pastrone^a, M. Pelliccioni^a, G.L. Pinna Angioni^{a,b}, F. Ravera^{a,b}, A. Romero^{a,b}, M. Ruspa^{a,c}, R. Sacchi^{a,b}, A. Solano^{a,b}, A. Staiano^a

INFN Sezione di Trieste ^a, Università di Trieste ^b, Trieste, Italy

S. Belforte^a, V. Candelise^{a,b,2}, M. Casarsa^a, F. Cossutti^a, G. Della Ricca^{a,b}, B. Gobbo^a, C. La Licata^{a,b}, M. Marone^{a,b}, A. Schizzi^{a,b}, A. Zanetti^a

Kangwon National University, Chunchon, Korea

A. Kropivnitskaya, S.K. Nam

Kyungpook National University, Daegu, Korea

D.H. Kim, G.N. Kim, M.S. Kim, D.J. Kong, S. Lee, Y.D. Oh, A. Sakharov, D.C. Son

Chonbuk National University, Jeonju, Korea

J.A. Brochero Cifuentes, H. Kim, T.J. Kim

Chonnam National University, Institute for Universe and Elementary Particles, Kwangju, Korea

S. Song

Korea University, Seoul, Korea

S. Choi, Y. Go, D. Gyung, B. Hong, H. Kim, Y. Kim, B. Lee, K. Lee, K.S. Lee, S. Lee, S.K. Park, Y. Roh

Seoul National University, Seoul, Korea

H.D. Yoo

University of Seoul, Seoul, Korea

M. Choi, H. Kim, J.H. Kim, J.S.H. Lee, I.C. Park, G. Ryu, M.S. Ryu

Sungkyunkwan University, Suwon, Korea

Y. Choi, J. Goh, D. Kim, E. Kwon, J. Lee, I. Yu

Vilnius University, Vilnius, Lithuania

V. Dudenas, A. Juodagalvis, J. Vaitkus

National Centre for Particle Physics, Universiti Malaya, Kuala Lumpur, Malaysia

I. Ahmed, Z.A. Ibrahim, J.R. Komaragiri, M.A.B. Md Ali³⁴, F. Mohamad Idris³⁵, W.A.T. Wan Abdullah, M.N. Yusli

Centro de Investigacion y de Estudios Avanzados del IPN, Mexico City, Mexico

E. Casimiro Linares, H. Castilla-Valdez, E. De La Cruz-Burelo, I. Heredia-De La Cruz³⁶, A. Hernandez-Almada, R. Lopez-Fernandez, A. Sanchez-Hernandez

Universidad Iberoamericana, Mexico City, Mexico

S. Carrillo Moreno, F. Vazquez Valencia

Benemerita Universidad Autonoma de Puebla, Puebla, Mexico

I. Pedraza, H.A. Salazar Ibarguen

Universidad Autónoma de San Luis Potosí, San Luis Potosí, Mexico

A. Morelos Pineda

University of Auckland, Auckland, New Zealand

D. Kofcheck

University of Canterbury, Christchurch, New Zealand

P.H. Butler

National Centre for Physics, Quaid-I-Azam University, Islamabad, Pakistan

A. Ahmad, M. Ahmad, Q. Hassan, H.R. Hoorani, W.A. Khan, T. Khurshid, M. Shoaib

National Centre for Nuclear Research, Swierk, Poland

H. Bialkowska, M. Bluj, B. Boimska, T. Frueboes, M. Górska, M. Kazana, K. Nawrocki, K. Romanowska-Rybinska, M. Szleper, P. Zalewski

Institute of Experimental Physics, Faculty of Physics, University of Warsaw, Warsaw, Poland

G. Brona, K. Bunkowski, A. Byszuk³⁷, K. Doroba, A. Kalinowski, M. Konecki, J. Krolikowski, M. Misiura, M. Olszewski, M. Walczak

Laboratório de Instrumentação e Física Experimental de Partículas, Lisboa, Portugal

P. Bargassa, C. Beirão Da Cruz E Silva, A. Di Francesco, P. Faccioli, P.G. Ferreira Parracho,

M. Gallinaro, N. Leonardo, L. Lloret Iglesias, F. Nguyen, J. Rodrigues Antunes, J. Seixas, O. Toldaiev, D. Vadruccio, J. Varela, P. Vischia

Joint Institute for Nuclear Research, Dubna, Russia

S. Afanasiev, P. Bunin, M. Gavrilenco, I. Golutvin, I. Gorbunov, A. Kamenev, V. Karjavin, V. Konoplyanikov, A. Lanev, A. Malakhov, V. Matveev^{38,39}, P. Moisenz, V. Palichik, V. Perelygin, S. Shmatov, S. Shulha, N. Skatchkov, V. Smirnov, A. Zarubin

Petersburg Nuclear Physics Institute, Gatchina (St. Petersburg), Russia

V. Golovtsov, Y. Ivanov, V. Kim⁴⁰, E. Kuznetsova, P. Levchenko, V. Murzin, V. Oreshkin, I. Smirnov, V. Sulimov, L. Uvarov, S. Vavilov, A. Vorobyev

Institute for Nuclear Research, Moscow, Russia

Yu. Andreev, A. Dermenev, S. Gninenko, N. Golubev, A. Karneyeu, M. Kirsanov, N. Krasnikov, A. Pashenkov, D. Tlisov, A. Toropin

Institute for Theoretical and Experimental Physics, Moscow, Russia

V. Epshteyn, V. Gavrilov, N. Lychkovskaya, V. Popov, I. Pozdnyakov, G. Safronov, A. Spiridonov, E. Vlasov, A. Zhokin

National Research Nuclear University 'Moscow Engineering Physics Institute' (MEPhI), Moscow, Russia

A. Bylinkin

P.N. Lebedev Physical Institute, Moscow, Russia

V. Andreev, M. Azarkin³⁹, I. Dremin³⁹, M. Kirakosyan, A. Leonidov³⁹, G. Mesyats, S.V. Rusakov

Skobeltsyn Institute of Nuclear Physics, Lomonosov Moscow State University, Moscow, Russia

A. Baskakov, A. Belyaev, E. Boos, M. Dubinin⁴¹, L. Dudko, A. Ershov, A. Gribushin, V. Klyukhin, O. Kodolova, I. Loktin, I. Myagkov, S. Obraztsov, S. Petrushanko, V. Savrin, A. Snigirev

State Research Center of Russian Federation, Institute for High Energy Physics, Protvino, Russia

I. Azhgirey, I. Bayshev, S. Bitioukov, V. Kachanov, A. Kalinin, D. Konstantinov, V. Krychkine, V. Petrov, R. Ryutin, A. Sobol, L. Tourtchanovitch, S. Troshin, N. Tyurin, A. Uzunian, A. Volkov

University of Belgrade, Faculty of Physics and Vinca Institute of Nuclear Sciences, Belgrade, Serbia

P. Adzic⁴², P. Cirkovic, J. Milosevic, V. Rekovic

Centro de Investigaciones Energéticas Medioambientales y Tecnológicas (CIEMAT), Madrid, Spain

J. Alcaraz Maestre, E. Calvo, M. Cerrada, M. Chamizo Llatas, N. Colino, B. De La Cruz, A. Delgado Peris, A. Escalante Del Valle, C. Fernandez Bedoya, J.P. Fernández Ramos, J. Flix, M.C. Fouz, P. Garcia-Abia, O. Gonzalez Lopez, S. Goy Lopez, J.M. Hernandez, M.I. Josa, E. Navarro De Martino, A. Pérez-Calero Yzquierdo, J. Puerta Pelayo, A. Quintario Olmeda, I. Redondo, L. Romero, J. Santaolalla, M.S. Soares

Universidad Autónoma de Madrid, Madrid, Spain

C. Albajar, J.F. de Trocóniz, M. Missiroli, D. Moran

Universidad de Oviedo, Oviedo, Spain

J. Cuevas, J. Fernandez Menendez, S. Folgueras, I. Gonzalez Caballero, E. Palencia Cortezon, J.M. Vizan Garcia

Instituto de Física de Cantabria (IFCA), CSIC-Universidad de Cantabria, Santander, Spain

I.J. Cabrillo, A. Calderon, J.R. Castiñeiras De Saa, P. De Castro Manzano, M. Fernandez, J. Garcia-Ferrero, G. Gomez, A. Lopez Virto, J. Marco, R. Marco, C. Martinez Rivero, F. Matorras, J. Piedra Gomez, T. Rodrigo, A.Y. Rodríguez-Marrero, A. Ruiz-Jimeno, L. Scodellaro, N. Trevisani, I. Vila, R. Vilar Cortabitarte

CERN, European Organization for Nuclear Research, Geneva, Switzerland

D. Abbaneo, E. Auffray, G. Auzinger, M. Bachtis, P. Baillon, A.H. Ball, D. Barney, A. Benaglia, J. Bendavid, L. Benhabib, J.F. Benitez, G.M. Berruti, P. Bloch, A. Bocci, A. Bonato, C. Botta, H. Breuker, T. Camporesi, R. Castello, G. Cerminara, M. D'Alfonso, D. d'Enterria, A. Dabrowski, V. Daponte, A. David, M. De Gruttola, F. De Guio, A. De Roeck, S. De Visscher, E. Di Marco⁴³, M. Dobson, M. Dordevic, B. Dorney, T. du Pree, D. Duggan, M. Dünser, N. Dupont, A. Elliott-Peisert, G. Franzoni, J. Fulcher, W. Funk, D. Gigi, K. Gill, D. Giordano, M. Girone, F. Glege, R. Guida, S. Gundacker, M. Guthoff, J. Hammer, P. Harris, J. Hegeman, V. Innocente, P. Janot, H. Kirschenmann, M.J. Kortelainen, K. Kousouris, K. Krajczar, P. Lecoq, C. Lourenço, M.T. Lucchini, N. Magini, L. Malgeri, M. Mannelli, A. Martelli, L. Masetti, F. Meijers, S. Mersi, E. Meschi, F. Moortgat, S. Morovic, M. Mulders, M.V. Nemallapudi, H. Neugebauer, S. Orfanelli⁴⁴, L. Orsini, L. Pape, E. Perez, M. Peruzzi, A. Petrilli, G. Petrucciani, A. Pfeiffer, D. Piparo, A. Racz, T. Reis, G. Rolandi⁴⁵, M. Rovere, M. Ruan, H. Sakulin, C. Schäfer, C. Schwick, M. Seidel, A. Sharma, P. Silva, M. Simon, P. Sphicas⁴⁶, J. Steggemann, B. Stieger, M. Stoye, Y. Takahashi, D. Treille, A. Triossi, A. Tsirou, G.I. Veres²³, N. Wardle, H.K. Wöhri, A. Zagozdzinska³⁷, W.D. Zeuner

Paul Scherrer Institut, Villigen, Switzerland

W. Bertl, K. Deiters, W. Erdmann, R. Horisberger, Q. Ingram, H.C. Kaestli, D. Kotlinski, U. Langenegger, D. Renker, T. Rohe

Institute for Particle Physics, ETH Zurich, Zurich, Switzerland

F. Bachmair, L. Bäni, L. Bianchini, B. Casal, G. Dissertori, M. Dittmar, M. Donegà, P. Eller, C. Grab, C. Heidegger, D. Hits, J. Hoss, G. Kasieczka, W. Lustermann, B. Mangano, M. Marionneau, P. Martinez Ruiz del Arbol, M. Masciovecchio, D. Meister, F. Micheli, P. Musella, F. Nessi-Tedaldi, F. Pandolfi, J. Pata, F. Pauss, L. Perrozzi, M. Quitnat, M. Rossini, A. Starodumov⁴⁷, M. Takahashi, V.R. Tavolaro, K. Theofilatos, R. Wallny

Universität Zürich, Zurich, Switzerland

T.K. Arrestad, C. Amsler⁴⁸, L. Caminada, M.F. Canelli, V. Chiochia, A. De Cosa, C. Galloni, A. Hinzmann, T. Hreus, B. Kilminster, C. Lange, J. Ngadiuba, D. Pinna, P. Robmann, F.J. Ronga, D. Salerno, Y. Yang

National Central University, Chung-Li, Taiwan

M. Cardaci, K.H. Chen, T.H. Doan, Sh. Jain, R. Khurana, M. Konyushikhin, C.M. Kuo, W. Lin, Y.J. Lu, S.S. Yu

National Taiwan University (NTU), Taipei, Taiwan

Arun Kumar, R. Bartek, P. Chang, Y.H. Chang, Y.W. Chang, Y. Chao, K.F. Chen, P.H. Chen, C. Dietz, F. Fiori, U. Grundler, W.-S. Hou, Y. Hsiung, Y.F. Liu, R.-S. Lu, M. Miñano Moya, E. Petrakou, J.f. Tsai, Y.M. Tzeng

Chulalongkorn University, Faculty of Science, Department of Physics, Bangkok, Thailand
B. Asavapibhop, K. Kovitanggoon, G. Singh, N. Srimanobhas, N. Suwonjandee

Cukurova University, Adana, Turkey

A. Adiguzel, M.N. Bakirci⁴⁹, S. Cerci⁵⁰, Z.S. Demiroglu, C. Dozen, E. Eskut, F.H. Gecit, S. Girgis, G. Gokbulut, Y. Guler, E. Gurpinar, I. Hos, E.E. Kangal⁵¹, G. Onengut⁵², M. Ozcan, K. Ozdemir⁵³, A. Polatoz, D. Sunar Cerci⁵⁰, H. Topakli⁴⁹, M. Vergili, C. Zorbilmez

Middle East Technical University, Physics Department, Ankara, Turkey

I.V. Akin, B. Bilin, S. Bilmis, B. Isildak⁵⁴, G. Karapinar⁵⁵, M. Yalvac, M. Zeyrek

Bogazici University, Istanbul, Turkey

E. Glmez, M. Kaya⁵⁶, O. Kaya⁵⁷, E.A. Yetkin⁵⁸, T. Yetkin⁵⁹

Istanbul Technical University, Istanbul, Turkey

A. Cakir, K. Cankocak, S. Sen⁶⁰, F.I. Vardarli

Institute for Scintillation Materials of National Academy of Science of Ukraine, Kharkov, Ukraine

B. Grynyov

National Scientific Center, Kharkov Institute of Physics and Technology, Kharkov, Ukraine

L. Levchuk, P. Sorokin

University of Bristol, Bristol, United Kingdom

R. Aggleton, F. Ball, L. Beck, J.J. Brooke, E. Clement, D. Cussans, H. Flacher, J. Goldstein, M. Grimes, G.P. Heath, H.F. Heath, J. Jacob, L. Kreczko, C. Lucas, Z. Meng, D.M. Newbold⁶¹, S. Paramesvaran, A. Poll, T. Sakuma, S. Seif El Nasr-storey, S. Senkin, D. Smith, V.J. Smith

Rutherford Appleton Laboratory, Didcot, United Kingdom

K.W. Bell, A. Belyaev⁶², C. Brew, R.M. Brown, L. Calligaris, D. Cieri, D.J.A. Cockerill, J.A. Coughlan, K. Harder, S. Harper, E. Olaiya, D. Petyt, C.H. Shepherd-Themistocleous, A. Thea, I.R. Tomalin, T. Williams, S.D. Worm

Imperial College, London, United Kingdom

M. Baber, R. Bainbridge, O. Buchmuller, A. Bundock, D. Burton, S. Casasso, M. Citron, D. Colling, L. Corpe, N. Cripps, P. Dauncey, G. Davies, A. De Wit, M. Della Negra, P. Dunne, A. Elwood, W. Ferguson, D. Futyan, G. Hall, G. Iles, M. Kenzie, R. Lane, R. Lucas⁶¹, L. Lyons, A.-M. Magnan, S. Malik, J. Nash, A. Nikitenko⁴⁷, J. Pela, M. Pesaresi, K. Petridis, D.M. Raymond, A. Richards, A. Rose, C. Seez, A. Tapper, K. Uchida, M. Vazquez Acosta⁶³, T. Virdee, S.C. Zenz

Brunel University, Uxbridge, United Kingdom

J.E. Cole, P.R. Hobson, A. Khan, P. Kyberd, D. Leggat, D. Leslie, I.D. Reid, P. Symonds, L. Teodorescu, M. Turner

Baylor University, Waco, USA

A. Borzou, K. Call, J. Dittmann, K. Hatakeyama, H. Liu, N. Pastika

The University of Alabama, Tuscaloosa, USA

O. Charaf, S.I. Cooper, C. Henderson, P. Rumerio

Boston University, Boston, USA

D. Arcaro, A. Avetisyan, T. Bose, C. Fantasia, D. Gastler, P. Lawson, D. Rankin, C. Richardson, J. Rohlf, J. St. John, L. Sulak, D. Zou

Brown University, Providence, USA

J. Alimena, E. Berry, S. Bhattacharya, D. Cutts, N. Dhingra, A. Ferapontov, A. Garabedian, J. Hakala, U. Heintz, E. Laird, G. Landsberg, Z. Mao, M. Narain, S. Piperov, S. Sagir, R. Syarif

University of California, Davis, Davis, USA

R. Breedon, G. Breto, M. Calderon De La Barca Sanchez, S. Chauhan, M. Chertok, J. Conway, R. Conway, P.T. Cox, R. Erbacher, G. Funk, M. Gardner, W. Ko, R. Lander, M. Mulhearn, D. Pellett, J. Pilot, F. Ricci-Tam, S. Shalhout, J. Smith, M. Squires, D. Stolp, M. Tripathi, S. Wilbur, R. Yohay

University of California, Los Angeles, USA

C. Bravo, R. Cousins, P. Everaerts, C. Farrell, A. Florent, J. Hauser, M. Ignatenko, D. Saltzberg, C. Schnaible, E. Takasugi, V. Valuev, M. Weber

University of California, Riverside, Riverside, USA

K. Burt, R. Clare, J. Ellison, J.W. Gary, G. Hanson, J. Heilman, M. Ivova PANEVA, P. Jandir, E. Kennedy, F. Lacroix, O.R. Long, A. Luthra, M. Malberti, M. Olmedo Negrete, A. Shrinivas, H. Wei, S. Wimpenny, B. R. Yates

University of California, San Diego, La Jolla, USA

J.G. Branson, G.B. Cerati, S. Cittolin, R.T. D'Agnolo, M. Derdzinski, A. Holzner, R. Kelley, D. Klein, J. Letts, I. Macneill, D. Olivito, S. Padhi, M. Pieri, M. Sani, V. Sharma, S. Simon, M. Tadel, A. Vartak, S. Wasserbaech⁶⁴, C. Welke, F. Würthwein, A. Yagil, G. Zevi Della Porta

University of California, Santa Barbara, Santa Barbara, USA

J. Bradmiller-Feld, C. Campagnari, A. Dishaw, V. Dutta, K. Flowers, M. Franco Sevilla, P. Geffert, C. George, F. Golf, L. Gouskos, J. Gran, J. Incandela, N. Mccoll, S.D. Mullin, J. Richman, D. Stuart, I. Suarez, C. West, J. Yoo

California Institute of Technology, Pasadena, USA

D. Anderson, A. Apresyan, A. Bornheim, J. Bunn, Y. Chen, J. Duarte, A. Mott, H.B. Newman, C. Pena, M. Pierini, M. Spiropulu, J.R. Vlimant, S. Xie, R.Y. Zhu

Carnegie Mellon University, Pittsburgh, USA

M.B. Andrews, V. Azzolini, A. Calamba, B. Carlson, T. Ferguson, M. Paulini, J. Russ, M. Sun, H. Vogel, I. Vorobiev

University of Colorado Boulder, Boulder, USA

J.P. Cumalat, W.T. Ford, A. Gaz, F. Jensen, A. Johnson, M. Krohn, T. Mulholland, U. Nauenberg, K. Stenson, S.R. Wagner

Cornell University, Ithaca, USA

J. Alexander, A. Chatterjee, J. Chaves, J. Chu, S. Dittmer, N. Eggert, N. Mirman, G. Nicolas Kaufman, J.R. Patterson, A. Rinkevicius, A. Ryd, L. Skinnari, L. Soffi, W. Sun, S.M. Tan, W.D. Teo, J. Thom, J. Thompson, J. Tucker, Y. Weng, P. Wittich

Fermi National Accelerator Laboratory, Batavia, USA

S. Abdullin, M. Albrow, G. Apollinari, S. Banerjee, L.A.T. Bauerdtick, A. Beretvas, J. Berryhill, P.C. Bhat, G. Bolla, K. Burkett, J.N. Butler, H.W.K. Cheung, F. Chlebana, S. Cihangir, V.D. Elvira, I. Fisk, J. Freeman, E. Gottschalk, L. Gray, D. Green, S. Grünendahl, O. Gutsche, J. Hanlon, D. Hare, R.M. Harris, S. Hasegawa, J. Hirschauer, Z. Hu, B. Jayatilaka, S. Jindariani, M. Johnson, U. Joshi, A.W. Jung, B. Klima, B. Kreis, S. Lammel, J. Linacre, D. Lincoln, R. Lipton, T. Liu, R. Lopes De Sá, J. Lykken, K. Maeshima, J.M. Marraffino, V.I. Martinez Outschoorn, S. Maruyama, D. Mason, P. McBride, P. Merkel, K. Mishra, S. Mrenna, S. Nahn,

C. Newman-Holmes[†], V. O'Dell, K. Pedro, O. Prokofyev, G. Rakness, E. Sexton-Kennedy, A. Soha, W.J. Spalding, L. Spiegel, N. Strobbe, L. Taylor, S. Tkaczyk, N.V. Tran, L. Uplegger, E.W. Vaandering, C. Vernieri, M. Verzocchi, R. Vidal, H.A. Weber, A. Whitbeck

University of Florida, Gainesville, USA

D. Acosta, P. Avery, P. Bortignon, D. Bourilkov, A. Carnes, M. Carver, D. Curry, S. Das, R.D. Field, I.K. Furic, S.V. Gleyzer, J. Hugon, J. Konigsberg, A. Korytov, K. Kotov, J.F. Low, P. Ma, K. Matchev, H. Mei, P. Milenovic⁶⁵, G. Mitselmakher, D. Rank, R. Rossin, L. Shchutska, M. Snowball, D. Sperka, N. Terentyev, L. Thomas, J. Wang, S. Wang, J. Yelton

Florida International University, Miami, USA

S. Hewamanage, S. Linn, P. Markowitz, G. Martinez, J.L. Rodriguez

Florida State University, Tallahassee, USA

A. Ackert, J.R. Adams, T. Adams, A. Askew, S. Bein, J. Bochenek, B. Diamond, J. Haas, S. Hagopian, V. Hagopian, K.F. Johnson, A. Khatiwada, H. Prosper, M. Weinberg

Florida Institute of Technology, Melbourne, USA

M.M. Baarmann, V. Bhopatkar, S. Colafranceschi⁶⁶, M. Hohlmann, H. Kalakhety, D. Noonan, T. Roy, F. Yumiceva

University of Illinois at Chicago (UIC), Chicago, USA

M.R. Adams, L. Apanasevich, D. Berry, R.R. Betts, I. Bucinskaite, R. Cavanaugh, O. Evdokimov, L. Gauthier, C.E. Gerber, D.J. Hofman, P. Kurt, C. O'Brien, I.D. Sandoval Gonzalez, C. Silkworth, P. Turner, N. Varelas, Z. Wu, M. Zakaria

The University of Iowa, Iowa City, USA

B. Bilki⁶⁷, W. Clarida, K. Dilsiz, S. Durgut, R.P. Gundrajula, M. Haytmyradov, V. Khristenko, J.-P. Merlo, H. Mermerkaya⁶⁸, A. Mestvirishvili, A. Moeller, J. Nachtman, H. Ogul, Y. Onel, F. Ozok⁵⁸, A. Penzo, C. Snyder, E. Tiras, J. Wetzel, K. Yi

Johns Hopkins University, Baltimore, USA

I. Anderson, B.A. Barnett, B. Blumenfeld, N. Eminizer, D. Fehling, L. Feng, A.V. Gritsan, P. Maksimovic, C. Martin, M. Osherson, J. Roskes, A. Sady, U. Sarica, M. Swartz, M. Xiao, Y. Xin, C. You

The University of Kansas, Lawrence, USA

P. Baringer, A. Bean, G. Benelli, C. Bruner, R.P. Kenny III, D. Majumder, M. Malek, M. Murray, S. Sanders, R. Stringer, Q. Wang

Kansas State University, Manhattan, USA

A. Ivanov, K. Kaadze, S. Khalil, M. Makouski, Y. Maravin, A. Mohammadi, L.K. Saini, N. Skhirtladze, S. Toda

Lawrence Livermore National Laboratory, Livermore, USA

D. Lange, F. Rebassoo, D. Wright

University of Maryland, College Park, USA

C. Anelli, A. Baden, O. Baron, A. Belloni, B. Calvert, S.C. Eno, C. Ferraioli, J.A. Gomez, N.J. Hadley, S. Jabeen, R.G. Kellogg, T. Kolberg, J. Kunkle, Y. Lu, A.C. Mignerey, Y.H. Shin, A. Skuja, M.B. Tonjes, S.C. Tonwar

Massachusetts Institute of Technology, Cambridge, USA

A. Apyan, R. Barbieri, A. Baty, K. Bierwagen, S. Brandt, W. Busza, I.A. Cali, Z. Demiragli, L. Di Matteo, G. Gomez Ceballos, M. Goncharov, D. Gulhan, Y. Iiyama, G.M. Innocenti,

M. Klute, D. Kovalskyi, Y.S. Lai, Y.-J. Lee, A. Levin, P.D. Luckey, A.C. Marini, C. McGinn, C. Mironov, S. Narayanan, X. Niu, C. Paus, D. Ralph, C. Roland, G. Roland, J. Salfeld-Nebgen, G.S.F. Stephans, K. Sumorok, M. Varma, D. Velicanu, J. Veverka, J. Wang, T.W. Wang, B. Wyslouch, M. Yang, V. Zhukova

University of Minnesota, Minneapolis, USA

B. Dahmes, A. Evans, A. Finkel, A. Gude, P. Hansen, S. Kalafut, S.C. Kao, K. Klapoetke, Y. Kubota, Z. Lesko, J. Mans, S. Nourbakhsh, N. Ruckstuhl, R. Rusack, N. Tambe, J. Turkewitz

University of Mississippi, Oxford, USA

J.G. Acosta, S. Oliveros

University of Nebraska-Lincoln, Lincoln, USA

E. Avdeeva, K. Bloom, S. Bose, D.R. Claes, A. Dominguez, C. Fangmeier, R. Gonzalez Suarez, R. Kamaliuddin, J. Keller, D. Knowlton, I. Kravchenko, F. Meier, J. Monroy, F. Ratnikov, J.E. Siado, G.R. Snow

State University of New York at Buffalo, Buffalo, USA

M. Alyari, J. Dolen, J. George, A. Godshalk, C. Harrington, I. Iashvili, J. Kaisen, A. Kharchilava, A. Kumar, S. Rappoccio, B. Roozbahani

Northeastern University, Boston, USA

G. Alverson, E. Barberis, D. Baumgartel, M. Chasco, A. Hortiangtham, A. Massironi, D.M. Morse, D. Nash, T. Orimoto, R. Teixeira De Lima, D. Trocino, R.-J. Wang, D. Wood, J. Zhang

Northwestern University, Evanston, USA

K.A. Hahn, A. Kubik, N. Mucia, N. Odell, B. Pollack, A. Pozdnyakov, M. Schmitt, S. Stoynev, K. Sung, M. Trovato, M. Velasco

University of Notre Dame, Notre Dame, USA

A. Brinkerhoff, N. Dev, M. Hildreth, C. Jessop, D.J. Karmgard, N. Kellams, K. Lannon, N. Marinelli, F. Meng, C. Mueller, Y. Musienko³⁸, M. Planer, A. Reinsvold, R. Ruchti, G. Smith, S. Taroni, N. Valls, M. Wayne, M. Wolf, A. Woodard

The Ohio State University, Columbus, USA

L. Antonelli, J. Brinson, B. Bylsma, L.S. Durkin, S. Flowers, A. Hart, C. Hill, R. Hughes, W. Ji, T.Y. Ling, B. Liu, W. Luo, D. Puigh, M. Rodenburg, B.L. Winer, H.W. Wulsin

Princeton University, Princeton, USA

O. Driga, P. Elmer, J. Hardenbrook, P. Hebda, S.A. Koay, P. Lujan, D. Marlow, T. Medvedeva, M. Mooney, J. Olsen, C. Palmer, P. Piroué, H. Saka, D. Stickland, C. Tully, A. Zuranski

University of Puerto Rico, Mayaguez, USA

S. Malik

Purdue University, West Lafayette, USA

V.E. Barnes, D. Benedetti, D. Bortoletto, L. Gutay, M.K. Jha, M. Jones, K. Jung, D.H. Miller, N. Neumeister, B.C. Radburn-Smith, X. Shi, I. Shipsey, D. Silvers, J. Sun, A. Svyatkovskiy, F. Wang, W. Xie, L. Xu

Purdue University Calumet, Hammond, USA

N. Parashar, J. Stupak

Rice University, Houston, USA

A. Adair, B. Akgun, Z. Chen, K.M. Ecklund, F.J.M. Geurts, M. Guilbaud, W. Li, B. Michlin, M. Northup, B.P. Padley, R. Redjimi, J. Roberts, J. Rorie, Z. Tu, J. Zabel

University of Rochester, Rochester, USA

B. Betchart, A. Bodek, P. de Barbaro, R. Demina, Y. Eshaq, T. Ferbel, M. Galanti, A. Garcia-Bellido, J. Han, A. Harel, O. Hindrichs, A. Khukhunaishvili, G. Petrillo, P. Tan, M. Verzetti

Rutgers, The State University of New Jersey, Piscataway, USA

S. Arora, A. Barker, J.P. Chou, C. Contreras-Campana, E. Contreras-Campana, D. Ferencek, Y. Gershtein, R. Gray, E. Halkiadakis, D. Hidas, E. Hughes, S. Kaplan, R. Kunnawalkam Elayavalli, A. Lath, K. Nash, S. Panwalkar, M. Park, S. Salur, S. Schnetzer, D. Sheffield, S. Somalwar, R. Stone, S. Thomas, P. Thomassen, M. Walker

University of Tennessee, Knoxville, USA

M. Foerster, G. Riley, K. Rose, S. Spanier, A. York

Texas A&M University, College Station, USA

O. Bouhali⁶⁹, A. Castaneda Hernandez⁶⁹, A. Celik, M. Dalchenko, M. De Mattia, A. Delgado, S. Dildick, R. Eusebi, J. Gilmore, T. Huang, T. Kamon⁷⁰, V. Krutelyov, R. Mueller, I. Osipenkov, Y. Pakhotin, R. Patel, A. Perloff, A. Rose, A. Safonov, A. Tatarinov, K.A. Ulmer²

Texas Tech University, Lubbock, USA

N. Akchurin, C. Cowden, J. Damgov, C. Dragoiu, P.R. Dudero, J. Faulkner, S. Kunori, K. Lamichhane, S.W. Lee, T. Libeiro, S. Undleeb, I. Volobouev

Vanderbilt University, Nashville, USA

E. Appelt, A.G. Delannoy, S. Greene, A. Gurrola, R. Janjam, W. Johns, C. Maguire, Y. Mao, A. Melo, H. Ni, P. Sheldon, B. Snook, S. Tuo, J. Velkovska, Q. Xu

University of Virginia, Charlottesville, USA

M.W. Arenton, B. Cox, B. Francis, J. Goodell, R. Hirosky, A. Ledovskoy, H. Li, C. Lin, C. Neu, T. Sinthuprasith, X. Sun, Y. Wang, E. Wolfe, J. Wood, F. Xia

Wayne State University, Detroit, USA

C. Clarke, R. Harr, P.E. Karchin, C. Kottachchi Kankanamge Don, P. Lamichhane, J. Sturdy

University of Wisconsin - Madison, Madison, WI, USA

D.A. Belknap, D. Carlsmith, M. Cepeda, S. Dasu, L. Dodd, S. Duric, B. Gomber, M. Grothe, R. Hall-Wilton, M. Herndon, A. Hervé, P. Klabbers, A. Lanaro, A. Levine, K. Long, R. Loveless, A. Mohapatra, I. Ojalvo, T. Perry, G.A. Pierro, G. Polese, T. Ruggles, T. Sarangi, A. Savin, A. Sharma, N. Smith, W.H. Smith, D. Taylor, N. Woods

†: Deceased

1: Also at Vienna University of Technology, Vienna, Austria

2: Also at CERN, European Organization for Nuclear Research, Geneva, Switzerland

3: Also at State Key Laboratory of Nuclear Physics and Technology, Peking University, Beijing, China

4: Also at Institut Pluridisciplinaire Hubert Curien, Université de Strasbourg, Université de Haute Alsace Mulhouse, CNRS/IN2P3, Strasbourg, France

5: Also at National Institute of Chemical Physics and Biophysics, Tallinn, Estonia

6: Also at Skobeltsyn Institute of Nuclear Physics, Lomonosov Moscow State University, Moscow, Russia

7: Also at Universidade Estadual de Campinas, Campinas, Brazil

-
- 8: Also at Centre National de la Recherche Scientifique (CNRS) - IN2P3, Paris, France
 - 9: Also at Laboratoire Leprince-Ringuet, Ecole Polytechnique, IN2P3-CNRS, Palaiseau, France
 - 10: Also at Joint Institute for Nuclear Research, Dubna, Russia
 - 11: Also at Helwan University, Cairo, Egypt
 - 12: Now at Zewail City of Science and Technology, Zewail, Egypt
 - 13: Now at Fayoum University, El-Fayoum, Egypt
 - 14: Also at British University in Egypt, Cairo, Egypt
 - 15: Now at Ain Shams University, Cairo, Egypt
 - 16: Also at Université de Haute Alsace, Mulhouse, France
 - 17: Also at Tbilisi State University, Tbilisi, Georgia
 - 18: Also at RWTH Aachen University, III. Physikalisches Institut A, Aachen, Germany
 - 19: Also at Indian Institute of Science Education and Research, Bhopal, India
 - 20: Also at University of Hamburg, Hamburg, Germany
 - 21: Also at Brandenburg University of Technology, Cottbus, Germany
 - 22: Also at Institute of Nuclear Research ATOMKI, Debrecen, Hungary
 - 23: Also at Eötvös Loránd University, Budapest, Hungary
 - 24: Also at University of Debrecen, Debrecen, Hungary
 - 25: Also at Wigner Research Centre for Physics, Budapest, Hungary
 - 26: Also at University of Visva-Bharati, Santiniketan, India
 - 27: Now at King Abdulaziz University, Jeddah, Saudi Arabia
 - 28: Also at University of Ruhuna, Matara, Sri Lanka
 - 29: Also at Isfahan University of Technology, Isfahan, Iran
 - 30: Also at University of Tehran, Department of Engineering Science, Tehran, Iran
 - 31: Also at Plasma Physics Research Center, Science and Research Branch, Islamic Azad University, Tehran, Iran
 - 32: Also at Università degli Studi di Siena, Siena, Italy
 - 33: Also at Purdue University, West Lafayette, USA
 - 34: Also at International Islamic University of Malaysia, Kuala Lumpur, Malaysia
 - 35: Also at Malaysian Nuclear Agency, MOSTI, Kajang, Malaysia
 - 36: Also at Consejo Nacional de Ciencia y Tecnología, Mexico city, Mexico
 - 37: Also at Warsaw University of Technology, Institute of Electronic Systems, Warsaw, Poland
 - 38: Also at Institute for Nuclear Research, Moscow, Russia
 - 39: Now at National Research Nuclear University 'Moscow Engineering Physics Institute' (MEPhI), Moscow, Russia
 - 40: Also at St. Petersburg State Polytechnical University, St. Petersburg, Russia
 - 41: Also at California Institute of Technology, Pasadena, USA
 - 42: Also at Faculty of Physics, University of Belgrade, Belgrade, Serbia
 - 43: Also at INFN Sezione di Roma; Università di Roma, Roma, Italy
 - 44: Also at National Technical University of Athens, Athens, Greece
 - 45: Also at Scuola Normale e Sezione dell'INFN, Pisa, Italy
 - 46: Also at University of Athens, Athens, Greece
 - 47: Also at Institute for Theoretical and Experimental Physics, Moscow, Russia
 - 48: Also at Albert Einstein Center for Fundamental Physics, Bern, Switzerland
 - 49: Also at Gaziosmanpasa University, Tokat, Turkey
 - 50: Also at Adiyaman University, Adiyaman, Turkey
 - 51: Also at Mersin University, Mersin, Turkey
 - 52: Also at Cag University, Mersin, Turkey
 - 53: Also at Piri Reis University, Istanbul, Turkey
 - 54: Also at Ozyegin University, Istanbul, Turkey

- 55: Also at Izmir Institute of Technology, Izmir, Turkey
- 56: Also at Marmara University, Istanbul, Turkey
- 57: Also at Kafkas University, Kars, Turkey
- 58: Also at Mimar Sinan University, Istanbul, Istanbul, Turkey
- 59: Also at Yildiz Technical University, Istanbul, Turkey
- 60: Also at Hacettepe University, Ankara, Turkey
- 61: Also at Rutherford Appleton Laboratory, Didcot, United Kingdom
- 62: Also at School of Physics and Astronomy, University of Southampton, Southampton, United Kingdom
- 63: Also at Instituto de Astrofísica de Canarias, La Laguna, Spain
- 64: Also at Utah Valley University, Orem, USA
- 65: Also at University of Belgrade, Faculty of Physics and Vinca Institute of Nuclear Sciences, Belgrade, Serbia
- 66: Also at Facoltà Ingegneria, Università di Roma, Roma, Italy
- 67: Also at Argonne National Laboratory, Argonne, USA
- 68: Also at Erzincan University, Erzincan, Turkey
- 69: Also at Texas A&M University at Qatar, Doha, Qatar
- 70: Also at Kyungpook National University, Daegu, Korea